# Melt Inclusion Study on Bingham Canyon Volcanics

## Constraining the magma source for the mineralizing fluids in a world class copper porphyry system

**Master Thesis**

**Author(s):**
Gilsbach, Lucas

**Publication date:**
2015

**Permanent link:**
https://doi.org/10.3929/ethz-b-000407668

DERDW
Departement Erdwissenschaften

ETH zürich

Institute of Geochemistry and Petrology

Fluids and Mineral Deposits Group

# Melt Inclusion Study on Bingham Canyon Volcanics:

## Constraining the magma source for the mineralizing fluids in a world class copper porphyry system

| | |
|---|---|
| Submitted: | Master thesis |
| for the degree of: | Master of Science |
| by: | Lucas Gilsbach |
| born in: | Wesel, Germany |
| Email: | glucas@student.ethz.ch |

| | |
|---|---|
| Main supervisor: | Prof. Dr. Christoph A. Heinrich |
| Co-Referee: | Dr. Joerg Philipp Weis |
| Additional Supervisor: | Prof. Dr. Olivier Bachmann |

# 1 Abstract

The Bingham Canyon porphyry copper-system is the largest gold and copper deposit in North America. Volcanic and subvolcanic activity accompanied the mineralization event resulting in a complex stack of debris and lava flow deposits of intermediate composition, now exposed in the vicinity of the mine. LA-ICPMS of silicate and sulfide melt inclusions in the volcanic rocks was combined with optical petrography to gain insights into the magmatic evolution at Bingham and constrain the composition of the magma releasing the mineralizing fluids.

Results from LA-ICPMS of silicate and sulfide melt inclusions in two volcanic rock samples and one subvolcanic intrusive reveal post entrapment modification of amphibole hosted melt inclusions.

Trace element compositions in unmodified silicate-melt inclusions suggest a subduction related genesis for the magma releasing the mineralizing fluids at Bingham. Magma evolution is characterized by fractional crystallization and (lower) crustal assimilation and resulted in a dacitic to rhyolitic magma recorded in plagioclase-hosted melt inclusions. Petrographic observations indicate the mixing of a second (mafic) magma with the evolved rhyolitic melt, explaining the dominance of intermediate volcanic rocks in the Bingham volcanic suite This second magma is possibly recorded in potassium rich, clinopyroxene-hosted silicate melt inclusions and perhaps contributed additional Cu to the system.

Cu-rich sulfide melt inclusions seem to have exerted an influence on the composition of the initial ore fluid in Bingham possibly supporting ideas that consider the pre-concentration of metals in a sulfide melt as an important step towards the generation of economic ore deposits.

# Table of Contents

# Table of figures

# 2 Introduction

## *2.1 Magmatic hydrothermal ore deposits.*

Copper-porphyry systems are an important type of magmatic hydrothermal ore deposits. Those generally form due to fluid movements in the upper crust and are associated with magmatic intrusions acting as the major fluid source. Thermal heat supplied by the intrusive bodies provides the energy necessary for fluid flow. In addition metals can be transferred from the magma to the circulating fluid phase. If the fluid flow is focused into a limited rock volume and metals precipitation happens in a restricted space, important metals deposits can form (Hedenquist and Lowenstern, 1994). Metals concentrated in these deposits are Cu, Sn, W, Mo and Au. They either occur as vein hosted deposits or by replacement of the initial rock.

Cu-porphyry systems dominantly form in magmatic arc environments in an overall compressive regime (Sillitoe, 2010) and sit on successively emplaced porphyritic intrusions of intermediate composition (Audétat and Simon, 2012). As mentioned, the origin of fluids, ligands and metals is seen in a magmatic source underlying the porphyritic stocks in mid crustal levels (Hedenquist and Lowenstern, 1994; Ulrich et al., 1999). Mafic magmas can help the mineralization potential of an igneous complex by supplying additional heat, metals, ligands and fluids to the system. If such a mafic magma mixes with a more felsic magmas in a mid-crustal magma chamber a sulfide phase can form and sequester the available ore metals (Halter et al., 2005). It is highly debated whether this processes actually helps or rather suppresses the formation of economic ore deposits. In an review article Wilkinson (2013) points out that the formation of a sulfide phase upon magmatic differentiation in crustal regions is an essential pre-requisite for the formation of Cu-porphyry systems. The sulfide melt in this case would “pre-concentrate” siderophile metals which are released to an evolving mineralizing fluid upon destabilization of the sulfide melt (Wilkinson, 2013 and herein mentioned references). Contrasting with this view and outlined in an review article by Richards (2014) it is argued that the presence of sulfide residuals in the source region of (Cu-porphyry generating) continental arc magmas has little impact on the concentration of mildly siderophile elements like Cu. Moreover the exsolution of a sulfide melt in mid to upper crustal regions is unlikely due to the more oxidized nature of evolved arc magmas and would rather suppress instead of help the formation of Cu-porphyry systems (Richards, 2014 and herein mentioned references).
However, if the ore metals become available to an aqueous or vapor fluid phase they can be transported through the crust and precipitated from the cooling hydrothermal fluids to form economic ore deposits. (Redmond et al., 2004). The fluid movement lead characteristic and spatially separated alteration zones in and around the porphyry stocks (Lowell and Guilbert, 1970).

Since the recognition that the main ingredients (metal, sulfur and fluids) of porphyry Cu- systems have magmatic origin (Hedenquist and Lowenstern, 1994; Ulrich et al., 1999), the application of melt inclusions in such systems yielded a unique opportunity to study the composition of the source releasing the mineralizing fluids. Melt inclusions form by entrapment of a melt in a growing crystal and can thus yield information about the chemistry of the melt out of which the crystal has grown (Kent, 2008). In addition they can be used to explore the evolution of a magmatic system over time (Audétat and Lowenstern, 2014 and herein mentioned references; Halter et al., 2004b; Zajacz and Halter, 2007).
Significant modifications of the melt inclusion can occur after entrapment due to diffusive re-equilibration (Kent, 2008; Spandler et al., 2007). Especially for Cu, Na, Ag and Li in quartz (Zajacz et al., 2009), Fe, Mg in olivine (Danyushevsky et al., 2000) and Ca, and Na in Plagioclase (Audétat and

Lowenstern, 2014) it has been shown that element ratios measured in melt inclusion are not necessarily representative of the parental melt out of which the crystal has grown. This stresses the importance of a critical interpretation of obtained melt inclusion compositions.
With this knowledge kept in mind melt inclusions have been used successfully to explore and understand processes in the magmatic and hydrothermal regime of igneous systems (Anderson et al., 2000; Halter et al., 2005). For example melt inclusions studies have led to the confirmation of previous suspicions that mafic magmas play a decisive role in the formation of porphyry Cu-system by supplying important amounts of metals and sulfur . In addition it could be shown that the porphyry stocks hosting the mineralization are the result of magma mixing and do not represent the composition of the magma that released the mineralizing fluids (Halter et al., 2005; Hattori and Keith, 2001; Maughan et al., 2002). Moreover, determining the chemistry of co-existing sulfide and silicate melt inclusion yields a great opportunity to understand the role of sulfur in porphyry Cu-systems.

### *2.2 Aim of the study*

The Bingham Cu-porphyry system is probably one of the best studied porphyry Cu-system in the world (Porter et al., 2012 and herein mentioned references). Numerous studies address the mechanisms of metal transportation and precipitation from hydrothermal fluids (e.g. (Gruen et al., 2010; Landtwing et al., 2010; Redmond et al., 2004). In a contribution from Steinberger et al. (2013) the approximate dimension of the magmatic body supplying the ore related components where modeled based on geophysical and geochemical mass balance considerations. However, little has been done in order to constrain the composition of this source. So far, genetic models for Bingham have been built on bulk rock data and modeling results, without any direct evidence from the magmatic regime supporting these findings.
This study is part of a larger project aiming to perform a melt inclusion study on the entire section of volcanic rocks in the Bingham mining district and constrain the chemistry of the magmatic source for the mineralizing fluids. For the first time silicate and sulfide melt inclusions from co-magmatic volcanic rocks of the Bingham Cu-porphyry system are analyzed by LA-ICPMS, the validity of this approach was tested by (Pettke et al., 2004). The analysis of melt inclusions will help to get direct compositional constrains in the magma releasing the mineralizing fluids. In addition the behavior of ore metals in the presence of co-existing sulfide and silicate melts can be explored. Detailed optical petrography and the combination of inclusions analysis of differently evolved volcanic rocks from the same magmatic complex will help to understand the evolution of and establish a genetic model for the Bingham porphyry system. This thesis deals with rocks sampled in the northern part of the exposed volcanic section, from Copperton in the north down to Rose Canyon. The area south of Rose Canyon is covered by a team from the University of Toronto lead by Zoltan Zajacs.

*2.3 Regional geology of the study area*

The study area is part of the Bingham mine district located in north – central Utah in the central Oquirrh mountains close to the eastern termination of the Basin and Range province (Fig. 1). It was subjected to two main phases of compression and extension during Paleozoic times. In the Jurassic the Elko orogeny was associated with regional metamorphism and in the Cretaceous the Servier orogeny was associated with a shallow dipping subduction zone in the western Cordillera (Maughan et al., 2002; Presnell and Parry, 1995; Presnell, 1997)

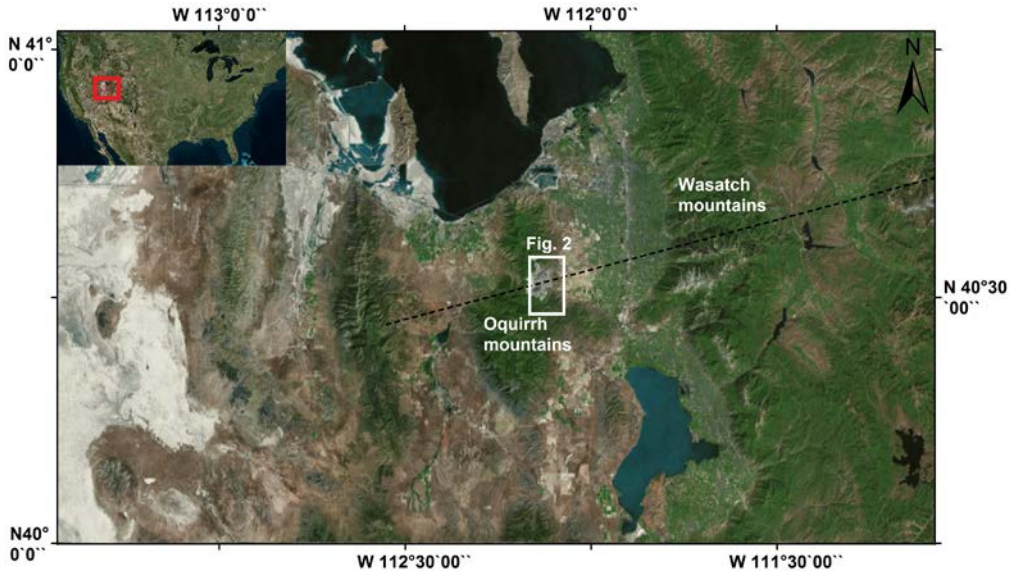


*Fig. 1: Location of the Bingham volcanic system in north central Utah (white square). Location of the Uinta cortez axis in stippled line from Maughan et al. (2002).*

A slap break off in Eocene times induced a change from a compressional to an extensional regime associated with the emplacement of an intrusive belt stretching in east west direction from the Wasatch to the Oquirrh mountains (Maughan et al., 2002; Porter et al., 2012; Presnell, 1997; Sillitoe, 2010). Its location coincides with the Uinta Cortez axis, an east west oriented suture zone of archean-proterozoic age which intersects the north trending Proterozoic Uinta aulacogen south of the mine. The Eocene intrusives are associated with northeast striking fault. After intrusion emplacement the area was subjected to basin and range tectonics leading to a 10°-30° tilting and exposure of the Eocene intrusives at Bingham (Maughan et al., 2002; Porter et al., 2012; Presnell, 1997).

*2.4 The Bingham porphyry Cu-deposit*

At Bingham the intrusive bodies are hosted in folded Paleozoic siliciclastic and carbonate rocks and have been studied intensively (Core et al., 2006; Gruen et al., 2010; Landtwing et al., 2010; Porter et al., 2012; Quadt et al., 2011; Redmond et al., 2004; Waite et al., 1997). They are represented by several porphyry stocks of latitic to monzonitic composition successively emplaced from 38.10Ma to 37.78 Ma and cross cut by late stage latite dykes (Porter et al., 2012; Quadt et al., 2011).

The oldest intrusive is the equigranular monzonite (EM) with an U-Pb age of 38.55 $^{+}/_{-}$ 0.19Ma (Parry et al., 2001). The EM is itself is intruded by a porphyritic quartz monzonite (QMP) the marginal parts of which is termed hybrid quartz monzonite porphyry. The QMP has elevated Cr content in mafic enclaves and studies of contemporaneously erupted volcanic rocks suggest that it formed by mixing a mafic and more calc-alkaline magma in shallow crustal levels. The mafic magmas possibly contributed significant amounts of Cu and fluids to the system (Porter et al., 2012 Maughan, 2002 #20). The QMP is the best mineralized rock and cut by latite porphyry dikes (LP) and quartz latite porphyry dykes (QLP) representing the youngest intrusives in the mine area. Two late stage mafic

biotite porphyry dykes also cut the QMP. Zircon age determination indicate that the QMP, the LP and the QLP were emplaced in a time interval of 0.32m.y.

The mineralization at Bingham consists of a tooth shaped Cu shell with elevated Au concentration at its top. On average the ore has a Cu/Au ratio of 16000:1 (Porter et al., 2012). The main ore host until today has been the EM with about 50% of all ore mined. The main Cu mineralization event was associated with the emplacement of the QMP and LP (Porter et al., 2012). Inside the Cu-shell sits a zone of Molybdenum mineralization. Mo mineralization post-dates the Cu-Au introduction and is associated with the late stage QLP dykes. Lead Zinc mineralization mainly consists of galena and sphalerite and can be found in a corona around the porphyry intrusions (Porter et al., 2012).

### *2.5 Bingham volcanics*

Volcanic activity accompanied the emplacement of the intrusive stocks with now east-ward dipping debris avalanche -, lahar deposits and lava flows exposed east and south of the mine (Fig. 2). Geologic relationships indicate that a former stratovolcano was centered near the modern open pit with an elevation of about 2km above the pre-mine surface (Landtwing et al., 2010; Steinberger et al., 2013).

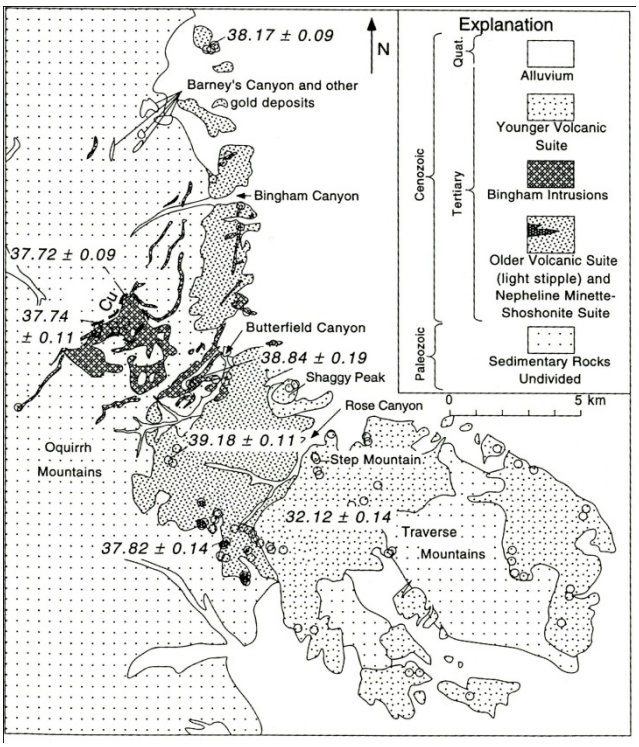


*Fig. 2:Simplified geological map of the Bingham canyon volcanics. The present day mine is 1km to the east. After Keith et al. (1997)*

The volcanic rock pile has also been subjected to several studies mainly focusing on petrographic observations and whole rock geochemical data (Keith et al., 1997; Maughan et al., 2002; Waite et al., 1997 Moore, 1973 #47). (Keith et al., 1997; Maughan et al., 2002). The study of Moore (1973) was the first implying that the volcanic rocks can be seen as an erupted equivalent to the mineralized intrusives which was later confirmed based on geological observations, geochronology, geochemistry and isotope compositions (Keith et al., 1997; Maughan et al., 2002; Waite et al., 1997).

The volcanic activity at Bingham can be subdivided into two main stages . The older volcanic suit with a basal age of 38.68 +/- 0.13 Ma (Maughan et al., 2002) and top age of 37.84 +/-0.14Ma (Deino and Keith, 1997) is largely coeval with the Bingham intrusives and crops out mainly north-west of Rose Canyon and east of the mine. It ranges in composition from minette (basanite) to dacite with the majority of volcanic rocks being intermediate in compositions. Rocks are generally potassium rich, expressed by the occurrence of shoshonitic lava flows in the older volcanic suite. The minette are the most mafic lavas in the area and contain the highest content of Cu (Keith et al., 1997). The younger volcanic suit is dated at 33-31Ma and crops out south of Rose Canyon. Despite its similar mineral assemblages it is most likely related to a separate magmatic system (Waite et al., 1997).

# 3 Methods

## *3.1 Field work*

Sample collection took place during a three week field trip to the Bingham mining district with the aim to sample unaltered volcanic rocks with a potential to preserve melt inclusions . Overall 129 samples were collected in the volcanic section east and south east of the mine and from drill cores. The sample location are marked on the geological map. Samples used for melt inclusion analysis are highlighted in red.

In the field a first selection of sample location was based on geologic maps of the area. Sampling was focused on lava flows, since some clasts in debris flows already indicated that rocks not related to the magmatic activity have been picked up during emplacement. To maximize the probability to find preserved inclusions only fresh rocks were sampled. In addition to sampling, GPS measurement, a short geologic description and if possible, orientation measurements were taken at every location. One particular representative outcrop for the encountered volcanic suite was mapped and examined in detail. If a lava flow or dyke crops out over its whole thickness, sample were taken from the margin and the core in order to have the possibility to examine the effect of variable cooling rates.

## *3.2 Optical petrography*

After a re-consideration of all samples those with the highest potential for MI preservation and with a special interest with regard to the magmatic history were selected for thin section preparation for o In total 21 thin sections were examined in detail using an Olympus BX60 microscope. Pictures documenting the observations were taken with a Leica DFC290HD camera and the Leica Application suit V3 software. All samples were than classified according to the IUGS subcomission on the systematic of igneous rocks based on their mineral content. In the end all samples were rated based on a scale of 0 (=no preserved inclusion) to 3 (=excellent) regarding their silicate- and sulfide-melt inclusion preservation. In addition the potential to analyze sulfide melt inclusions in every sample was rated based on the same system.

## *3.3 LA-ICPMS analysis*

Three samples for LA-ICPMS were selected based on two criteria. First, the presence and quality of preserved silicate and sulfide melt inclusions. Second, the samples should represent the variability of the rocks in the Bingham volcanic suit. Thus a sample from the felsic and more mafic end of the suit was selected. The sample representing the felsic end of the older volcanic suit (TBC13.10A, Location: W112°`5`12.1`` N40°30`50.2``) is from the Lark intrusion and based on optical petrography classified as a tholeiitic andesite, straddling the border to quartz dacite in the Streckeisen diagram for volcanic rocks. The mafic sample is a tholeiitic basalt based on optical petrography (TBC3.1A, Location: W112°7`28.7`` N40°29`58.4``). The third sample (BV6.2I, Location: W112°5`49.4`` N40°33`8.1``) is an andesitic basalt sampled from a lava flow. In all samples silicate melt inclusions were analyzed. Only the tholeiitic basalt contains sulfide inclusions. Both other samples contain few sulfide inclusions which were not suitable for analysis due to their size.

After preparing thick sections with 50um and 120um thickness melt inclusions for analysis were selected. To guarantee the representativeness of the entrapped melt only inclusion larger than 20um were analyzed. In order to be able to ensure homogenous entrapment and track post entrapment modifications several inclusions in one assemblage or growth zone were analyzed together. A total of

273 silicate melt inclusions were analyzed of which 190 had a clear distinguishable signal and could be processed.
After inclusion selection sulfide bearing rock chips were cleaned by treating them with Aqua Regia (1 part $HNO_3$ 3 parts HCL) two times for one hour and then cleaning with a Al-emulsion and treating for 15 hours with Aqua Regia again.
The LA-ICPMS analysis was done by ablating entire unexposed melt inclusions using 193nm ArF Laser coupled with a Elan 6100 DRC mass spectrometer. A very detailed explanation of the approach and the ablation procedure can be found in Halter et al. (2002a), Heinrich et al. (2003) and Pettke et al. (2004). The ablation chamber had a volume of $1cm^3$. For analysis of sulfide inclusions 5ml/min of $H_2$ were added to the carrier gas in order to enhance the sensitivity for Au (Guillong and Heinrich, 2007). Analytical parameters of the system are reported in Table 1. Prior and after the analysis of a set of melt inclusions two standards were measured. The external standard used was NIST 610.

Data quantification and uncertainty calculation was done using the Matlab script SILLS( v1.2) and the signal deconvolution and data quantification approach of Halter et al. (2002b) implemented into excel. The formulas used to calculate the element concentrations plus their derivation can be found in the same publication. A linear drift correction was applied using the analysis of the two bracketing standards.

*Table 1: Analytical parameters of LA-ICPMS system*

| | |
|---|---|
| *Laser parameters* | |
| Energy density of sample surface | 8-10J/$cm^2$ |
| Pulse rate | 10Hz |
| He carrier gas flow | He, 1.1L/min |
| $H_2$ carrier gas flow | $H_2$, 5ml/min |
| Pit size[1] | Adjusted to inclusion size |
| *Mass spectrometer parameters* | |
| Nebulizer gas flow | Ar, 0.73L/min |
| Auxillary gas flow | Ar, 0.8L/min |
| Plasma gas flow | Ar, 15.5L/min |
| Plasma Power | 1550W |
| Oxide production rate | ThO/Th <0.5% |
| *Element menu* | |
| Analytes silicate menu[2] | $B^{11}$, $Na^{23}$, $Mg^{24}$, $Al^{27}$, $Si^{29}$, ($P^{31}$), $K^{39}$, $Ca^{42}$, ($Sc^{45}$), $Ti^{47}$, $V^{51}$, $Cr^{53}$, $Mn^{55}$, $Fe^{57}$, ($Co^{59}$), ($Ni^{60}$), $Cu^{65}$, $Rb^{85}$, $Sr^{88}$, $Y^{89}$,( $Zr^{90}$), ($Nb^{93}$), $Cs^{133}$, $Ba^{137}$, $La^{139}$, ($Ce^{140}$), ($Nd^{146}$), ($Sm^{147}$), ($Ho^{165}$), ($Yb^{173}$), $Pb^{208}$, $Th^{232}$, $U^{238}$ |
| Analytes sulfide menu | $Si^{29}$, $S^{32}$, $Fe^{57}$, $Co^{59}$, $Cu^{65}$, $Zn^{66}$, $As^{75}$, $Mo^{95}$, $Ag^{107}$, $Sb^{121}$, $Au^{197}$, $Pb^{208}$ |
| Dwell time | Between 10ms (normal) and 40ms (Au and Cu) |
| RSD of plasma flickering | 0.3% |

[1] The pit size was adjusted for every inclusion to guarantee ablation of the entire inclusion and an optimal ratio of ablated inclusion vs. ablated host (mass factor x)
[2] () Elements not measured during first run due to a readjustment of the element menu

The host, mixed and background windows from the ablation signal were set using SILLS. Using signal intensities and dwell times for a certain element, the composition of the host was calculated in excel using equation 1. Element concentration were obtained after a relative sensitivity factor (RSF) was calculated by normalizing the host to 100% total oxides (equation. 2).

$$C_i^{samp} = \frac{C_i^{Std} * I_i^{Samp}}{I_i^{Std} * RSF} \quad (1)$$

$$RSF = \frac{C_{ox}^{Std} * I_{ox}^{Samp}}{I_{ox}^{Std} * C_{ox}^{samp}} \quad (2)$$

In order to obtain the composition of the melt entrapped in the inclusion the amount of host hit during the ablation has to be subtracted from the mixed signal. This was done using a mass factor x, describing the ratio of ablated inclusion to ablated host (equation 3).

$$x = \frac{m^{Incl}}{m^{MIX}} = \frac{C_i^{Host} - C_i^{MIX}}{C_i^{HOST} - C_i^{INCL}} \quad (3)$$

Re-arranging equation 3 allows the calculation of the concentration ($C_i^{INCL}$) of an element in the inclusion. However, in order to calculate x one element concentration in the inclusion has to be known a priori (internal standard).

*Silicate melt inclusions*

For silicate melt inclusions $Al_2O_3$ was chosen as an internal standard since its variation in the older volcanic suite is the smallest of all major elements (Waite et al., 1997). The assumed $Al_2O_3$ content was based on the average value of published bulk rock chemical data (Table 2).

Water content in all inclusion was assumed to be 4%, based on the presence of Amphiboles and published experimental data (Moore and Carmichael, 1998). Variation in the water content by $^{+}$/- 2% affects the final melt composition within the analytical uncertainty.

Iron was assumed to be present as $Fe^{2+}$. Changing the FeO/(FeO+$Fe_2O_3$) of the melt from 1 to 0 only affect the melt composition marginally, well within the uncertainty. An exception of this are inclusion in the tholeiitic basalt which will be discussed later.

Table 2 shows a summary of the assumed input parameters used to quantify melt inclusions in all samples.

*Table 2: Summary of assumptions used to quantify melt inclusion compositions*

| Sample number | TBC3.1A | TBC13.10A | BV6.2I |
|---|---|---|---|
| Outcrop | Dyke | Lark intrusion | Lava flow |
| Rock | Tholeiitic Basalt | Tholeiitic Andesite | Andesitic Basalt |
| Assumed $Al_2O_3$ conc. | 14.2% | 15.1% | 15.7 |
| Assumed water content | 4% | 4% | 4% |
| FeO/(FeO+Fe2O3) | 1 | 1 | 1 |
| Bulk rock reference | (Stavast et al., 2006) | (Maughan et al., 2002; Waite et al., 1997) | (Maughan et al., 2002; Waite et al., 1997) |

For the andesitic basalt sample the two mineral approach of Zajacz and Halter (2007) was tested because petrographic observations indicate simultaneous growth of clinopyroxene and plagioclase , both hosting Si-melt inclusions. However, the approach was not successful since no intersection of useful element ratios could be obtained for the compositions of melt inclusions in the two minerals.

*Table 3: Effect of varying the internal standard by 1wt% $Al_2O_3$ for a melt inclusion hosted in plagioclase*

| Internal standard variation | | | |
|---|---|---|---|
| $Al_2O_3$ from bulk rock | | Internal standard +1wt% | Internal standard --1wt% |
| | | Deviation | Deviation |
| $SiO_2$ | 60.75 | 0% | 0% |
| $TiO_2$ | 0.31 | 14% | 15% |
| $Al_2O_3$ | 15.69 | 6% | 6% |
| FeO | 4.46 | 14% | 15% |
| MnO | 0.06 | 14% | 15% |
| MgO | 1.91 | 14% | 15% |
| CaO | 3.33 | 12% | 13% |
| $Na_2O$ | 6.87 | 1% | 2% |
| $K_2O$ | 2.63 | 12% | 13% |
| Cu | 81.55 | 14% | 15% |
| Rb | 52.92 | 14% | 15% |
| Sr | 910 | 13% | 14% |
| Y8 | 6.34 | 14% | 15% |
| Zr | 197.1 | 14% | 15% |
| Nb | 20.05 | 14% | 15% |
| Ba | 575.70 | 8% | 9% |
| Cs | 1.125 | 14% | 15% |
| La | 40.94 | 11% | 12% |
| Ce | 62.731 | 12% | 12% |
| Nd | 18.99 | 13% | 13% |
| Th | 9.62 | 15% | 15% |
| U2 | 5.63 | 15% | 15% |
| Ho | 0.31 | 15% | 15% |

Uncertainties in the obtained concentration occur due to background noise in the ICP signal, uncertainty due to counting statistics and the sequential counting of the MS leading to an incomplete sampling. The quantification of each contribution to the overall uncertainty is explained in Halter et al. (2002b) and was included into the calculation of element concentrations in this study.

An additional source of error is the uncertainty on the mass factor x. As illustrated above x is dependent on our initial assumption of the internal standard. Thus the uncertainty on x can only be evaluated by the uncertainty on the calculated concentration of the internal standard, which is our initial assumption. This forbids an analytical quantification of this uncertainty. However, in order to test the sensitivity of the results for a variation in $Al_2O_3$ content, element concentrations were calculated by using the selected internal standard and a deviation of +/- 1%. This variation covers 60% of the entire $Al_2O_3$ content in bulk rocks from the Bingham volcanic suite, excluding the nepheline minette, which were not sampled during this study. From Table 3 it can be seen that a change of the internal standard by 1% does not affect the melt composition significantly. The ratio of $\frac{C_i^{Al \pm 1\ \% Al}}{C_i^{Al\ int.std.}}$ is 15% on average. Thus, the uncertainty on x was not propagated through the quantification.

*Sulfide melt inclusions*

Sulfide melt inclusions were quantified using the same approach explained for silicate melt inclusions. Sulfur was not quantified but a positive peak in the ablations signal was used to identify sulfide melt inclusions. Processing of the inclusions was done assuming that the inclusions are stoichiometric FeS. This assumption is valid since the eutectic point in the Fe-S system is close to a proportion of 50:50, so within the analytical uncertainty of S with our instrumental setup (Barton and Skinner, 1979). For deconvolution of the mixed host-sulfide signal, Si was used as an matrix only tracer.

# 4 Results

## *4.1 Field work*

The volcanic section is dominated by interlayered debris and lava flows with thickness from 1m to tens of meters. They swell and pinch rapidly and are laterally not traceable, defying a stratigraphic classification. In addition the outcrop situation is not good enough to allow to construct a stratigraphic succession. However, volcanics directly east of the mine are most likely stratigraphically below those outcropping in the rose canyon area (Fig. 2). A representative outcrop for the encountered lithologies in Fig. 5.

*Debris flows*

Debris flow mostly have an ashy matrix and contain blocks up to 50cm in size. The matrix content varies from 20% to 80% in different debris flow and even within a single flow by 20-30%. Clasts are mostly of dacitic composition but often heavily altered such that only the magmatic texture is preserved. The highest degree of alteration was found in the lower section of the volcanic rock pile where some blocks of vuggy quartz most likely have been picked up close to the former crater or vent system. Some limestone blocks point to a reworking of older rocks by the debris flows. The textural appearance of the debris flows is dominantly massive. In some places a fining upward sequence can be recognized with debris flow at the base and finer grained pyroclastic deposits on top (Fig. 3). A clear bedding in debris flows is only visible in some ash beds. Finer pyroclastic beds also show internal coarsening upward cycles (Fig. 3).


*Fig. 3 Coarsening upward cycles in ash layers overlying debris flow deposits. The bedding is clearly recognizable and dips with 20° towards SE. The text for general composition of debris flows. (Locatioin on geological map RCX6_4*

*Lava flows*

Lava flows in the mapping area are dominantly basalts and andesites with a reddish to brown weathering color. biotite, plagioclase and amphiboles are the dominating phenocrysts. Pyroxene occurs in subordinate amounts, seldom olivine was found. Amphiboles are often flow aligned. In places epidote alteration and a thick oxidation crust in the lava flows can be found. Structurally lava flows can be subdivided in two categories. Narrow jointed blocky lava flows, and more massive lava flows with a wider spacing of joints, often oriented 90° to each other. Some aa-type lava flows could be found in the northern part of the mapping area (Fig. 4).

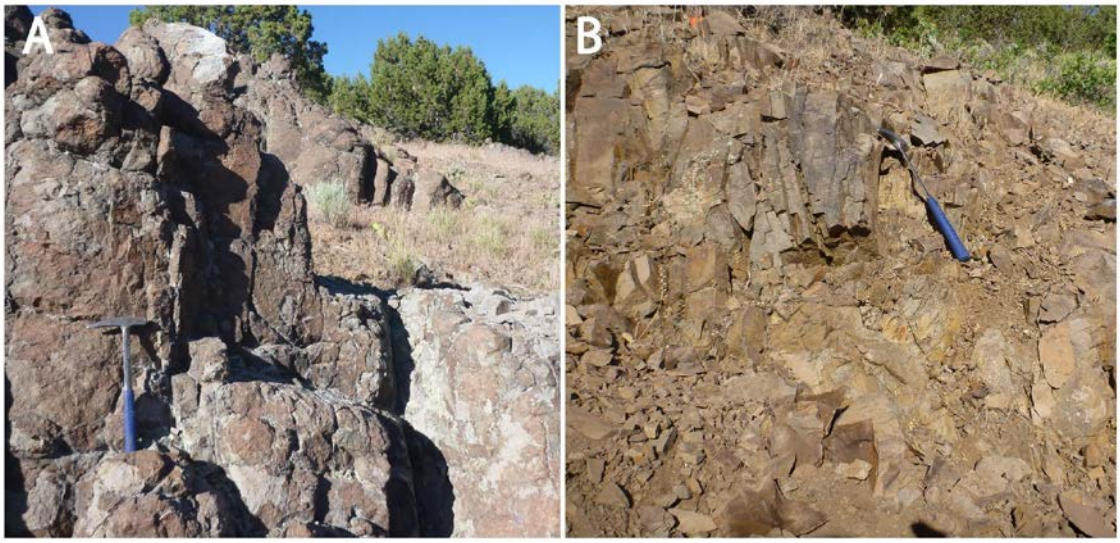


*Fig. 4: Two different types of lava flow in the mapping area that can be distinguished based on their appearance A:. Rounded lava flow in the southern part of the mapping area (Location on geological map – TBCX12_8). B: Blocky lava flow with narrow jointing (Location on geological map – TBCX13_9).*

*Dykes and Plugs*

Near the Bingham mine in Butterfield Canyon a set of porphyry dykes was sampled. Needle like up to 2cm large amphiboles are the dominating phenocrysts. Plagioclase, biotite and clinopyroxenes with oxidized rims occur in smaller amounts. The texture is isotropic and they have a composition ranging from basalt to latiteandesite. Dykes sampled and examined during this study are intruded into Paleozoic limestones.

Two subvolcanic intrusives are exposed in the mapping area. The dacite intrusion of Lark crops out near the entrance of Butterfield canyon (compare map). It is extremely friable and has a porphyric texture. Dominant phenocrysts are plagioclase, biotite and subordinate quartz. A bit south of the Lark intrusive, a quartzlatite plug crops out at shaggy peak (compare map). It has a porphyric texture but in places flow foliated fine grained layers of 1.5-5cm thickness occur. The rock has abundant smoky, euhedral quartz, plagioclase, biotite and alkalifeldspar. The contact to the surrounding lava flows is mostly covered by debris and a precise localization is difficult.

*Orientation data*

Orientation data in the mapping area a sparse since a bedding is normally not visible in the lava and debris flows. However, some ash layers preserve a well visible bedding (Fig. 3). In accordance with published data the measurement indicate a dip of the whole rock pile towards SE with around 20°.

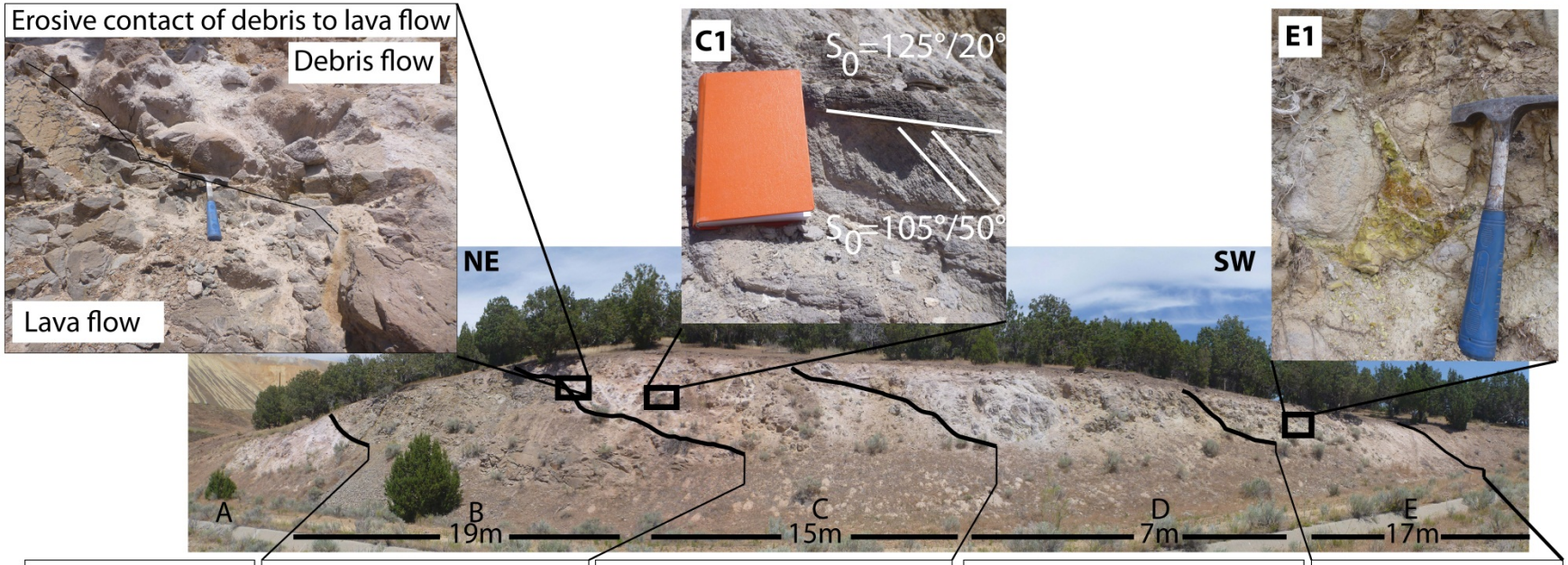


**A**
Blocky ash flow with almost glassy components, grey to black color. Matrix rich with around 60% ashy matrix

**B**
Lava flow of andesitic-dacitic compostion with 1mm phenocrysts of biotite, amphibole and pyroxene. Blocky weathering and homogeneous textural appearance. Handspecimen with 60% of grey matrix.

**C**
Heterogeneous debris flow with erosive base to underlying lava flow. Crossbedding (C1) in finer parts indicates dip and flow direction approximately towards E. Clasts probably of dacitic composition (based on texture) but reddish oxidation is common. Greyish, yellowish and whitish altered clasts occur together. Most minerals are destructively altered.Texture of rock is poorly preserved, best in reddish oxidized blocks. Shape of mm sized amphiboles partly preserved. Ash matrix around 30-40%

**D**
More massive debris flow. Dacitic blocks in ashy matrix are the dominant constituents. Clasts with greyish alteration and reddish oxidation are abundant and occur together with yellowish and whitish, pervasively altered blocks. Blocks range in size from 40cm down to several cm. Matrix content 10-20%

**E**
Same composition as C but without indications of bedding. Clasts include vuggy quartz (E1) and sometimes show a greenish alteration.

*Fig. 5: Representative outcrop showing the encountered geology in the mapping area. Interlayered debris and lava flow of andesitic-dacitic composition dominate.*

*Location on map: BVX5_4; W112°5`51``N40°32`11.5``.*

*4.2 Sample description*

In the following a description of the samples selected for the later melt inclusion study is presented. All samples are highlighted on the geological map. A summary of all outcrops sampled during field work plus the results from optical petrography can be found in an excel table in the digital supplement.

Three rock samples were selected for melt inclusion analysis. During petrographic work on these samples special attention was paid to the crystallization sequence, growth zoning and location of melt inclusions.

*Tholeiitic basalt*

Location on map: TBC3.1A W112°7`28.7`` N40°29`58.4``.

The tholeiitic basalt was sampled from a dyke near Butterfield Canyon. The outcrop shows a reddish-brownish weathering color (Fig. 6A). Stavast et al. (2006) classified the rocks as latite, close to the border of andesite, dacite and trachyte in the TAS diagram. However, with almost 70% of all phenocrysts being mafic the examined rock clearly classifies as basalt according the Streckeisen classification.

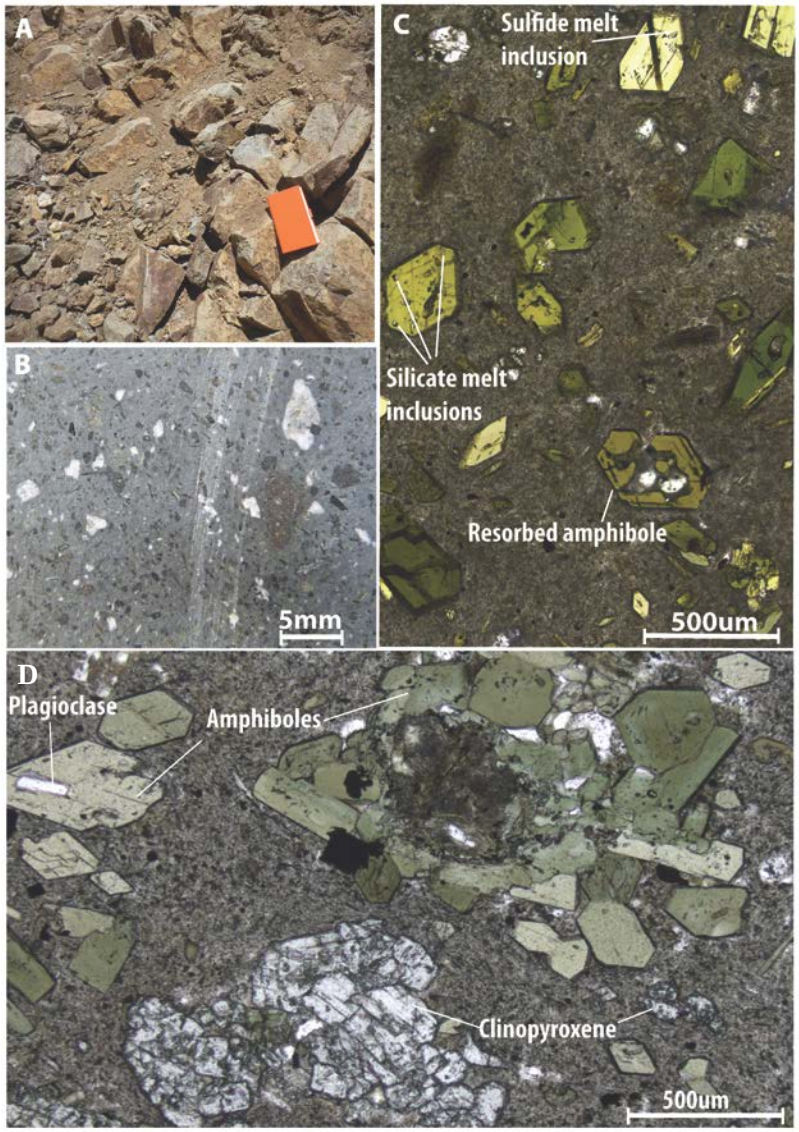


*Fig. 6: A: Outcrop location of tholeiitic basalt close to mine tailings. See geological map for location. B: Hand specimen with plagioclase, amphibole and pyroxene phenocysts. Plagioclase is poorly preserved in thin sections. C:Thin section picture of tholeiitic basalt. Resorbed amphiboles can be found. Melt inclusions do not show different compositions in light yellow amphiboles and dark green hornblends. D: Plagioclase inclusions in amphiboles and cumulates of amphiboles and clinopyroxenes.*

The hands pecimen is porphyric with tabular plagioclase and needle shaped amphiboles (up to 2mm, compare Fig. 6B). Pyroxenes hav a grey color.

In the thin section, the dominating phenocrysts are euhedral amphiboles (Fig. 6C), up to 2.1mm with abundant inclusions of biotite and plagioclase, often along outer growth zones (Fig. 6D). Titanite and apatite also occur as inclusions. A strong zoning can be recognized in some amphiboles. Broken amphiboles are often intruded by the cryptocrystalline matrix and resorption textures can be found (Fig. 6C). Amphiboles are mostly dark green hornblends and some yellow-brownish amphiboles ( possibly oxyhornblends) (Fig. 6C).

Subhedral to anhedral clinopyroxenes account for around 30% of the phenocrysts. Their size averages at 0.5mm and they experienced intense fracturing evident from former crystals now broken into piece. The rims of clinopyroxens sometimes show a chloride alteration and they occur in cumulates with amphiboles (Fig. 6D). Plagioclase is up to 3.5mm in diameter. It shows a strong sericitization along fractures and has pronounced growth zones. Quartz accounts for 5% of the phenocrysts and can contain inclusions of amphibole. The presence of large calcite crystals in a nearby dyke (TBC3_2d), might indicates assimilation of country rock.

The crystallization sequence is evident from mineral inclusions and intergrowth textures. Pyroxenes, amphiboles and possibly plagioclase crystallized together, although inclusions of plagioclase in amphibole might point to an earlier growth of the latter. Quartz is the last mineral to crystallize.

Opaque minerals are abundant in the matrix and to a lesser extent as inclusions in rock forming minerals. Magnetite with hematite rims is dominating. It occurs mostly in the matrix rarely in amphiboles but never in plagioclase. Pyrrhotite is the most common sulfide and is found in amphiboles and rarely plagioclase. It can also occur as an inclusion in magnetite. In few cases pyrrhotite is associated with chalcopyrite which also occurs as inclusions in amphibole together with pyrite (Fig. 7D).

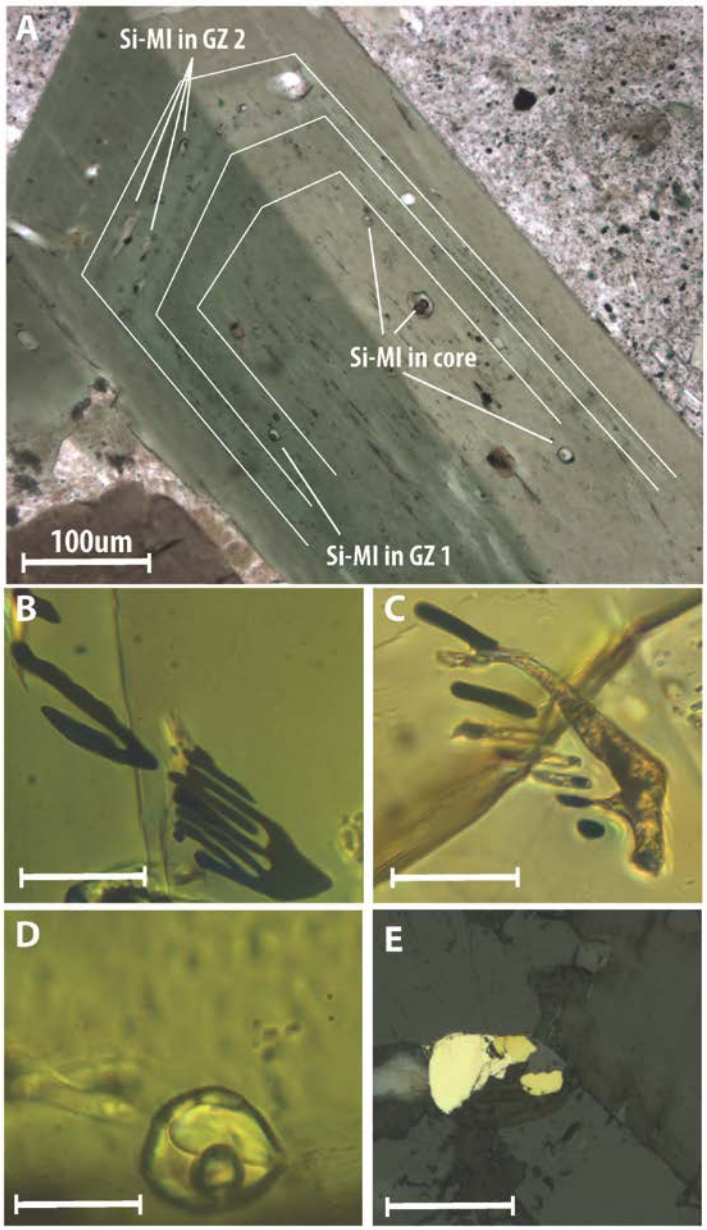


*Fig. 7: A. Melt inclusion along growth zones(GZ) in amphiboles. In the analyzed samples no systematic variation of inclusion composition in different growth zones could be observed. B: Sulfide melt inclusions trapped as liquid phase. C. Mixed silicate sulfide melt inclusions. D: Crystallized melt inclusion with coexisting bubble and liquid phase. E: Sulfide inclusion in reflected light showing pyrite and chalcopyrite. All scale bars in B,C,D, E are 20um.*

Melt inclusions analyzed in this sample were preserved in amphiboles. No suitable inclusion for LA-ICPMS were found in pyroxenes and plagioclase. Inclusions in amphiboles occur along growth zones, as assemblages in the center of the mineral or as individual inclusions (Fig. 7A). They sometimes co-exist with tiny fluid inclusions. A variety of different inclusion can be identified by optic petrography. They can be either finely or coarsely crystallized or largely glassy and some inclusions have glassy and crystallized parts. Inclusions are in most cases bubble bearing and bubble volumes range from 5-20%, in some rare cases can be up to 30%. Bubbles are often deformed. In some cases inclusions have an entrapped fluid phase coexisting with the vapor bubble (Fig. 7D). The presence of opaque daughter phases is common

and always along the inclusion boundary. There can be several daughter phases in one inclusion. Some inclusions are free of opaque phases. Host crystallization along the inclusions wall is evident in some cases.

Sulfide inclusions (Fig. 7B) are trapped together with silicate melt inclusions in amphiboles. The shape of sulfide inclusions indicates entrapment as a liquid phase. Sulfide and silicate melt inclusions occur next to each other. In one case sulfide and silicate melts where together entrapped in one mixed, silicate-sulfide melt inclusion (Fig. 7C)

*Tholeiitic andesite*

Location on map: TBC 13.10A, W112°`5`12.1`` N40°30`50.2``

The Lark sample has a very friable texture in outcrop and hand specimen (Fig. 8A). The weathering in outcrop is rounded. It is porphyric and biotite, amphiboles and plagioclase are visible phenocrysts. The matrix is grey and fine grained (Fig. 8b). Euhedral plagioclase (up to 3mm, 25%) is the main mineral in the Lark sample. Intergrowth of different plagioclase crystals are abundant and a sieve texture is common (Fig. 8D). Zircons occur as inclusions. Biaxial quartz (1.5mm, 5%) is xenomorph, has inclusions of amphiboles and characteristic embayments intruded by matrix, possibly due to a resorption of the mineral indicating disequilibrium conditions after crystal growth (Fig. 8C). Oxyhornblends (1mm, 3%) are zoned and have numerous apatite inclusions. Along the rims and cleavage they show clay alteration. Euhedral biotite (3mm,

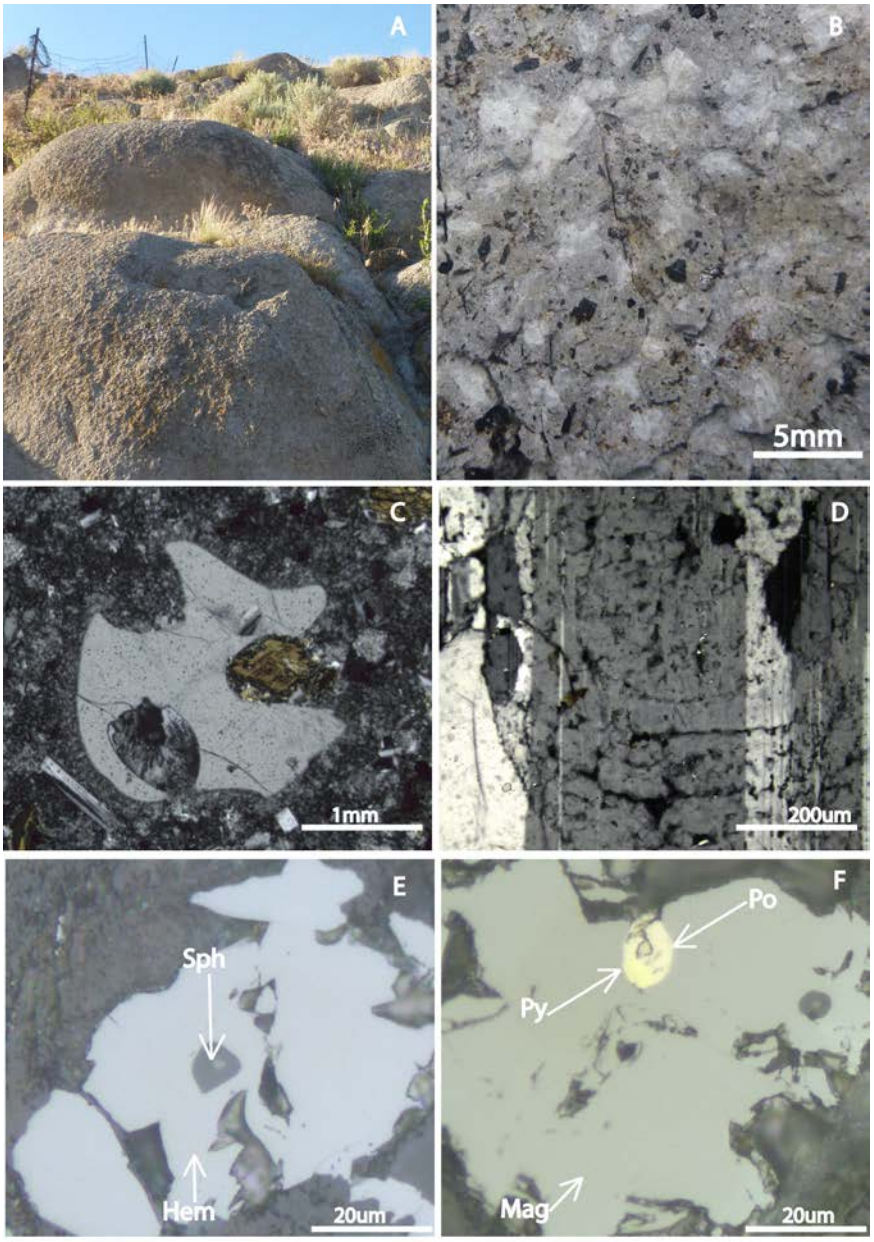


*Fig. 8: Tholeiitic andesite of Lark. A:Outcrop location marked on the map. Extremely friable texture and a rounded weathering is characteristic in this place. B: Hand specimen with visible plagioclase (white), amphiboles and biotite. Quartz occurs in subordinate amounts. C: Resorbed quartz. D: Sieve textures in plagioclase. .E: Sphalerite inclusions in hematite. F: Sulfide inclusion with pyrite and pyrrhotite in magnetite.*

8%) with apatite inclusions is the most abundant mafic mineral.
Opaque minerals in the Lark sample is almost exclusively magnetite with hematite rims. It occurs in fractures of minerals and in the matrix. Sulfides present are pyrrhotite, sphalerite and pyrite. Sphalerite is found in corroded amphiboles and is associated with hematite (Fig. 8E). Pyrrhotite is extremely rare but seldom 1-2um sized inclusions are found in plagioclase sometimes with rims of chalcopyrite. Occasionally pyrite occurs together with pyrrhotite in hematite (Fig. 8F). Due to the rarity and small size no suitable sulfides were found for laser ablation.

Melt inclusion in the Lark sample are numerous in plagioclase and quartz (Fig. 9). They occur in the core (Fig. 9A), and along growth zones in plagioclase (Fig. 9B), can be glassy, finely and coarsely crystallized or a show both, finer and coarser crystallized parts. Inclusions of different types co-exists

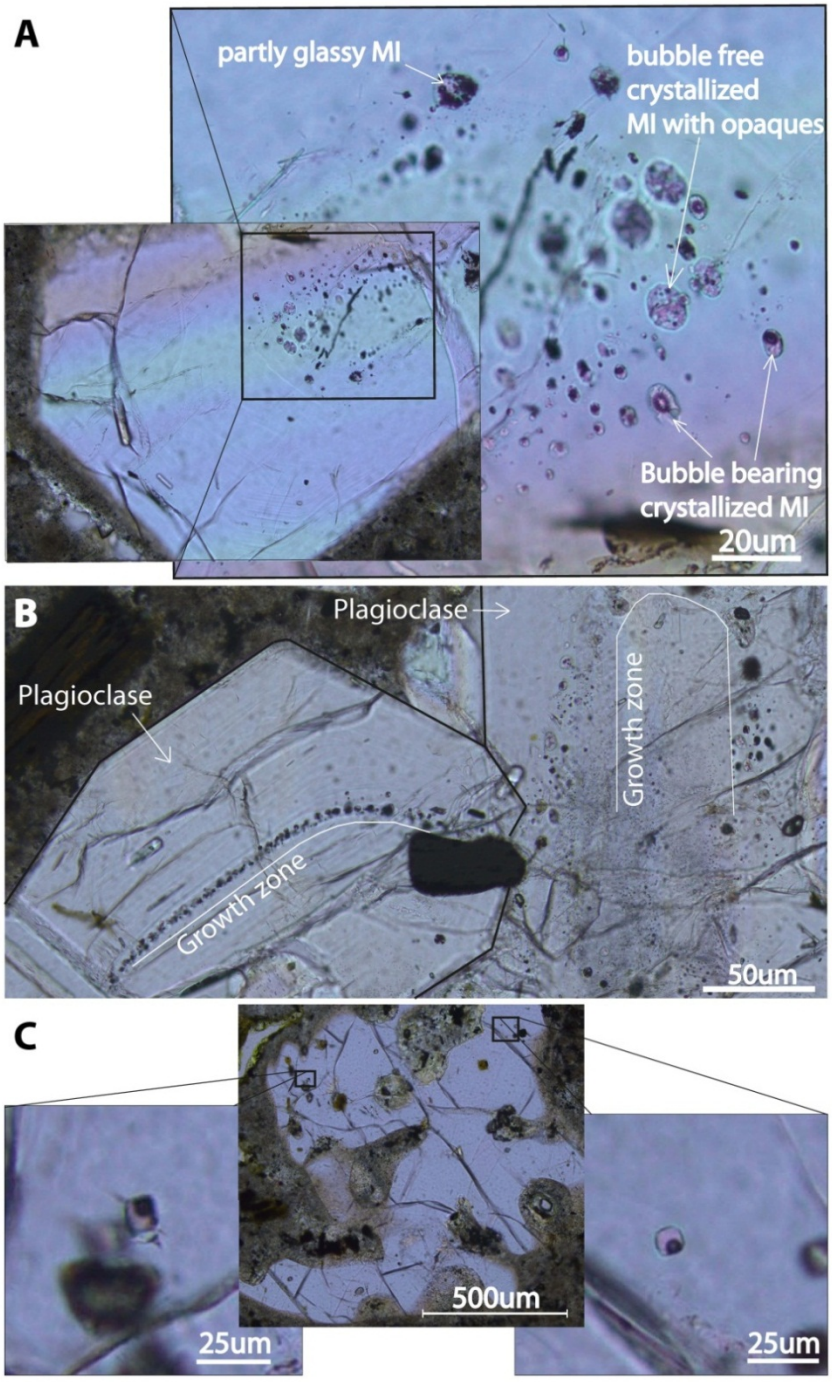


*Fig. 9: Thick section photographs: A: Melt inclusions of different types co-exists in the core of a plagioclase crystal. B: Melt inclusions mostly occur along growth zones and in the core of plagioclase. C: Melt inclusions in resorbed quartz indicating a magmatic origin and out of equilibrium conditions after crystals growth*

in assemblages (Fig. 9A). Melt inclusions can contain several opaque daughter phases. Bubbles range in volume from 5-25% and are often deformed. The shape is often rounded, but especially along growth zones they can be rectangular and irregular. They range in size from some um to 100um.
Melt inclusions in quartz are coarsely crystallized and bubble bearing (Fig. 9C). The presence of melt inclusions points to the magmatic origin of quartz. Unfortunately melt inclusions in quartz could not be analyzed due to dissolution of the sample while cleaning with aqua regia.

*Andesitic basalt*

Location on map: BV6.2I, W112°5`49.4`` N40°33`8.1``

The andesitic basalt was sampled from a lava flow which overlies a debris flow. It has a blocky appearance and reddish weathering color (Fig. 10A). The hand specimen has large plagioclase phenocrysts and small pyroxenes. Amphiboles appear rusty but have a distinct elongated shape. Greenish minerals could be saussuritizised plagioclase or epidote (Fig. 10B). The matrix is not distinguishable with the hand lens, but has a greyish-greenish color.

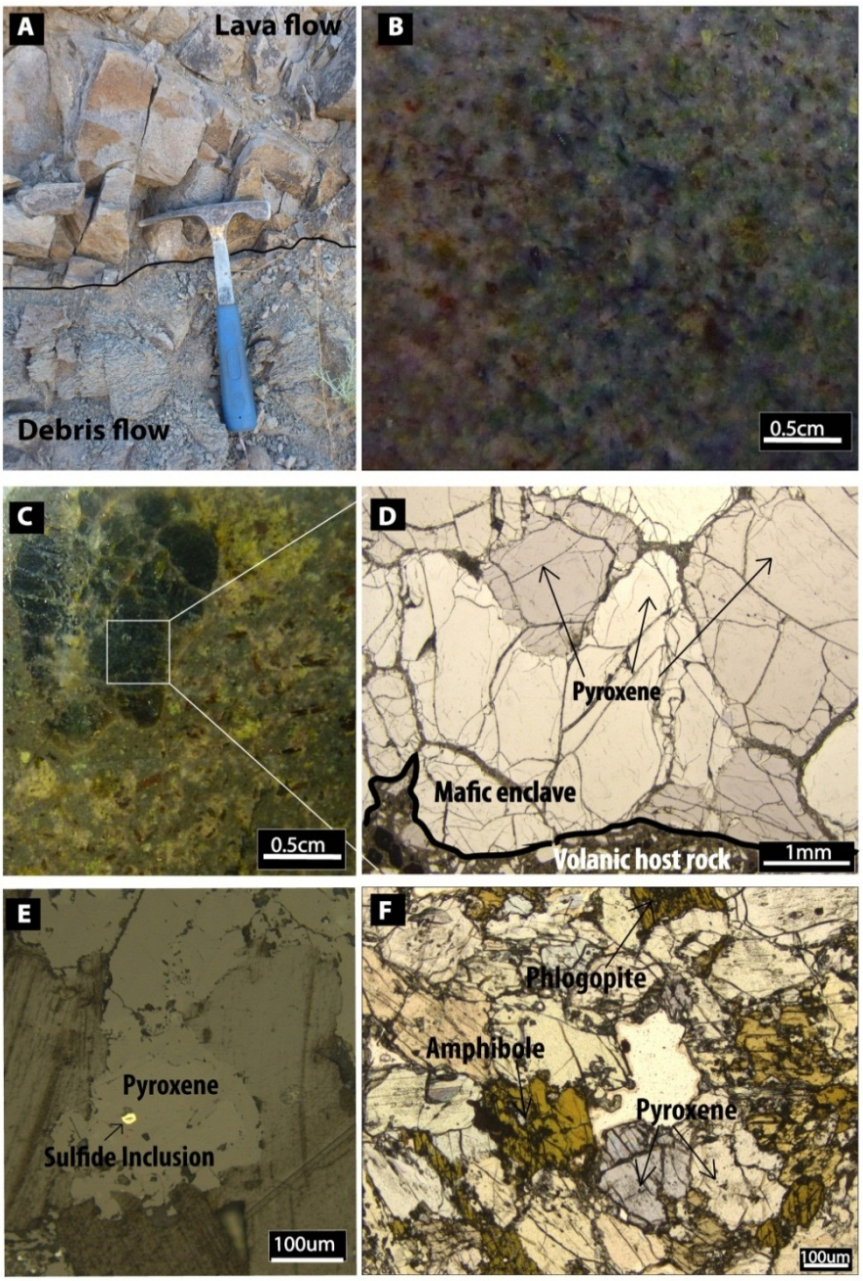


*Fig. 10: A: Sample location for the andesitic basalt. The sample as taken from a lava flow overlying debris flow deposits B. Photography of hand specimen showing greenish color originating from saussuritizised plagioclase or epidote. C: Mafic enclave in a neighboring lava flow contains almost exclusively orthopyroxenes. D:. Orthopyroxenes in mafic cumulates have sulfide inclusions. F: Mafic cumulate with pyroxene amphiboles and most likely phlogopite.*

The thin section is dominated by euhedral zoned and sometimes sieve textured plagioclase (1.5mm, 20%). Clinopyroxens (1mm, 8%) are the main mafic phase, appear oxidized along the rims and show inclusions of opaques. Clinopyroxens have intergrowth textures with plagioclase, indicating the simultaneous crystallization (Fig. 11A). Biotite (1mm, 5%) and amphibole (1mm, 2%) are heavily altered, brown in color and in most cases only relicts are left.

A nearby lava flow of the same composition was rich in mafic enclaves

(Fig. 10C,D,F). The mafic enclaves varied in composition but generally contain orthopyroxenes, brown amphiboles and mica, likely phlogopite, and variable amounts of interstital plagioclase. All mafic minerals are euhedral in shape and around 1mm in size. Phlogopite can show intergrowth with pyroxenes and inclusions of pyroxene in amphiboles and vice versa, point to a simultaneous crystallization of all mafic phases. Amphiboles often have oxides rims and are sieve textured.
One enclave almost exclusively contained orthopyroxenes (Fig. 10D)with up to 5mm large crystals.
Opaque minerals are dominantly magnetite and hematite, mostly located in the matrix but also present in pyroxene and plagioclase.
Sulfide inclusions are around 2um in size. They are found in pyroxene. Noteworthy, as discussed later, is the presence of sulfide inclusions in orthopyroxenes in a mafic cumulate next to the sample location (Fig. 10E).

Melt inclusions occur in plagioclase and clinopyroxenes and range in size from 20-30um. In plagioclase they occur along growth zones and are glassy or coarsely crystallized with several inclusions of daughter phases (Fig. 11B). They show complex elongated shapes and are partly rectangular. The complex overlap and shape of inclusions in growth zones makes an analysis of a single inclusion without partly ablating the neighboring one difficult. Inclusions in the mineral center are generally rounded
Inclusions in clinopyroxens are almost exclusively coarsely crystallized and contain a bubble of around 10% of the inclusion volume. One or more opaque daughter phases are found in almost every inclusion along the margin. Generally, inclusion in plagioclase and pyroxene differ significantly in their appearance (Fig. 11C,D).
In addition melt inclusions in orthopyroxenes from the mafic cumulate were found but not analyzed.

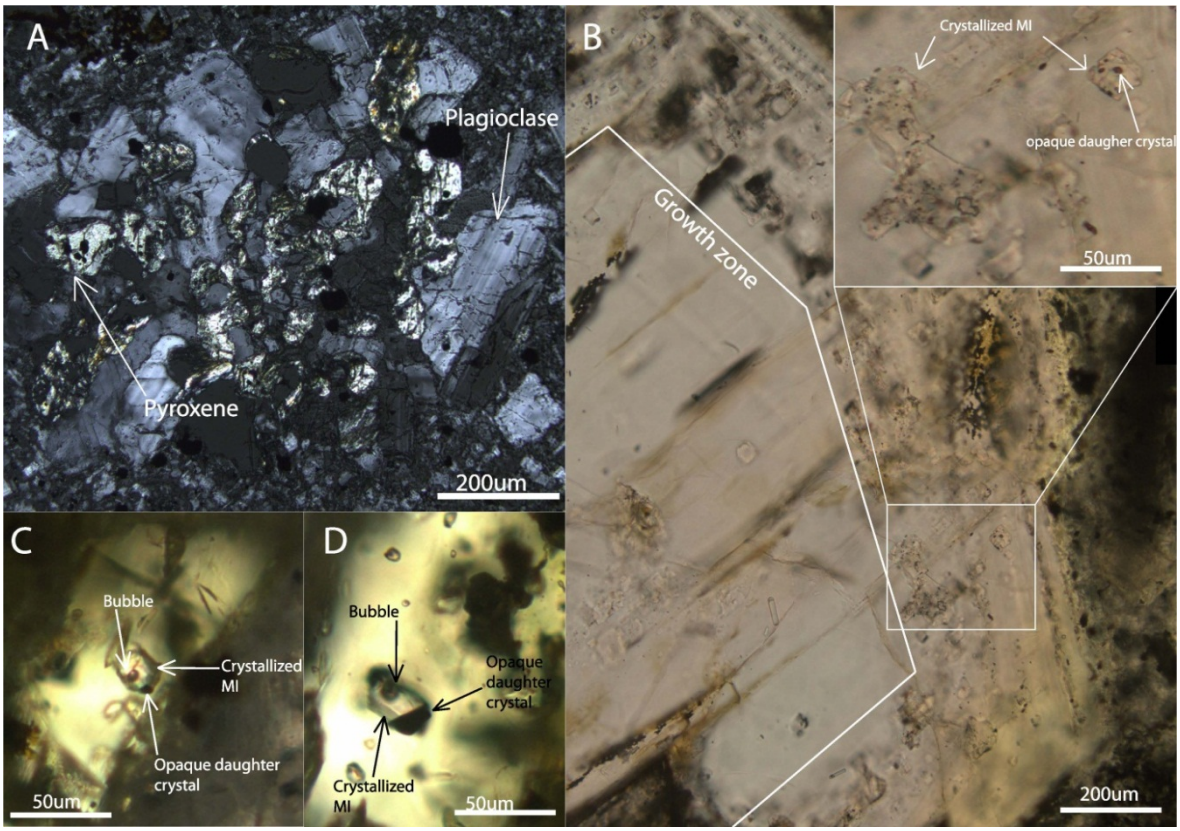


*Fig. 11: Andesitic basalt samples from lava flow. A: Intergrowth texture of plagioclase and amphibole indicate simultaneous crystallization. B: Melt inclusions in plagioclase are crystallized and generally occur along outer growth zones. They have an irregular shape and they often contain several small opaque daughter phases but no bubbles. C and D: Melt inclusions in pyroxene are crystallized, have opaque daughter phases and are bubble bearing.*

*4.3 Depletion of amphibole-hosted Si-melt inclusions*

As described in section 3.3 processing of melt inclusions was done by assuming an $Al_2O_3$ concentration in the melt inclusions derived from bulk rocks. Half of the inclusions of the tholeiitic basalt sample could not be processed using this internal standard, meaning the obtained inclusion to mixed-signal ratio (equation 3) was larger than one, which is not possible. This problem could be overcome by changing the internal standard. Surely those inclusions cannot be used for the later interpretation since a constant internal standard within one set inclusions is the basic assumption of the whole approach. However, since the possibility of post entrapment modification has been reported in the literature (Spandler et al., 2007) it is of great interest if lowering the $Al_2O_3$ content is actually correlated with a real decrease in the $Al_2O_3$ concentration in the inclusion. Two lines of evidence suggest that this is the case and that the composition of the inclusions was actually modified after entrapment.

Firstly, inclusions where a suitable x could only be obtained by lowering the $Al_2O_3$ considerably below the host concentration (≤10%) indeed show a lowering of the Al concentration in the mixed ablation signal compared to the host (Fig. 12). In addition to a depletion of Al, the negative spikes of nearly all other elements, especially those which are normally enriched is striking. The negative spike cannot be related to changes in ablation efficiency since element like Si stay constant.

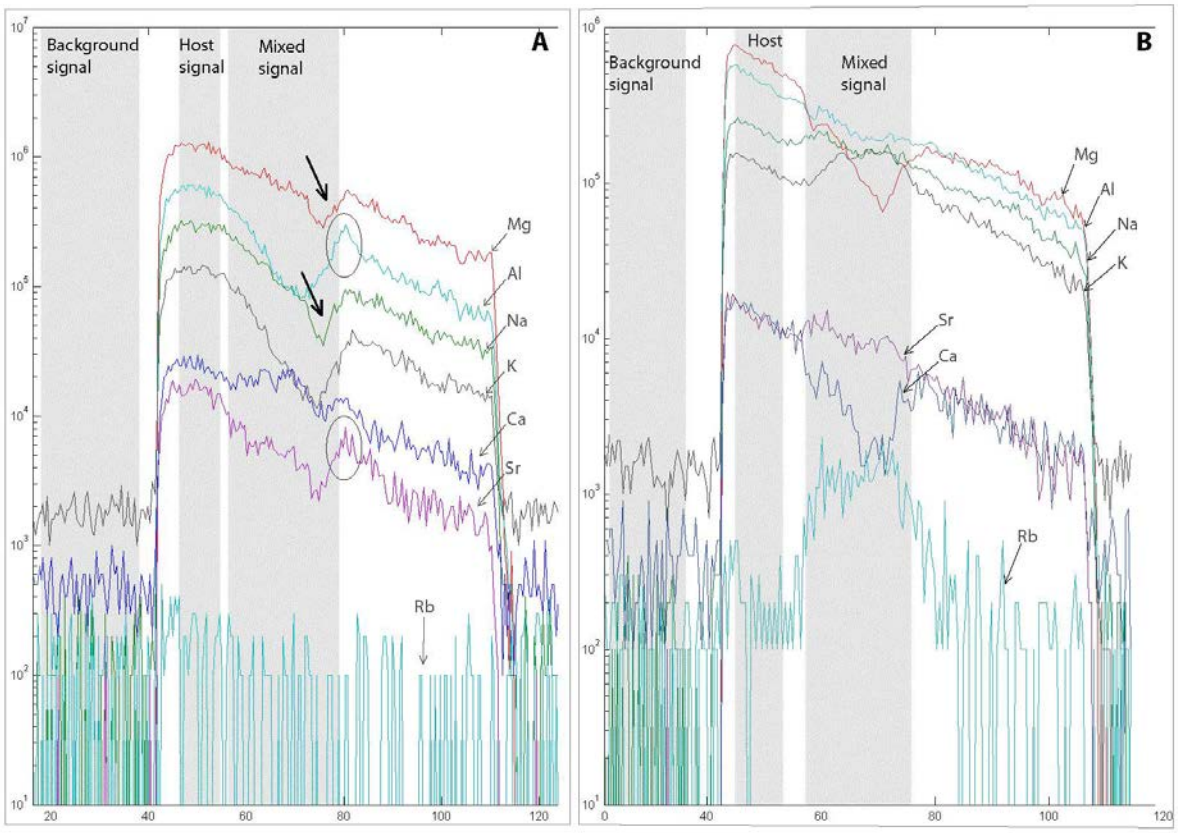


*Fig. 12: A: LA-ICPMS signal of depleted melt inclusion in tholeiitic basalt. The negative spike of Al relative to the host is clearly visible. Average host concentration 11% $Al_2O_3$. Note the conspicuous depletion of Mg, Sr and Na (arrows) and the constant Ca signal. Enriched Al and Sr host signals in the vicinity of the inclusion can be observed in some inclusions (ovals). B: LA-ICPMS signal of inclusion with $Al_2O_3$ content corresponding to bulk rocks. Enrichment of Rb and K is characteristic, depletion of Ca and Mg as well. U and Th are also generally enriched (not shown).*

Secondly considering equation 3, we can subdivide between two cases. First, a constellation where $C^{Host} > C^{Incl}$ and the second where $C^{Host} < C^{Incl}$.
For the first case, x becomes larger than 1 if $C^{Incl} > C^{Mix}$ which is not possible since this would imply $C^{Host} > C^{Incl} > C^{Mix}$. X becomes 1 if $C^{Incl} = C^{Mix}$. Thus, a suitable x between 0 and 1 can only be obtained by lowering the $C^{Incl}$ justified by the negative spike in the ablation signal. The first value for which a suitable x is obtained represents a maximum value for x (equation 3). Consequently, concentrations obtained with that x, are upper limits in the case of element which show a negative spike ($C^{Incl} < C^{Host}$) in the inclusion signal, and a lower limit for those which show a positive spike ($C^{Incl} > C^{Host}$) in the inclusion signal (compare equation 4).
In the second case, the argumentation is exactly the same but vice versa, with the results that for elements with a positive spike obtained concentrations are lower limits, for those with a negative spike upper limits.

$$C_i^{Incl} = C^{Host} - \frac{C_i^{Host} - C_i^{Samp}}{x} \quad (4)$$

The reason, mechanisms and extent for the depletion is unknown and it is beyond the scope of this thesis to evaluate it. However, this observation might contribute to the ongoing discussion in the scientific community to which extent post entrapment modification occurs in melt inclusions.
What can be said is that $Al_2O_3$ variations occur within one inclusion assemblage petrographic appearance of the inclusion (Fig. 13). In addition inclusions with very low $Al_2O_3$ contents show an enriched or at least constant Ca signal compared to the unmodified inclusions (compare Fig. 12A and B). Host enrichments in the direct vicinity of modified inclusions are rare, but have been observed (Fig. 12A).

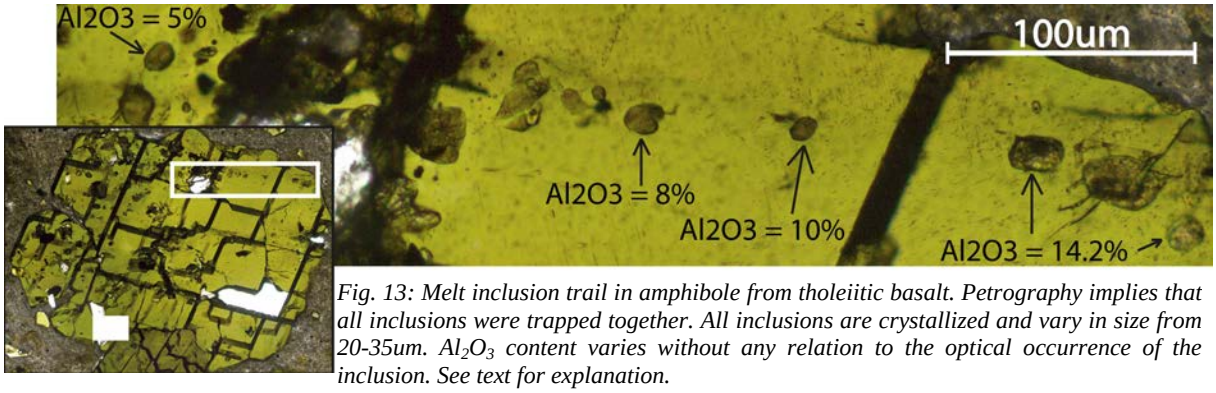


*Fig. 13: Melt inclusion trail in amphibole from tholeiitic basalt. Petrography implies that all inclusions were trapped together. All inclusions are crystallized and vary in size from 20-35um. $Al_2O_3$ content varies without any relation to the optical occurrence of the inclusion. See text for explanation.*

The obtained concentrations for the inclusions with an Al2O3 below 10% compared to those with an internal standard derived from bulk rocks are displayed in Fig. 15 and Fig. 14
In Fig. 15 it can be seen that the range of concentration for certain elements largely overlaps for both types of inclusions (mostly major oxids, especially $Na_2O$), for other it is notable different (most trace elements, especially V, Sr, Ba,Rb and Th). But, considering Fig. 14A and B, it is well illustrated that the compositional variation for the unmodified inclusions have the same trend as the bulk rocks from the Bingham volcanic suite. In contrast to that, the variation for the modified inclusions does not show this correlation. This clearly shows, that even if the concentrations of some elements in the modified and unmodified inclusions overlap, element ratios differ significantly.

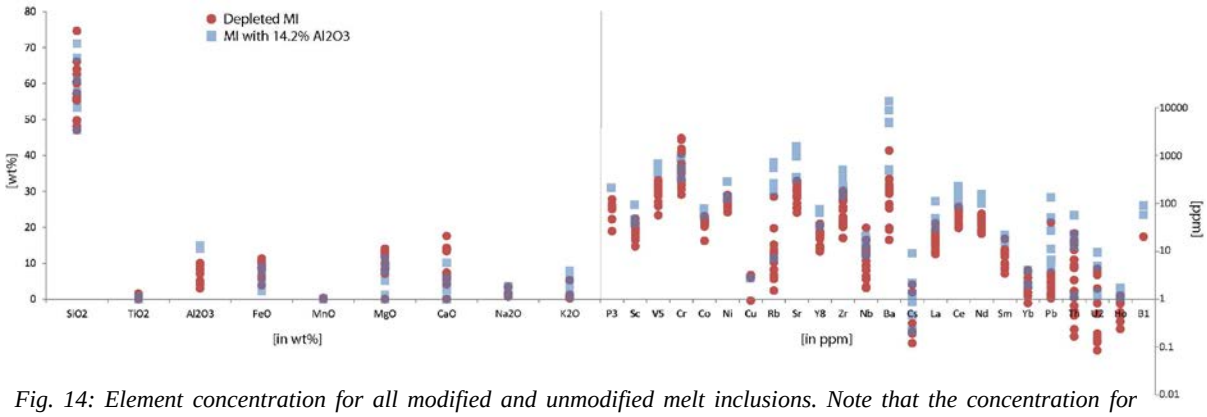


*Fig. 14: Element concentration for all modified and unmodified melt inclusions. Note that the concentration for modified inclusions was obtained using an upper limit value for x implying that for nearly all elements the displayed concentrations are also upper limits, see text for explanation. The compositional range overlaps largely for major elements, however trace elements show a general shift of depleted inclusions towards lower concentration values.*

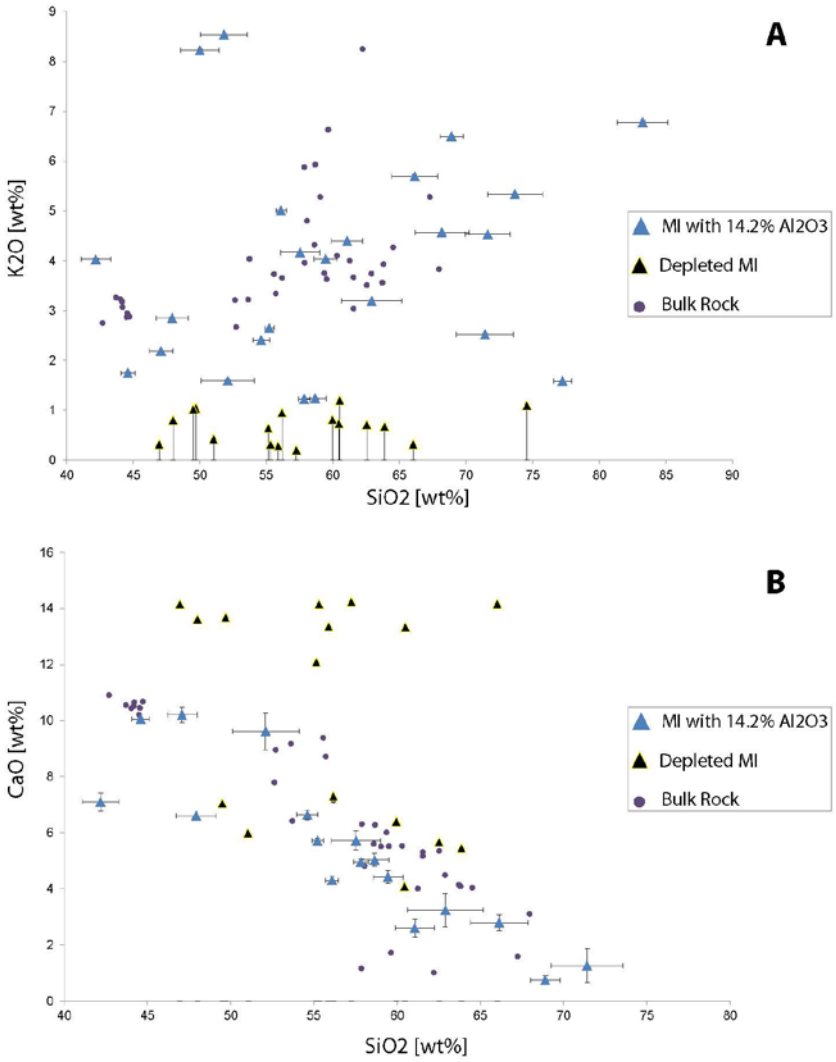


*Fig. 15: Cross plot of $SiO_2$ vs. $K_2O$ and CaO for depleted and unmodified MI. Although the compositional variation between both inclusion types overlap for most major elements the concentration ratios within the modified inclusions have change considerably. A: Modified inclusions are depleted in mobile LILE elements like K. Displayed concentrations are upper limits for modified inclusions (see text for explanation). B: The concentration range of depleted and undepleted inclusions overlaps for several elements. However, the range in the undepleted inclusions closely follows the bulk rock trend, whereas the variation in the depleted inclusions is completely random. Note that the concentrations for Ca are tendentially upper limits since Ca is enriched in the LA-ICPMS signal in depleted inclusions compared to unmodified ones.*

As mentioned, the outlines above only account for inclusions were $Al_2O_3$ had to be lowered below 10%. Several other inclusions could not be processed either, but it was sufficient to lower to $Al_2O_3$ content slightly by 1-3%, so down to 10-13%. Those inclusions did not show a negative spike in the ablation signal but most likely their lower $Al_2O_3$ content also reflects a true depletion. This fact will be picked up later.

*4.4 Host compositions*

Compositions of the host minerals in which MI were analyzed are shown in table Table 4. Amphiboles from the tholeiitic basalt have an average $SiO_2$ content of 46wt%. They have the most primitive character with the highest values of compatible elements (Cr, Ni, V) compared to the other host minerals. Cu is below detection limit.

Plagioclase compositions in the tholeiitic andesite from Lark and the andesitic basalt are similar for all major oxides. The same accounts for most trace elements. However, Cu, Rb, Ba, Pb, La, Ce are a bit higher concentrated in the plagioclase from the andesitic basalt. There is a conspicuous bimodal distribution with one set of plagioclase having Ba concentrations of around 300ppm and the other set of with around 1200ppm. Both concentrations were measured in the same plagioclase crystal in the same growth zone, implying a heterogeneous mineral composition.

Clinopyroxene have a bit higher Ca than Mg concentrations and generally an intermediate composition. They are the most Cu rich host minerals with around 11ppm Cu.

*Table 4: Average composition and standard deviation for melt inclusionhost minerals in the three analyzed rock samples. Number of analysis for averages: Tholeiitic basalt 15, tholeiitic andesite 15, andesitic basalt (Plag 10; Px 14). x = below limit of detection*

| | Tholeiitic basalt Average conc. amph in [wt%] | *Std. Deviation* | Tholeiitic andesite Average conc. plag in [wt%] | *Std. Deviation* | Basaltic andesite Average conc. plag in [wt%] | *Std. Deviation* | Average conc. cpx in [wt%] | *Std. Deviation* |
|---|---|---|---|---|---|---|---|---|
| $SiO_2$ | 46.80 | 2.35 | 63.21 | 1.85 | 62.93 | 1.31 | 56.26 | 1.25 |
| $TiO_2$ | 1.37 | 0.26 | 0.01 | 0.00 | 0.01 | 0.01 | 0.24 | 0.06 |
| $Al_2O_3$ | 11.48 | *1.42* | 23.12 | *1.19* | 23.42 | *1.05* | 1.33 | *0.27* |
| FeO | 14.22 | *1.21* | 0.17 | *0.04* | 0.32 | *0.04* | 9.24 | *1.32* |
| MnO | 0.21 | *0.04* | 0.00 | *0.00* | 0.00 | *0.00* | 0.27 | *0.03* |
| MgO | 12.70 | *1.11* | 0.01 | *0.02* | 0.02 | *0.00* | 13.70 | *0.68* |
| CaO | 10.02 | *1.16* | 5.14 | *0.42* | 5.26 | *0.37* | 18.39 | *1.53* |
| $Na_2O$ | 1.89 | *0.21* | 7.55 | *0.54* | 6.70 | *0.32* | 0.54 | *0.09* |
| $K_2O$ | 1.32 | *0.26* | 0.80 | *0.09* | 1.33 | *0.25* | 0.03 | *0.07* |
| | in [ppm] | | in [ppm] | | | | | |
| P | 104.88 | *36.58* | 44.75 | *14.14* | 46.76 | *21.86* | 275.69 | *305.99* |
| Sc | 39.47 | *9.15* | 0.54 | *0.05* | 1.07 | *0.17* | 45.88 | *18.32* |
| V | 343.65 | *63.35* | x | *x* | x | | 168.08 | *40.79* |
| Cr | 676.75 | *669.07* | x | *x* | x | | 364.70 | *511.33* |
| Co | 55.47 | *8.11* | x | *x* | 0.60 | | 51.02 | *10.80* |
| Ni | 123.43 | *69.50* | 2.34 | *1.12* | 1.02 | *0.39* | 116.48 | *33.83* |
| Cu | x | *x* | 1.74 | *0.35* | 4.38 | *2.19* | 10.89 | *6.89* |
| Rb | 6.71 | *5.54* | 2.78 | *2.22* | 7.80 | *2.97* | 5.33 | *6.71* |
| Sr | 280.33 | *74.65* | 1898.56 | *149.99* | 1748.69 | *296.85* | 59.68 | *7.40* |
| Y | 32.34 | *9.15* | 0.16 | *0.14* | 0.44 | *0.33* | 39.57 | *7.18* |
| Zr | 74.49 | *18.99* | 2.68 | *3.63* | 1.22 | *1.24* | 48.11 | *13.13* |
| Nb | 11.29 | *2.93* | 0.27 | *0.37* | 0.14 | *0.12* | 0.22 | *0.26* |
| Ba | 325.16 | *121.64* | 564.69 | *97.35* | 837.82 | *468.72* | 9.73 | *17.20* |
| Cs | x | *x* | 0.22 | *0.28* | 0.09 | *0.05* | 0.16 | *0.22* |
| La | 29.48 | *9.06* | 4.45 | *1.04* | 26.30 | *9.55* | 32.14 | *7.36* |
| Ce | 91.74 | *27.35* | 5.16 | *1.07* | 26.94 | *10.46* | 109.27 | *21.54* |
| Nd | 64.44 | *18.71* | 1.13 | *0.35* | 4.66 | *2.43* | 82.03 | *14.65* |
| Sm | 12.61 | *3.16* | 0.29 | *0.23* | 0.53 | *0.04* | 16.93 | *3.67* |
| Yb | 3.70 | *1.72* | 0.14 | *0.04* | 0.10 | *0.05* | 3.54 | *1.25* |
| Pb | 3.44 | *1.69* | 21.84 | *4.17* | 37.96 | *1.66* | 1.87 | *1.13* |
| Th | 0.51 | *0.43* | 0.30 | *0.43* | 0.25 | *0.29* | 0.60 | *0.38* |
| U | 0.14 | *0.12* | 0.22 | *0.30* | 0.06 | *0.05* | 0.23 | *0.25* |
| Ho | 1.26 | *0.31* | 0.02 | *0.01* | 0.03 | *0.02* | 1.59 | *0.38* |
| B | 51.89 | *10.16* | 23.36 | *1.89* | x | | x | |

*4.5 Classification of melt inclusion composition*

In the following inclusions which could not be processed using the internal standards of Table 2 were not considered. (39 melt inclusions out of 79 analyzed in amphiboles). In order to guarantee representative melt composition, only inclusions with a mass ratio higher than 0.2 in amphiboles and plagioclase were considered. In pyroxene hosted MI the value was chosen to be 0.15, since only 4 inclusions had a mass ratio larger than 0.2 (see discussion).

Since we are dealing with melts, strictly speaking a classification according to a nomenclature developed for rocks is not valid. But, in order to get a feeling for the chemical composition it is useful to do so, since putting a certain name on the inclusion composition gives a better feeling for their chemistry than concentration numbers.

As evident from Fig. 16 the analyzed melt inclusions span a wide range of composition with regard to $SiO_2$.

Inclusions analyzed in the tholeiitic basalt basically follow the bulk rock trend defined by the Bingham volcanic suite. They range from 44wt% $SiO_2$ to around 80%wt $SiO_2$ but the majority of the analyzed inclusions is of intermediate and acidic composition. Variation in alkali content is also large with the lowest inclusions having around 2wt% $Na_2O + K_2O$, the highest around 11%. But these cases are

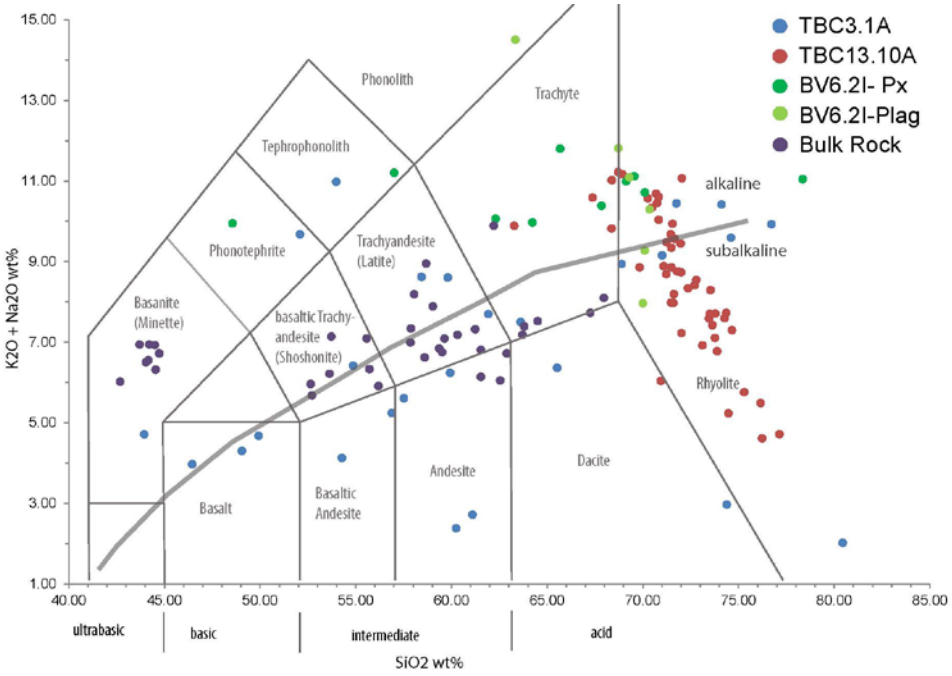


*Fig. 16: TAS diagram for classification of melt inclusion composition. Subdivison of alkaline vs. subalkaline after Irvine and Baragar (1971). Normalized to 100% volatile free basis. Names after the IUGS. In brackets names used in other studies on Bingham volcanics (Maughan et al., 2002; Waite et al., 1997).*

outliers from an otherwise well-defined trend from low to high $SiO_2$ with increasing alkali content along the alkaline sub-alkaline boundary. The inclusions straddle the borders between the basaltic-trachyandesite, trachyandesite, basaltic andesite, andesite and dacite field in the TAS diagram. Some samples with high $SiO_2$ are classified as rhyolite melts

Inclusions in the tholeiitic andesite from Lark have a rather uniform composition with regard to their $SiO_2$ content. They range from around 68% to about 77wt% $SiO_2$ which is a rhyolite melt. In contrast to that their alkali content is variable from 4wt% up to 11wt%, but the majority would classify as sub-alkaline. They are, besides some extreme inclusions from the tholeiitic basalt the most acidic inclusions analyzed.

Inclusions in pyroxene from the andesitic basalt vary in $SiO_2$ content from 47wt% to 68wt% and are generally alkaline. They mostly plot in the trachyte field, straddling the border to rhyolite.
Inclusions in plagioclase from the same sample are in accordance with the plagioclase inclusions from the tholeiitic andesite. They are rhyolite melts with variable alkali content, classifying some as sub-alkaline some as alkaline. Both, the plagioclase hosted melt inclusions from the andesitic basalt and those from lark are chemically located at the evolved end of the bulk rock composition of the Bingham volcanic suite.

In order to further subdivide the alkaline melts identified above, Middlemost (1975) used a cross plot of $Na_2O$ vs. $K_2O$. As we can see in figure Fig. 17 melt inclusions from the tholeiitic andesite belong to the K-series. They often have higher $Na_2O$ than $K_2O$ concentrations, whereas the plagioclase inclusions from the andesitic basalt have higher $K_2O$ contents compared to $Na_2O$ and partly belong to high K-series melts.

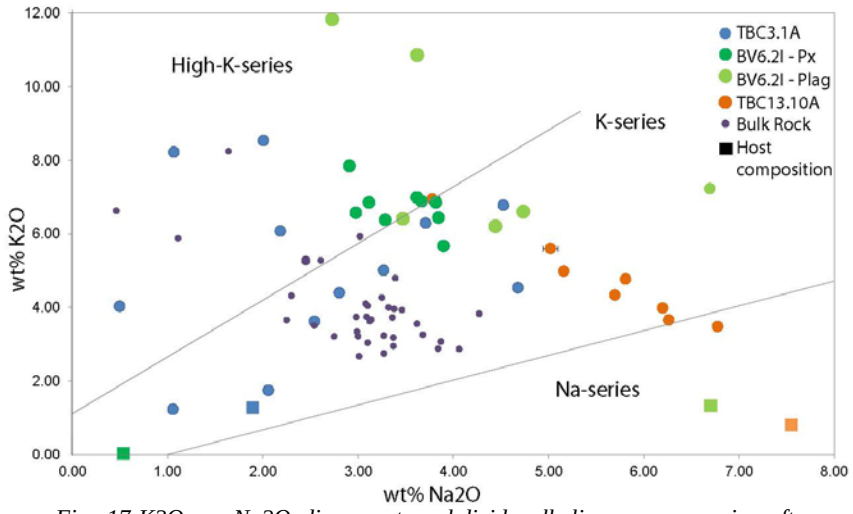


*Fig. 17:K2O vs. Na2O diagram to subdivide alkaline magma series after (Middlemost, 1975).*

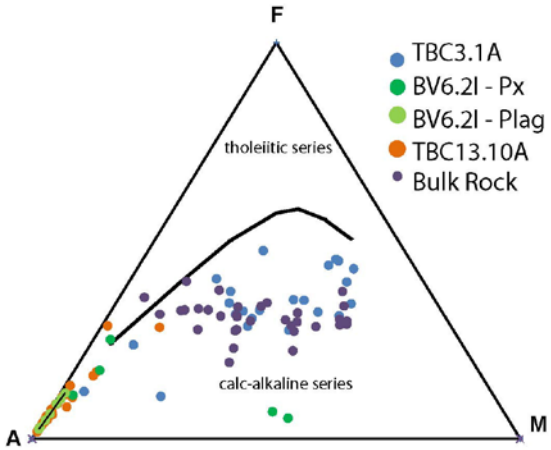


*Fig. 18: AFM Diagram showing the clear affiliation of the analyzed melts to the calc-alkaline magmatic suite. Boundary line after(Kuno, 1968)*

Inclusions in pyroxenes from the andesitic basalt are also higher in $K_2O$ than $Na_2O$ and plot around the border of K-series to high-K-series Melt inclusions from the tholeiitic basalt are divers plotting in the K-series to high-K- series field.

The overall trend of all analyzed inclusions is clearly calc-alkaline (Fig. 18). Plagioclase hosted MI with a rhyolitic composition plot at the evolved end of the trend. Pyroxene hosted MI have high K contents, going along with less enrichment of Fe leading to a position at the alkali end or the base of Fig. 18.

*4.6 Silicate melt inclusion composition*

In the following the results of the LA-ICPMS analysis of melt inclusions are presented in more detail. For concentrations of all analyzed inclusions , especially those not displayed here, the reader is referred to the appendix.

In this section $SiO_2$ is used as a fractionation indicator, since the #Mg is depending on the oxidation state of the magma and the ferric iron content. Since we only assumed this parameter, the significance of the #Mg number has to be taken with caution in our case. Other tracers such as Cs could not be used because they were not detected consistently in all inclusions.

*Tholeiitic basalt*

Analyzed melt inclusions in the tholeiitic basalt are exclusively hosted in amphibole. Fig. 19 shows

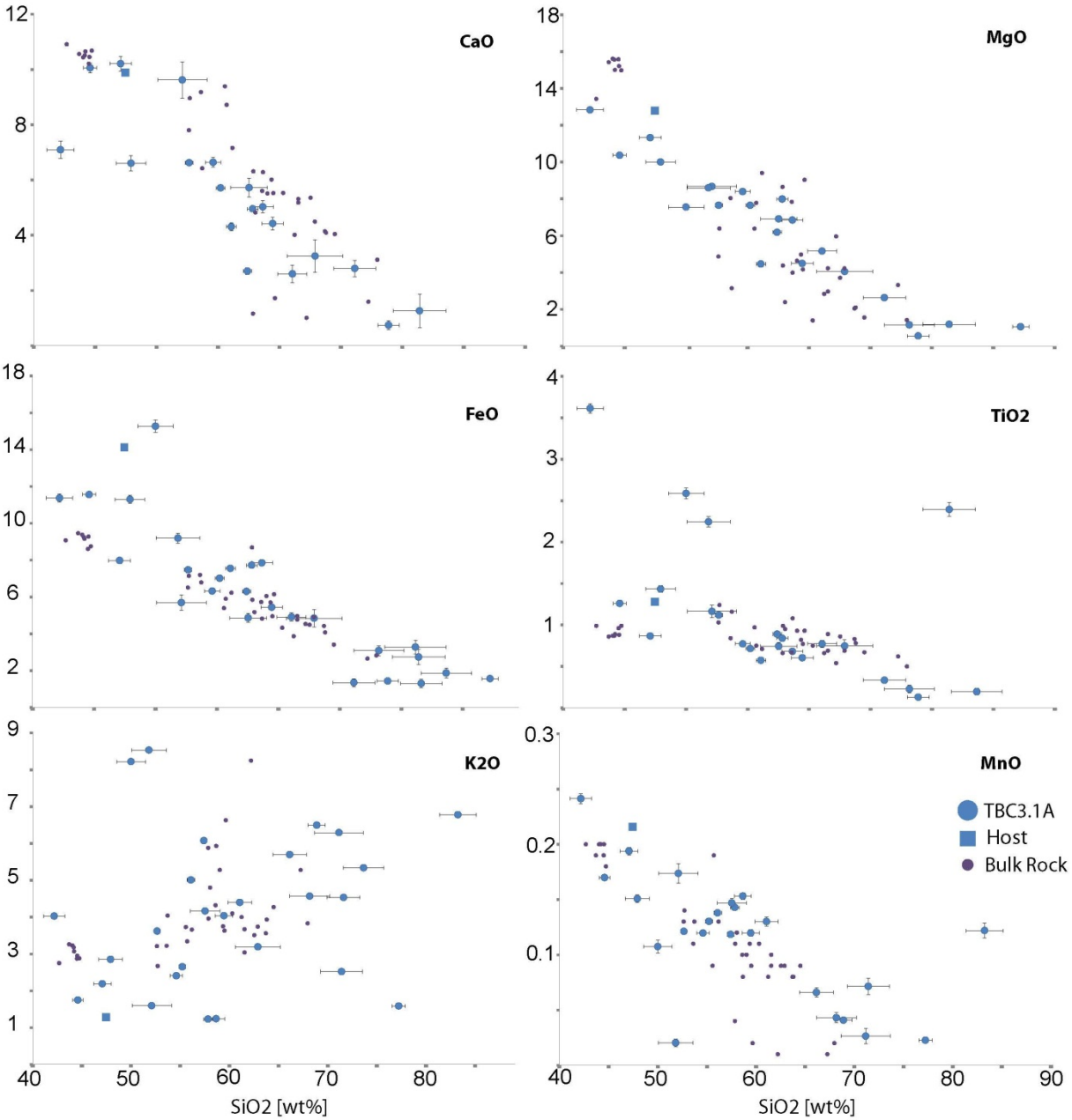


*Fig. 19: Haker diagrams for major oxides in amphibole hosted MI for the tholeiitic basalt. Concentrations in wt%. A clear correlation with the bulk rock trend defined by the Bingham volcanic suite is visible for all element, except $K_2O$.*

the concentration of major oxides vs. silicate content. Generally, it can be noted that all major oxides show a trend with respect to $SiO_2$. Except $K_2O$ (and $Na_2O$, not displayed) all element concentrations decrease with increasing acidity of the melt. This trend is in remarkable good agreement with the bulk rock trend from the Bingham volcanic suite. Exception is $K_2O$ where a clear positive sloping trend is visible, however it is not well correlated with the bulk rocks, but absolute values are in the same range.
The range in composition for the major oxides is large. CaO ranges from 11% in the most mafic inclusions to around 1% in the most acid ones. MgO and FeO vary in the same range with a constant FeO/MgO ratio of approximately 1. $TiO_2$ varies largely between 1.3wt% in the mafic inclusions to 0.25wt% in the felsic ones, with some outlier at 2.5wt%. MnO decreases from around 0.25wt% to 0.05wt% in evolved inclusions. $K_2O$ is lowest in the basic inclusions with around 2wt% and increases to 6wt% in $SiO_2$ rich inclusions.
Concentrations for trace elements are displayed in Fig. 20. Generally an accordance with bulk rock data can be observed, but it is less clear compared to the major oxides. LILE elements generally are in the same range and trend as the bulk rocks, except Sr which is concentrated on average with 350ppm in the inclusions, but with around 800pm in the bulk rocks. Rb and Th have a constant ratio up to intermediate inclusions of around 60-65wt% $SiO_2$. HFSE are generally concentrated in the same amount as in bulk rocks. The trend is also overlapping in many cases (Rb, Y, Nb, Pb). For other HFSE

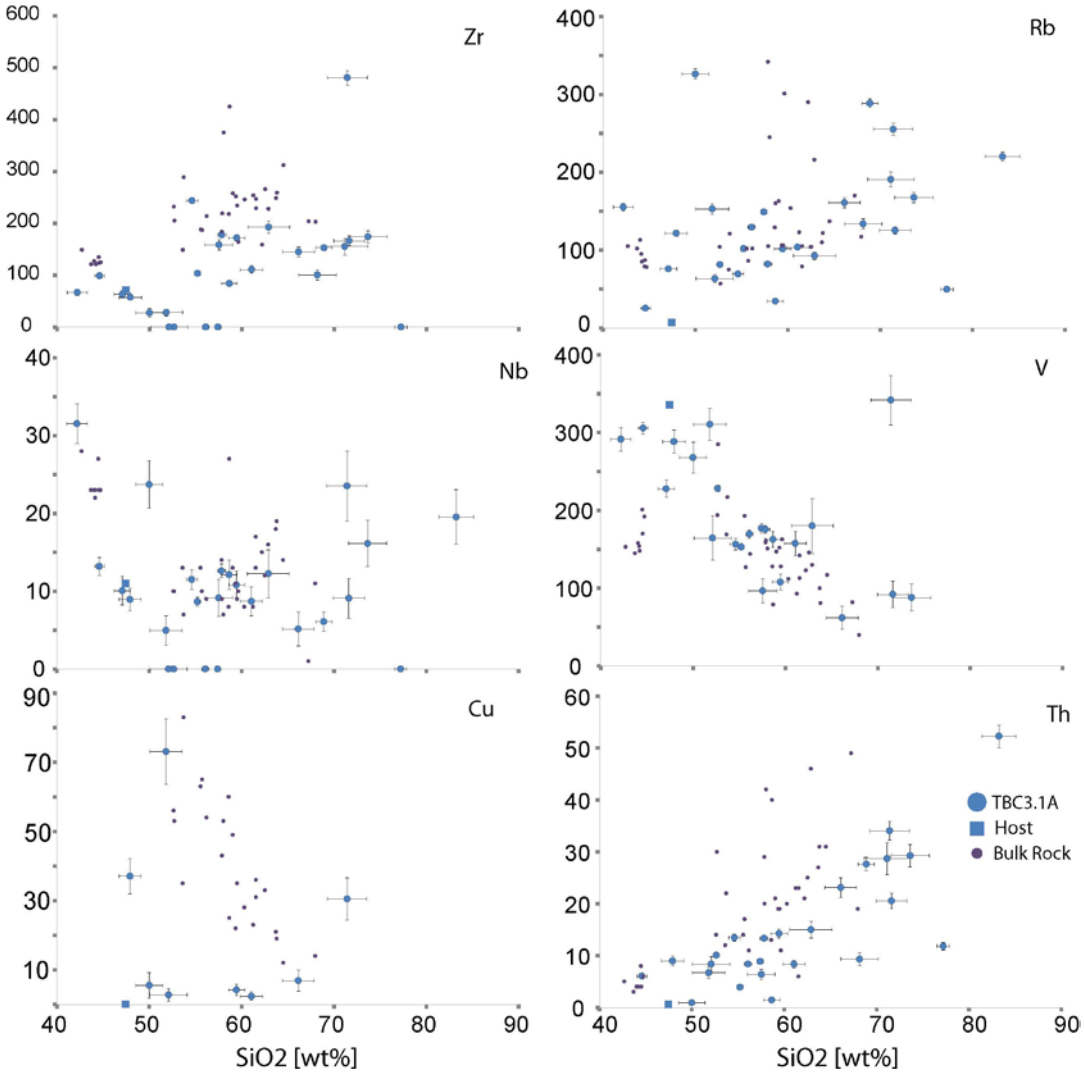


*Fig. 20: Harker diagram for trace elements in amphibole hosted melt inclusion from tholeiitic basalt. Concentrations in ppm. LILE elements are equally concentrated and show the same trend as the bulk rocks from the Bingham volcanic suite. HFSE are often in good accordance with the trend displayed by the bulk rocks.*

elements the trend of bulk rocks and melt inclusion composition is the same, but the element concentrations in the inclusion are shifted to lower values (Zr, Th, U). Notable is the U-shaped trend for Nb, which has its lowest concentrations in intermediate inclusions and increases towards basic and acid ones. Compatible elements like Cr and V are in the basic to intermediate inclusions in accordance bulk rocks. Ni is constant from 100ppm in the basic to around 50ppm in the intermediate rocks. Cu concentrations are rather low with a maximum value of 70ppm.

In figure Fig. 21A a multi element plot for melt inclusions of different evolved stages are displayed. A general enrichment of mobile incompatible elements, compared to HFSE elements and mantle compatible elements is evident. A pronounced Nb and Zr anomaly is visible. A high variability of LILE without any relation to $SiO_2$ content can be noted. However, immobile HFSE show a good internal correlation.

Chondrite normalized REE (Fig. 21B) in amphiboles show a strong enrichment of LREE elements compared to HREE but a flat slope from Sm to Yb. The $SiO_2$ content does not have an influence on the pattern .

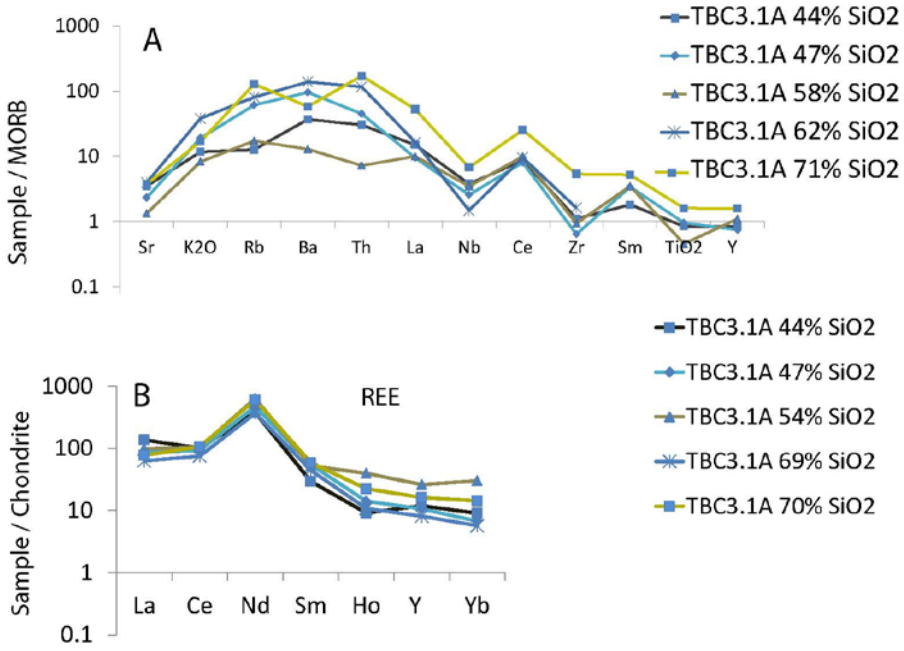


*Fig. 21: A: MORB normalized (Pearce, 1982, 1983) multi element plot for amphibole-hosted melt inclusions from tholeiitic basalt. A strong enrichment in LILE and negative spikes for Nb and Zr can be noted. B: Chondrite normalized (Haskin et al., 1968; Nakamura, 1974) REE element plot. LREE enrichment and a constant value for HREE are visible*

*Tholeiitic andesite*

Major oxides in plagioclase hosted melt inclusions in the tholeiitic andesite plot at the felsic end of the trend displayed by the bulk rocks of the Bingham volcanic suite (Fig. 22). $K_2O$ and $Na_2O$ (not shown) vary between 8wt% and 1.5%wt. Opposed to that, the concentrations of all other major oxides vary in a narrow range. Melt inclusions in the tholeiitic andesite are especially low in MgO and MnO hardly above 0.01wt%. CaO is concentrated with around 2.2wt% and FeO with 0.5wt%.

Trace element concentration is from melt inclusions in the tholeiitic andesite generally plot at the end of the compositional trend defined by the Bingham volcanic suite. LILE elements range in the same order as the bulk rocks, with Rb varying from 50-150ppm, Ba from 500-2000ppm (not displayed). Sr is slightly enriched with values up to 1200ppm (not displayed). The compatible elements Cr, Ni and V are mostly below detection limit stressing the evolved character of the melt inclusion composition.

HFSE are also in good accordance to the bulk rock trend at comparable $SiO_2$ content. Exception are Zr and Th which are significantly lower. The majority of the plagioclase hosted melt inclusions have Nb contents of 1-10ppm whereas most bulk rocks have concentrations of around 10-15ppm.

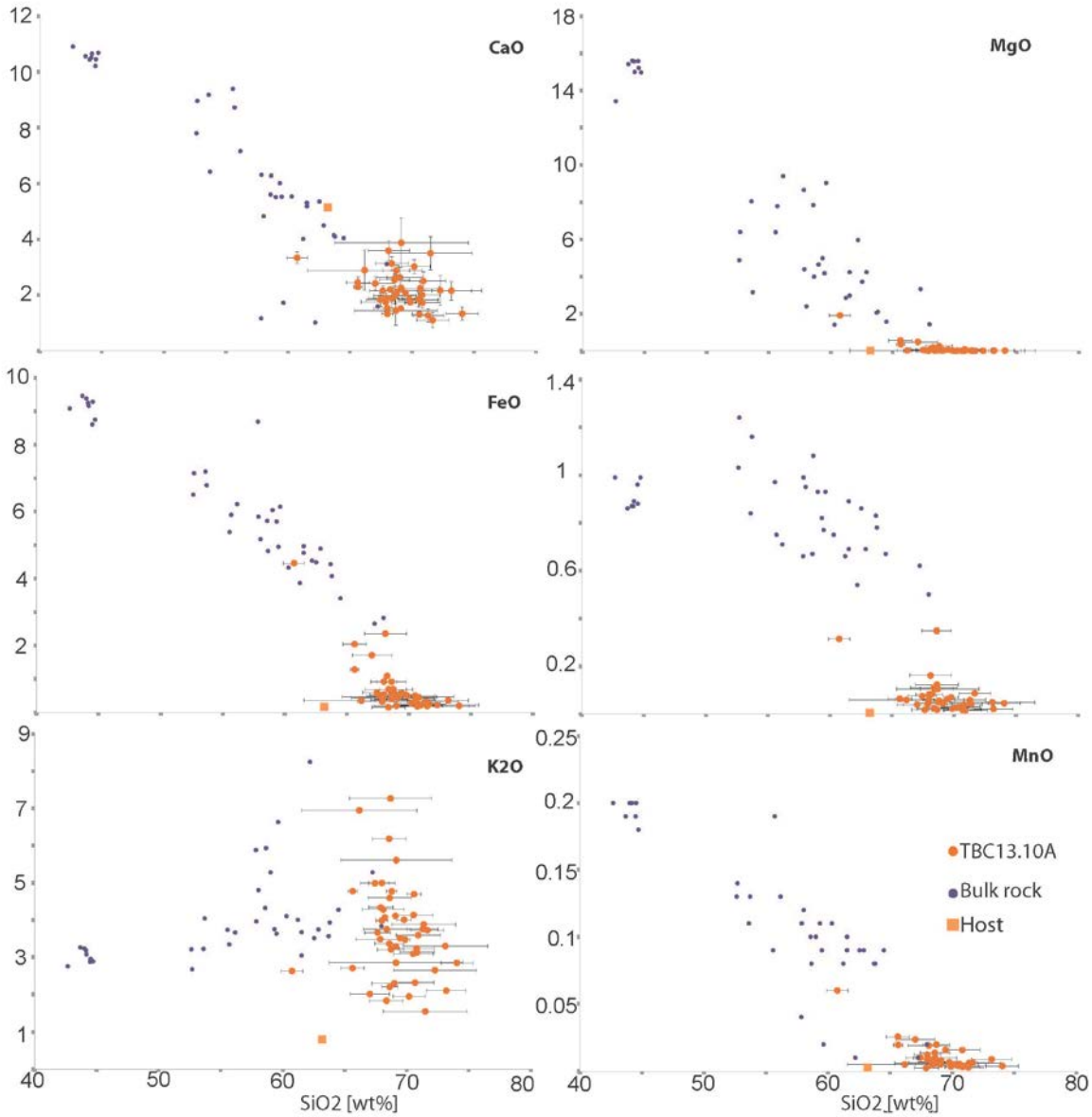


*Fig. 22: Harker diagram for major oxides in plagioclase hosted melt inclusions from tholeiitic andesite. All concentration in wt%. Major oxide composition is similar to the evolved rocks of the Bingham volcanic suite.*

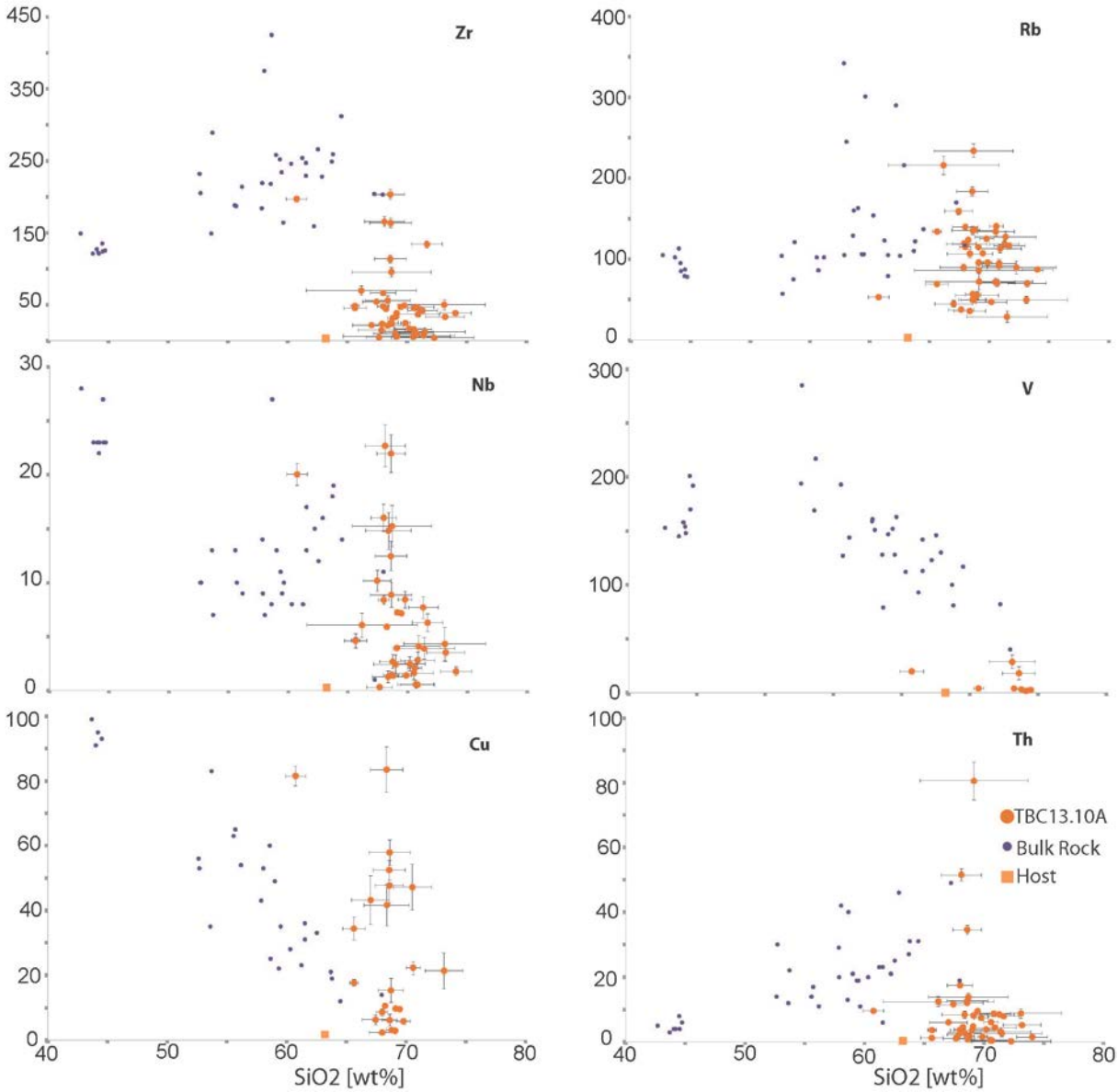


*Fig. 23: Haker diagram for trace elements in plagioclase hosted melt inclusions from tholeiitic andesite. Concentrations in ppm. Element concentrations are in the range of the bulk rock trend, with Th and Zr being lowered.*

The multi element plot in Fig. 24A also shows the enrichment in LILE characteristic for all analyzed inclusions. A pronounced Ti and Nb anomaly can be noted.

The REE pattern shows a prominent enrichment in LREE and depletion of HREE. However the HREE pattern is constant internally. A consistent La/Y ratio of 13.54 also indicates the LREE enrichment.

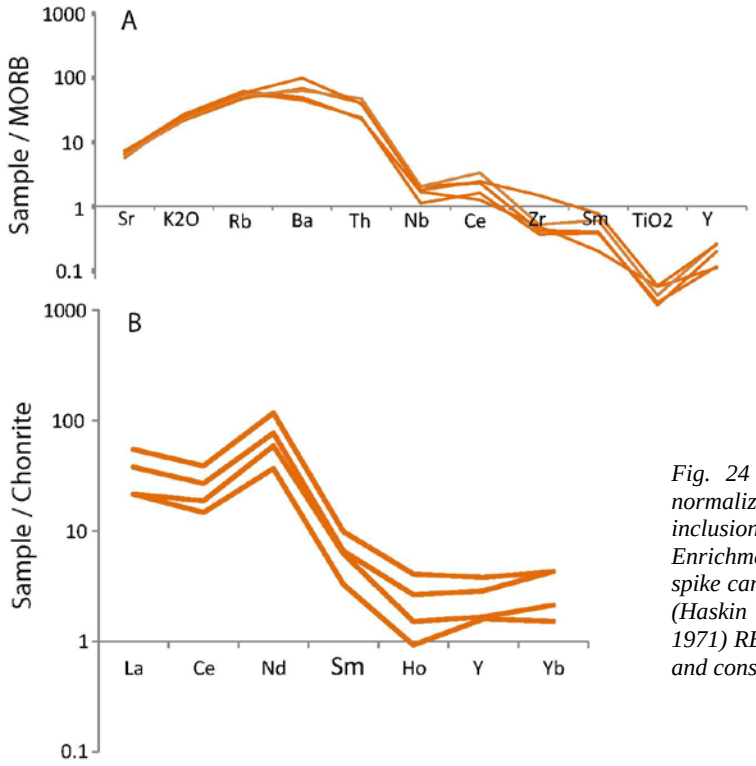


*Fig. 24 A: MORB (Pearce, 1982, 1983) normalized multi element plot for melt inclusions from tholeiitic andesite. Enrichment of LILE and Ti +Nb negative spike can be noted. B: Chondrite normalized (Haskin et al., 1968; Irvine and Baragar, 1971) REE pattern with enrichment of LREE and constant HREE*

*Andesitic basalt*

Melt inclusions in the andesitic basalt were analyzed in clinopyroxenes and plagioclase. As can be seen in Fig. 25 inclusion composition in the different hosts differ for some major oxides. Generally, plagioclase hosted melt inclusions plot near the silicic end of the bulk rock trend defined by the Bingham volcanic suite. One exception is $K_2O$ for which concentrations in the inclusions are higher.
Pyroxene hosted melt inclusions mimic the trend defined by the Bingham volcanic suite, however for $K_2O$ and FeO it does not coincide with that trend. Pyroxene-hosted MI show a considerable scatter in $SiO_2$ content from 47wt% to 68wt%. Except for $K_2O$ and FeO variation in major oxides go with $SiO_2$ content. FeO content in plagioclase and pyroxene hosted MI are considerably lower than in the bulk rock with a constant or very slightly increasing trend from 1wt% FeO at 47wt% $SiO_2$ to 2wt% FeO at 68% $SiO_2$ in pyroxene-hosted melt inclusions
Harker diagrams for trace elements are shown in Fig. 26. In general MI in pyroxenes are enriched in LILE elements compared to whole rocks. Elements like Rb and Th are significantly elevated in the pyroxene hosted melt inclusions compared to those in plagioclase but also to the bulk rock. Rb for example has an average concentration in the bulk rocks of the Bingham volcanic suite of around 240ppm whereas the pyroxene-hosted melt inclusions have an concentration of around 350ppm. Same account for Th where the concentration in the pyroxene-hosted MI is more than twice as high as in the bulk rocks. Ba on the other side is depleted in pyroxene-hosted MI compared to bulk rocks. Th, Rb and Ba also show pronounced positive and negative spikes in a MORB normalized multi element plot (Fig. 27A). Pyroxene hosted inclusions have HFSE enriched compared to bulk rocks with values around 350ppm Zr and 25ppm Nb (Fig. 26). They show a decoupling of LILE. A pronounced Ti anomaly when normalized on MORB is shown in Fig. 27A. Compatible elements like Cr and Cu are enriched with Cu values up to 440ppm in pyroxene hosted MI. The richest volcanic rocks in the Bingham volcanic suite, the nepheline minette in comparison have a Cu concentration of around 100ppm (Waite et al., 1997). Cr concentrations (not displayed) are available for only two inclusions in pyroxenes. One inclusions has a Cr concentration of 1171ppm, the other 528ppm which is slightly

above bulk rock concentrations. The abundance of mantle compatible elements is high for the normally intermediate composition of the melt inclusions.

Plagioclase hosted melt inclusions are rather depleted in incompatible mobile elements compared to whole rocks but also enriched compared to MORB (Fig. 27A). Nb and most other HFSE in plagioclase-hosted inclusions mostly overlap with bulk rock concentrations. However, Zr and Sc (not displayed) are depleted in plagioclase hosted MI. Compatible elements are depleted in plagioclase-hosted MI relative to the host rocks. An exception is Cu where two inclusions show elevated Cu concentrations of 120 and 320ppm. However, these inclusions occur in the same mineral, in the same growth zone as those with low Cu inclusions. Normally, Cu concentrations in plagioclase-hosted MI are below Cu concentrations in pyroxene-hosted MI at comparable $SiO_2$.

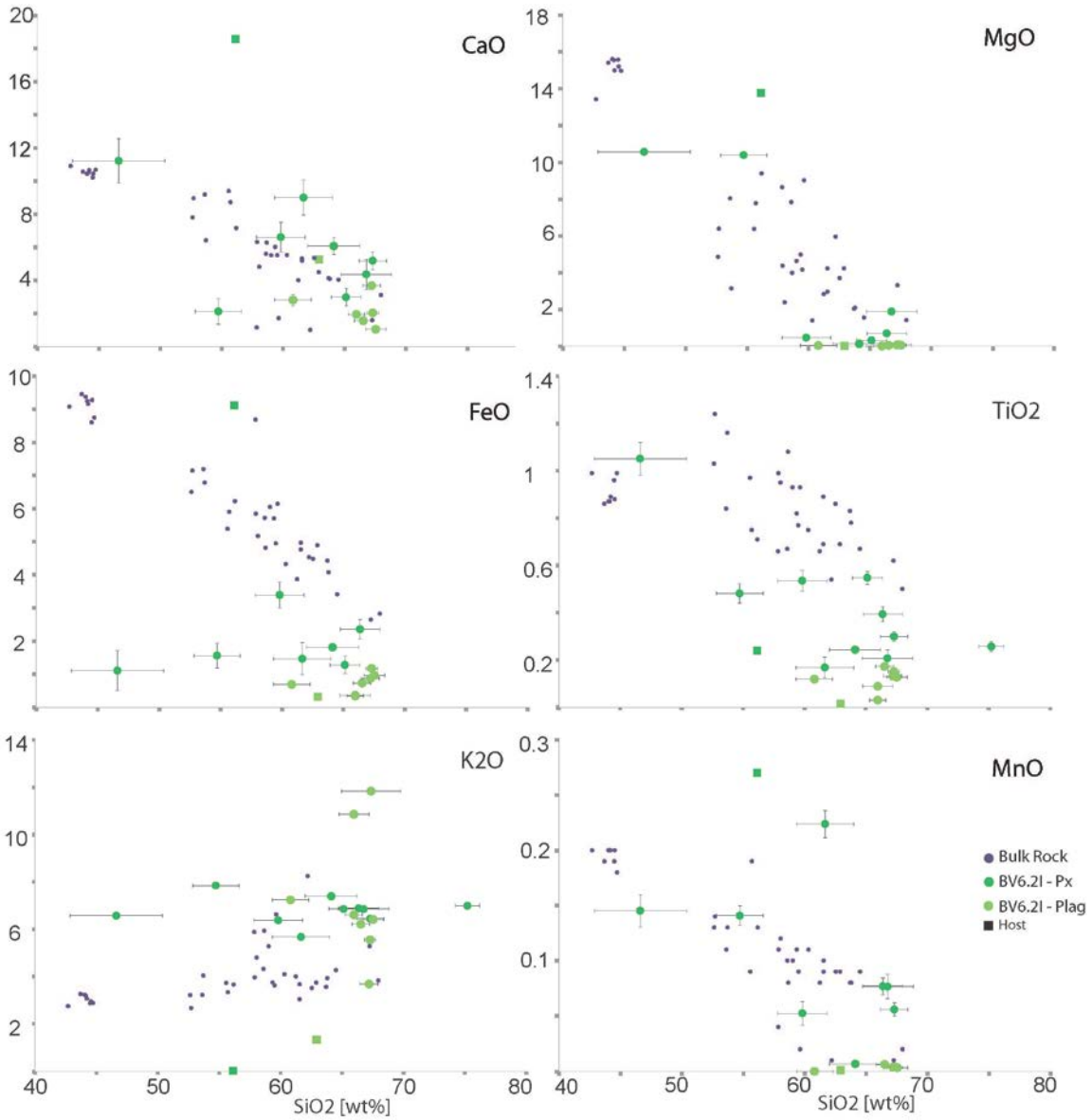


*Fig. 25: Harker diagram for major oxides of melt inclusions from andesitic basalt: All concentrations in wt%. Plagioclase- hosted melt inclusions are normally located at the felsic end of the bulk rock trend defined by the Bingham volcanic suit, except for $K_2O$. Pyroxene hosted melt inclusions follow the bulk rock trend for most oxides but show a considerable scatter. FeO and $K_2O$ are not related to the bulk rocks.*

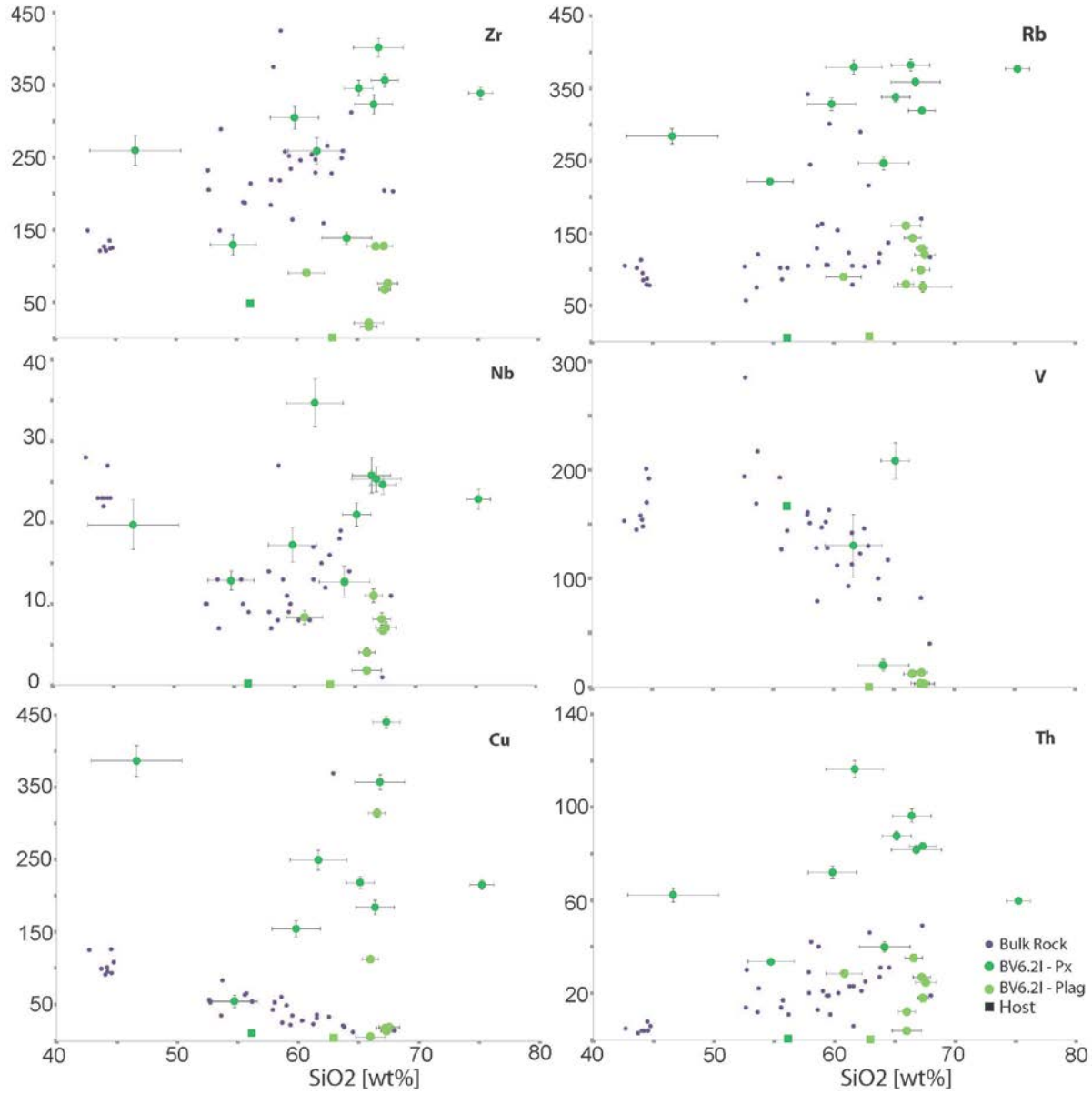


*Fig. 26: Harker diagram for trace elements in melt inclusions from andesitic basalt. All concentration in ppm. Pyroxene hosted melt inclusions are enriched in LILE and HFSE. In few inclusions compatible elements were measured but pyroxene hosted MI have high Cu concentration up to 400ppm. Plagioclase hosted MI are rather depleted compared to host rocks but two inclusions also have elevated Cu concentrations.*

Concentrations of REE are strongly enriched in both plagioclase and pyroxene compared to Chondrite (Fig. 27). In pyroxenes REE concentrations are generally the highest relative to all other measured MI at comparable $SiO_2$. A strong enrichment of the LREE compared to the HREE is stressed by an average La/Y ratio of 24. But the ratio is extremely variable from 40 to 7. Plagioclase inclusions show a similar pattern but an even more pronounced preference of LREE over HREE with an average La/Y ratio of 43 and similar wide in range from 67 to 39.

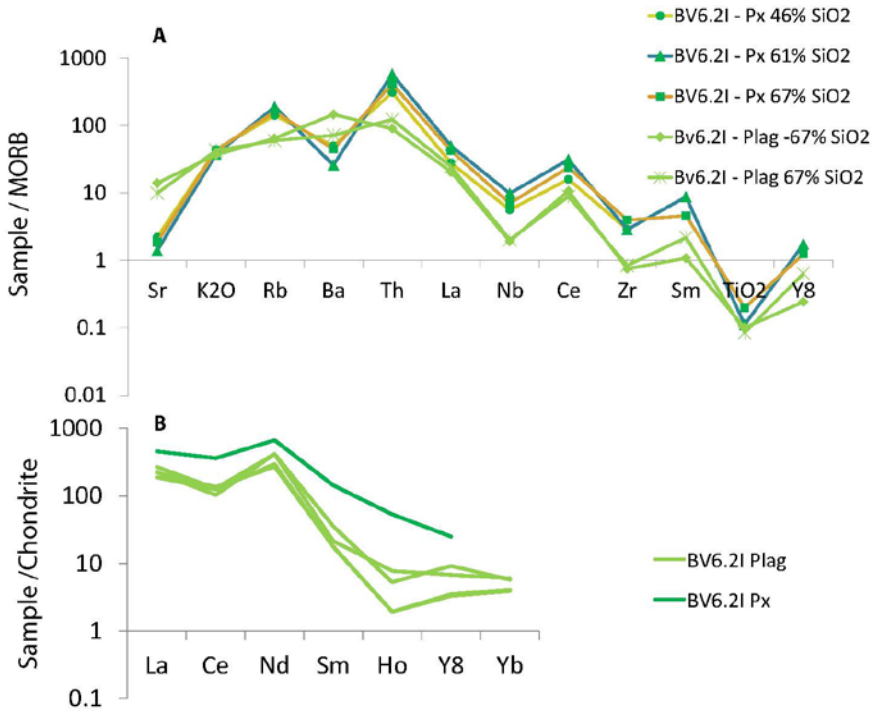


*Fig. 27 A: MORB (Pearce, 1982, 1983) normalized multi-element plot for plagioclase and pyroxene-hosted MI in andesitic basalt. Decoupling of LILE and HFSE element in pyroxene hosted MI is visible. Strong Ti, Nb and Ba anomaly are evident. Plagioclase-hosted inclusions have generally lower trace element concentrations, except Ba but also show LILE and HFSE decoupling and a negative Ti spike. B: Chondrite normalized (Haskin et al., 1968; Nakamura, 1974) REE abundances in pyroxene and plagioclase hosted melt inclusions show a strong enrichment of LREE compared to HREE.*

### *4.7 Sulfide melt inclusion composition*

Sulfide melt inclusions were measured in amphiboles from the tholeiitic basalt (section 4.2). The highest metal concentrations in sulfide melt inclusions were measured for Cu with about 2.4wt% on average. Most of the measured Cu-concentrations range between 1wt% - 4wt% , one outlier has a concentration of 9wt% (Table 4). Ni and Co show concentrations of around 1.1 and 0.2 wt% respectively. Gold was only detected in one inclusions (0.1ppm). However, as can be seen in Table 4 the limits of detection for Au are extremely high pointing to the fact that the inclusions might not be as Au poor as suggested by only 1 successful detection. Zn has concentrations of around 900ppm but with a range from almost 1900ppm to 100ppm. Mo concentrations are very low in the order of several ppm which is 50 times lower than the average of the ore mined up to today (Porter et al., 2012).

Compared to Cu-concentrations in sulfide melt inclusions from the large Alumbrera Cu-porphyry system – Argentina, the ranges from both system overlap very well. However, on average the concentration of Cu seem to be higher in sulfide melt inclusions from Bingham (Fig. 28).

Set against the composition of intermediate density (ID) fluid inclusions from the deep center in Bingham, which are considered to best represent the initial input fluid, Cu and Zn concentrations are elevated in the sulfide melt inclusions (Fig. 29). However, both compositions can be fitted to a line crossing (1/1) meaning that the Cu/Zn ratio is similar in the ID-fluid inclusions and the sulfide melt inclusions.

*Table 5: Composition of amphibole-hosted sulfide melt inclusions from tholeiitic basalt. Element composition and 1 σ error in ppm. Processing of sulfide melt inclusions was done by assuming that the melt composition is stoichiometric FeS.*

*<33.46 below limit of detection*

| Sample | $^{57}$Fe | $^{59}$Co | $^{60}$Ni | $^{65}$Cu | $^{66}$Zn | $^{75}$As | $^{77}$Se | $^{95}$Mo | $^{107}$Ag | $^{121}$Sb | $^{197}$Au | $^{208}$Pb |
|---|---|---|---|---|---|---|---|---|---|---|---|---|
| 15jn01c18 | 635000 | | 4738.41 | 15880.47 | 1904.14 | <32.46 | | <11.75 | <3.90 | 13.75 | <3.06 | |
| | 15522 | | 211 | 144 | 191 | <32.4 | | <11.75 | <3.90 | 8 | <3.06 | |
| 15jn01c19 | 635000 | | 9698.51 | 39640.92 | 1535.56 | <73.46 | | <23.90 | <6.80 | <24.80 | <6.24 | |
| | 26175 | | 474 | 299 | 301 | <73.46 | | <23.90 | <6.80 | <24.80 | <6.24 | |
| 15jn08a03 | 635000 | 1634.80 | 9683.97 | 26638.42 | 177.17 | <1.60 | 46.38 | 4.47 | 5.98 | <0.38 | 0.12 | 4.75 |
| | 679 | 4 | 21 | 30 | 8 | <1.60 | 4 | 0 | 0 | <0.38 | 0 | 0 |
| 15jn08a04 | 63500. | 1170.34 | 11164.93 | 36317.94 | 816.84 | <26.15 | <159.95 | <6.99 | 30.25 | <6.48 | <1.26 | 11.81 |
| | 5363 | 24 | 102 | 149 | 105 | <26.15 | <159.95 | <6.99 | 2 | <6.48 | <1.26 | 5 |
| 15jn08a07 | 635000 | 2566.69 | 10336.18 | 21746.47 | 448.07 | <20.86 | <129.36 | <6.06 | 5.25 | <5.33 | <1.02 | 3.53 |
| | 4400 | 26 | 99 | 119 | 62 | <20.86 | <129.36 | <6.06 | 1 | <5.33 | <1.02 | 5 |
| 15jn08a08 | 635000 | 1388.88 | 4407.17 | 8477.43 | 350.87 | <12.6 | <84.91 | <3.14 | 3.51 | <7.05 | <0.55 | <2.27 |
| | 8201 | 31 | 87 | 40 | 113 | <12.6 | <84.91 | <3.14 | 1 | <7.05 | <0.55 | <2.27 |
| 15jn08a09 | 635000 | 633.60 | 6227.27 | 30574.59 | 747.61 | <89.17 | <574.71 | <28.33 | <5.92 | 42.52 | <4.46 | <15.35 |
| | 29472 | 108 | 310 | 264 | 413 | <89.17 | <574.71 | <28.33 | <5.92 | 12 | <4.46 | <15.35 |
| 15jn09e04 | 635000 | 12742.31 | 75552.31 | 92495.95 | <2390.06 | <742.18 | <6026.33 | <280.74 | <86.92 | <236.52 | <47.57 | <150.90 |
| | 196988 | 869 | 2744 | 1695 | <2390.06 | <742.18 | <6026.33 | <280.74 | <86.92 | <236.52 | <47.57 | <150.90 |
| 15jn09e05 | 635000 | 4210.72 | 16240.53 | 31009.80 | 1797.20 | <131.88 | <1062.62 | <39.60 | <8.07 | <43.79 | <8.40 | <24.06 |
| | 54140 | 260 | 924 | 354 | 621 | <131.88 | <1062.62 | <39.60 | <8.07 | <43.79 | <8.40 | <24.06 |
| 15jn09e06 | 635000 | 834.62 | 18721.24 | 6635.08 | <682.69 | <200.36 | <1682.96 | <84.78 | <17.84 | <71.34 | <17.99 | <34.32 |
| | 33675 | 157 | 696 | 308 | <682.69 | <200.36 | <1682.96 | <84.78 | <17.84 | <71.34 | <17.99 | <34.32 |
| 15jn09e07 | 635000 | 871.52 | 3060.67 | 2557.58 | 946.45 | <97.92 | <827.83 | <34.1 | <11.15 | <71.34 | <7.95 | <24.65 |
| | 16499 | 64 | 210 | 112 | 286 | <97.92 | <827.83 | <34.1 | <11.15 | <71.34 | <7.95 | <24.65 |
| 15jn09f03 | 635000 | 1917.99 | 1409.34 | 21805.73 | <79.47 | <25.87 | 259.19 | <7.72 | 5.38 | <71.34 | <1.92 | <4.3426 |
| | 11473 | 45 | 61 | 109 | <79.47 | <25.87 | 123 | <7.72 | 2 | <71.34 | <1.92 | <4.3426 |
| 15jn09f04 | 635000 | 1502.54 | 3775.91 | 26708.85 | 506.36 | 12.24 | <100.20 | 6.89 | 4.48 | <71.35 | <0.96 | 13.20 |
| | 3548 | 18 | 48 | 96 | 52 | 7 | <100.20 | 2 | 1 | <71.35 | <0.96 | 4 |
| 15jn09f06 | 635000 | 1407.04 | 7370.73 | 23095.79 | 1224.53 | <25.97 | <225.10 | <9.25 | 5.04 | <71.35 | <2.16 | 20.60 |
| | 9231 | 38 | 118 | 140 | 132 | <25.97 | <225.10 | <9.25 | 2 | <71.35 | <2.16 | 10 |
| 15jn09h05 | 635000 | 1466.60 | 2681.96 | 11056.59 | 112.96 | <43.01 | <349.33 | <16.14 | <3.46 | <71.35 | <2.98 | <9.16 |
| | 10219 | 52 | 137 | 131 | 85 | <43.01 | <349.33 | <16.14 | <3.46 | <71.35 | <2.98 | <9.16 |
| 15jn09h06 | 635000 | 2645.59 | 14300.03 | 25534.15 | 518.04 | <19.86 | <156.27 | <7.26 | 3.47 | <71.35 | <1.37 | 54.24 |
| | 6517 | 37 | 138 | 132 | 53 | <19.86 | <156.27 | <7.26 | 1 | <71.35 | <1.37 | 5 |
| 15jn09h07 | 635000 | 1453.17 | 6033.15 | 13485.15 | 1601.05 | <62.31 | <482.44 | <22.42 | <6.58 | <71.35 | <4.81 | <14.85 |
| | 21428 | 101 | 287 | 233 | 182 | <62.31 | <482.44 | <22.42 | <6.58 | <71.35 | <4.81 | <14.85 |
| 15jn09h08 | 635000 | 733.25 | 9458.14 | 2188.49 | <80.64 | <33.3 | <260.96 | <11.46 | <2.79 | <71.35 | <1.66 | 12.94 |
| | 6411 | 29 | 115 | 42 | <80.64 | <33.3 | <260.96 | <11.46 | <2.79 | <71.35 | <1.66 | 6 |

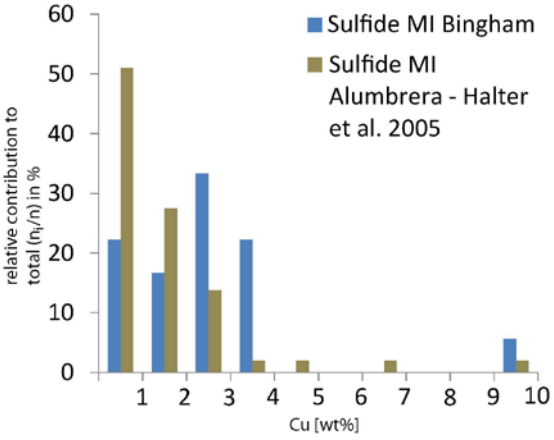


*Fig. 28: Comparison of Cu content of sulfide melt inclusions from Bingham and Alumbrera. Displayed is the number of concentration measurements per 1% category (ni) normalized on the total number of analyzed sulfide melt inclusions (n). Bingham sulfide melt inclusions seem to be richer in Cu on average. n Bingham:18; n Alumbrera:51*

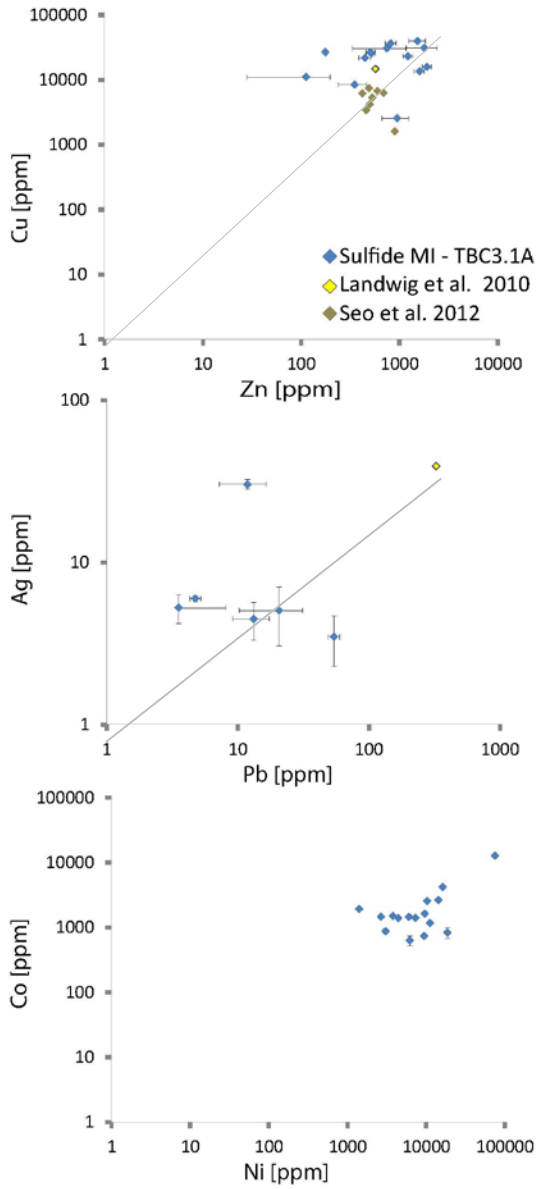


*Fig. 29: Metal concentrations in sulfide melt inclusions compared concentrations measured in intermediate density fluid (ID) inclusions from Bingham considered to represent the initial input fluid. Sulfide melt /fluid ratios are similar for Cu and Zn. Ag and Pb are higher concentrated in the intermediate density fluid.*

Ag and Pb are in contrast to that rather depleted in the sulfide melt inclusions relative to the ID-fluid inclusions (Fig. 29). The linear fit between both types of inclusions is less well constrained but tentatively the Ag/Pb ratio is also similar in fluid and sulfide melt inclusions. Interestingly, the Ag concentration of most sulfide melt inclusions is around 3-5ppm which matches quite well the average Ag-grade of the ore mined in Bingham (3-4ppm , compare Porter et al. (2012)). No ID-fluid concentrations for Co and Ni are available from the literature. From Fig. 29 we can see that Ni concentrations are around 1% in the sulfide melt inclusions, Co is less concentrated with around 0.2%.

In Fig. 30 we can see a comparison of average and best estimate composition values from sulfide melt inclusions and ID-density fluid inclusions. It has to be noted that values from Landtwing et al. (2010) rather represent upper limit concentration values (see reference). The first thing which can be stated is that Cu and Zn are richer in the sulfide melt inclusions, the other elements (Mo, Ag, As, Pb, Au) have higher concentrations in the ID-fluid inclusions. A notably well correlation can be established between sulfide melt and fluid inclusion composition. Most concentrations (besides Pb) plot nicely on a linear trend in the log-log diagram. This indicates that the concentrations in the sulfide melt inclusions and those in the ID-fluid inclusions are related by a function of the form $y=Ax^n$.

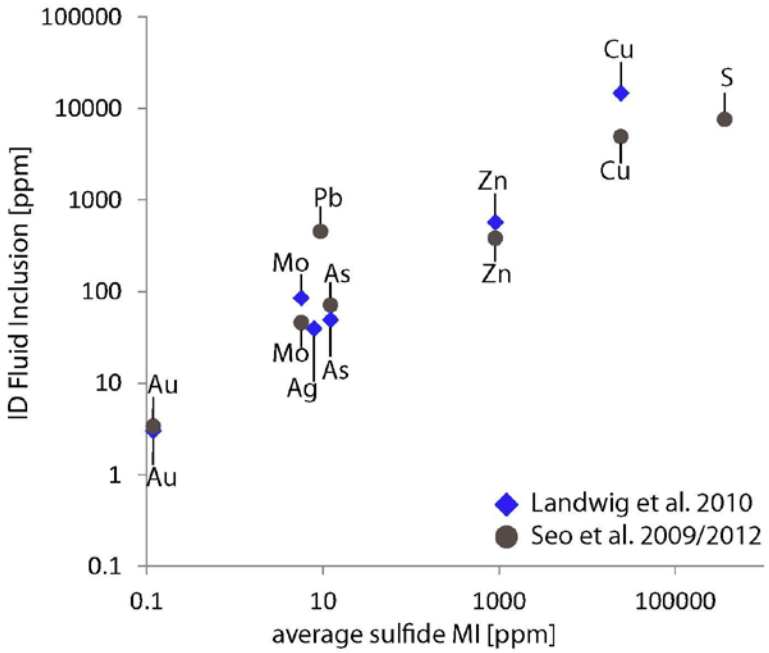


*Fig. 30: Average composition of sulfide melt inclusions against average (Seo et al., 2009, 2012) and best estimate values (Landtwing et al., 2010) of intermediate density fluid inclusions, considered to match closest with the initial input fluid at Bingham*

# 5 Discussion

## *5.1 Data reliability*

Because problems with post entrapment modification have already been reported for amphibole-hosted Si-melt inclusion in this study, a critical view on the obtained results is necessary.

Amphibole hosted Si-melt inclusions which have been regarded as unmodified so far, show a good correlation for all elements with the bulk rock trend. This can be taken as a sign towards their reliability. The large variability in the LILE for different $SiO_2$ values (Fig. 21A) might point to the modification (probably enrichment) by fluids, especially since no systematic variation (with $SiO_2$) in the LILE content can be observed. At this stage it cannot be stated when this possible enrichment occurred, during ore formation or later. But it possibly implies that the LILE content might not display the composition of the originally entrapped melt since we would expect a change in concentration with ongoing melt evolution, leading to a general increase of incompatible LILE in the melt which we do not observe (Fig. 19and Fig. 20). If we assume post entrapment diffusive modification to occur those should follow the general partition coefficients (Kd) for LILE in hornblende. Since K generally has the highest Kd value of all LILE in basic, intermediate and felsic liquids we would expect a negative spike for K in the multi-element plot (Fig. 21A). The same argumentation can be made for Rb which has the lowest Kd value of all LILE, and thus should be enriched in the melt. This pattern is not displayed in Fig. 21, possibly indicating that the amount of post entrapment modification due to fluid flow is minor.

An additional source of error is the internal standard. Since amphibole-hosted Si-MI in the tholeiitic basalt show a clear fractional crystallization trend (see discussion below), a constant $Al_2O_3$ for all inclusions is simply not correct since $Al_2O_3$ would also change during fractional crystallization. A proper internal standard in this case must be selected according to the stage of magma evolution. In this light, the previously reported $Al_2O_3$ content of around 10-13% in some amphibole-hosted melt inclusions might not be due to a depletion but actually reflect lower $Al_2O_3$ contents in primitive melt inclusions.

In the following, the compositional trend of amphibole-hosted melt inclusions from the tholeiitic basalt is considered to be reliable.

Difficulties during processing pyroxene-hosted melt inclusions in the andesitic basalt give a first reason to treat the results with caution. Using the internal standard of Table 2 only 8 out of 51 analyzed inclusions had a mass factor larger than 0.15, which is regarded as a lower limit for a reliable quantification. Most mass factors are in the range of 0.01. In addition the sum of major oxides in these inclusions did not add up to 100%, but was generally higher. Varying the internal standard by ± 5% (which is the whole $Al_2O_3$ range of the Bingham volcanics) does not improve the situation significantly. A minority of inclusions does yield slightly better x values, excluding the choice of the internal standard leading to the very low mass factors. Plagioclase-hosted MI in the same sample could be processed without any problems pointing to the fact that the source for the processing problems is restricted to clinopyroxene-hosted MI.

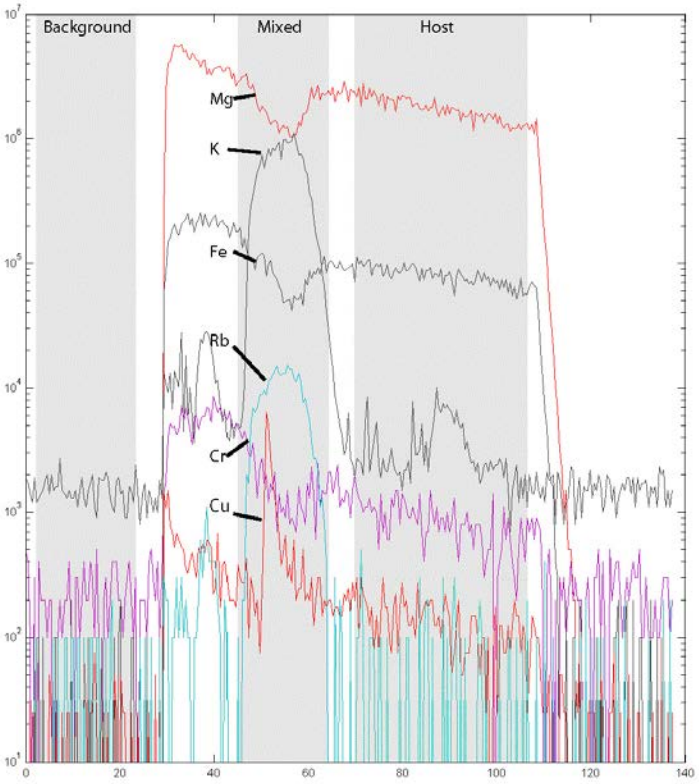


*Fig. 31: LAICPMS signal for a pyroxene-hosted melt inclusion in andesitic basalt, showing a clear positive spike for Cu,. Cr is relativy to the host (300ppm) depleted. Calculated concentration of Cr in this inclusions are 4times higher than in the host.*

In addition to the processing difficulties the enrichment in nearly all trace elements in pyroxene-hosted MI form the andesitic basalt is a conspicuous feature (compare Fig. 26 and appendix). When plotting element concentrations normalized on an immobile, incompatible element it becomes obvious that pyroxene-hosted MI from the andesitic basalt do not show especially high ratios. Normalizing helps to exclude the influence of late stage fluid flow and different degrees of fractional crystallization. An ideal candidate for normalization is La. It is immobile during fluid transport, it behaves incompatible during fractional crystallization and has roughly the same Kd for all minerals in which MI were analyzed. In Fig. 32 the ratios of some element (mobile and immobile) vs. La are shown. The enrichment in K, Cu or Zr of the pyroxene-hosted MI from the andesitic basalt compared to other MI are not visible anymore. Since we know that Cu is definitely enriched in the clinopyroxene-hosted melt inclusions (Fig. 31), the low Cu/La-ratio for clinopyroxene-hosted inclusions in Fig. 32 is striking. Changing La for another element which should have the same properties (e.g. Nb and Y but those have different Kd in the different phases) gives the same result, indicating that La is not the reason for the low Cu-ratios of clinopyroxene-hosted MI. Possibly a post entrapment enrichment of variable degree for Cu and HFSE should be considered during further work because optic petrography indicates that clinopyroxenes and plagioclase, which have significantly less Cu rich MI, have grown together. In this this context the high Cu-concentration of the clinopyroxene hosts might be of importance. Modifications of Cu-content in clinopyroxene-hosted MI have not been reported so far however, it was shown that it can occur in quartz-hosted MI. (Kamenetsky and Danyushevsky, 2005).

A similar pattern of strongly enriched K, Rb, Ba, Zr and Nb pyroxene-hosted MI was reported by Reubi and Blundy (2008) and has been attributed to grain scale processes during solid phase – melt reactions in a gabbroic dominated environment. A notable difference is that their inclusions showed pronounced different Ba/Sr ratios compared to other analyzed melt inclusions, not observed in this study.

The findings above indicate the results of pyroxene hosted melt inclusions should be treated with caution and limit the reliability of the obtained data. The elevated concentration of nearly all trace elements, might point to a systematic processing relict or a post entrapment enrichment since the LA-ICPMS signal are of very good quality and do not leave any room for picking the wrong inclusion interval.

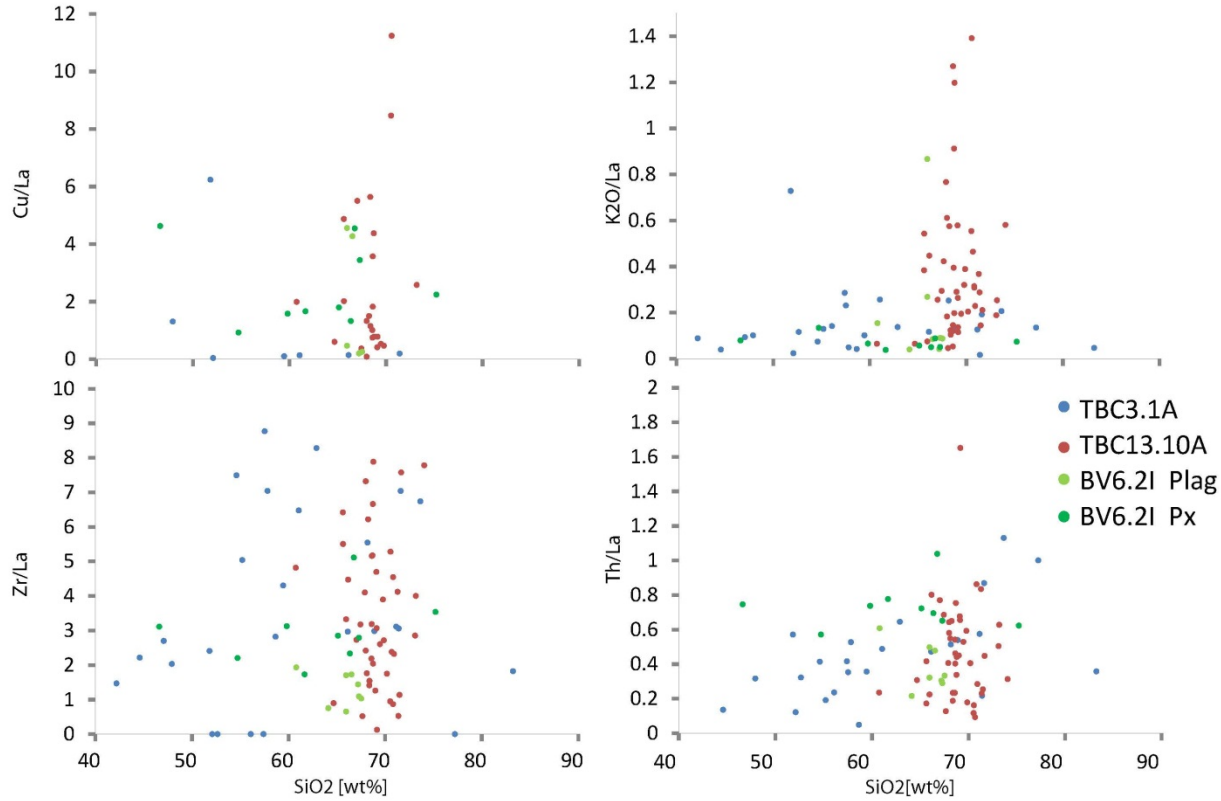


*Fig. 32 Element ratios using La as a normalizing factor. Normalization reveals that pyroxene hosted melt inclusions from the andesitic basalt have similar ratios for most LILE and HFSE as inclusions hosted in other phase, questioning their TBC3.1A: Tholeiitic basalt; TBC13.10A Tholeiitic andesite; BV6.2I Andesitic basalt.*

Compositions of the plagioclase hosted melt inclusions from Lark, show a well-defined point cloud in Fig. 22 and Fig. 26. The pattern in Fig. 27 is consistent for all inclusions. No processing difficulties were encountered. This implies that their quantification, based on the indications we have, is reliable.

However, variations in $K_2O$, $Na_2O$, Rb, Ba and Cu in plagioclase hosted MI from the tholeiitic andesite are very large for a given $SiO_2$ content (compare Fig. 22, Fig. 23, Fig. 24). In the first place it can be noted that almost all variable elements are mobile elements. So, possibly the variable content of these elements is related to a variable amount of fluid entrapped in the inclusion. As described above bubble sizes in plagioclase-hosted inclusions from the tholeiitic andesite range from 5-25%. However, no correlation between the bubble size and the $K_2O$ content of an inclusions can be made, indicating that the amount of fluid in the inclusion is probably not the reason for the element variations. In

addition there is no correlation between the inclusion position (core or rim of mineral) and $K_2O$ content.

Another possible reason for the variation in mobile elements might be difficulties during signal deconvolution (i.e. accidentally including different amount of host plagioclase into the inclusion signal). This can be tested by plotting highly variable elements like $Na_2O$ and $K_2O$ against an element which should be only present in the melt (i.e. incompatible in plagioclase) for example Zr. As can be seen in Fig. 33 there is no correlation between the $Na_2O+K_2O$ and Zr content in plagioclase-hosted MI from the tholeiitic andesite. This indicates that the large variations are not due to variable contribution of the host plagioclase to the signal.

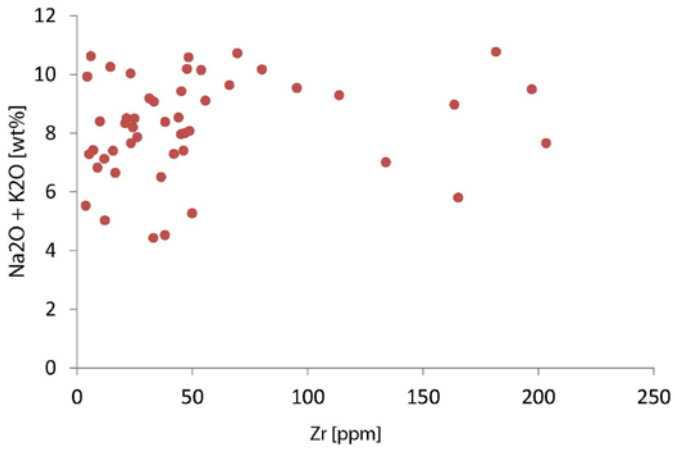


*Fig. 33: Ratio for Na2O+K2O vs. Zr in plagioclase-hosted MI from the tholeiitic andesite. No correlation between Zr and Na2O+K2O can be observed, making variable amount of host contribution as a reason for high element variability unlikely, See text for further explanation.*

No correlation among the highly variable elements in plagioclase-hosted MI from the tholeiitic andesite could be noted. If the variation of these elements would have a common reason, we might expect to see this by a correlation of the elements under discussion.

With the data in hand it is difficult to find an explanation for the observed variations. Possibly the observed variations only reflect natural variation in the magmatic composition. Similar ranges in composition with respect to $K_2O$ have been reported in other studies (Blundy et al., 2008; Halter et al., 2004a, 2005; Kamenetsky et al., 1995).

Thus, it is assumed that the calculated concentrations are correct and reflects natural variation in magmatic composition.

*5.2 Origin and evolution of magmas in the Bingham porphyry Cu-system*

The compositional trend displayed by amphibole-hosted Si-melt inclusions in the tholeiitic basalt is a clear sign of fractional crystallization. The decreasing Ca, Mg, Fe and Ti content can be explained by fractionation of clinopyroxene, and possibly olivine and amphibole (Fig. 19and Fig. 20). Since K and Na are incompatible in all these phases the rise in concentration is consistent with this interpretation. Petrographic observation of mafic cumulates support fractional crystallization being an active process in the magmatic system (Winter, 2010).

A Ti anomaly is displayed only by some amphibole hosted Si-MI in the tholeiitic basalt (Fig. 21A). There is no correlation to the Si content of the inclusion, excluding the crystallization of a mineral phase (e.g. Magnetite) at a certain point during fractional crystallization to be the reason for this. In addition fractional crystallization should lead to less evolved MI in the core of a mineral and more evolved MI in the outer growth zones. However, there is no such correlation in the amphibole-hosted Si-MI from the tholeiitic basalt. Both facts might show that next to fractional crystallization other processes are also important in the magmatic regime.

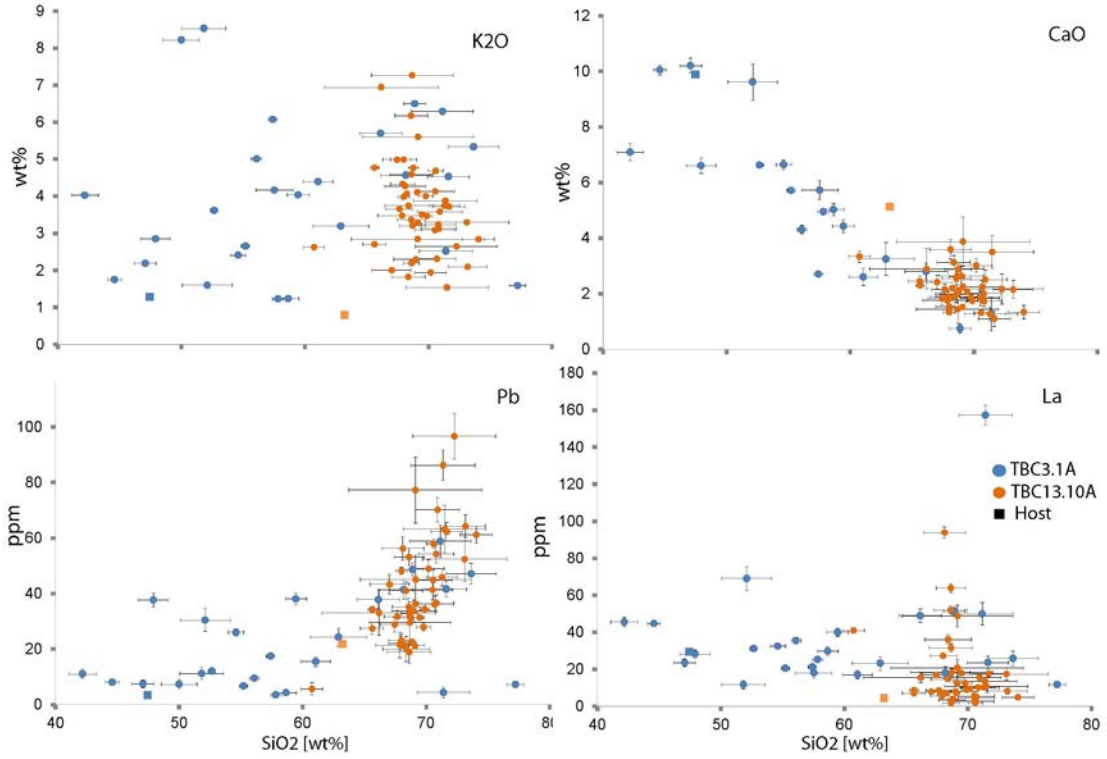


*Fig. 34:$SiO_2$ variation diagrams for amphibole-hosted MI from the tholeiitic basalt and plagioclase hosted MI from the tholeiitic andesite. $K_2O$ and CaO are rather mobile, La and Pb rather immobile and have comparable partition coefficients for hornblends and plagioclase in dacitic melts. A clear overlap of inclusions with comparable $SIO_2$ content can be recognized. Plagioclase-hosted MI from the tholeiitic andesite fit well in the trend defined by the MI from the tholeiitic basalt. This indicates that plagioclase is a late stage crystallization product of the same magma that crystallized the amphiboles in . TBC13.10A: Tholeiitic andesite; TBC3.1A: Tholeiitic basalt.*

However, in the context of fractional crystallization being at least partly involved in magma genesis at Bingham, plagioclase hosted melt inclusions from the tholeiitic andesite can be interpreted as the trachytic-rhyolitic end members in this fractional crystallization sequence. The main reason for this interpretation is that they often overlap with the element compositions recorded in equally evolved melt inclusions from the tholeiitic basalt, indicating that both have grown out of the same melt (Fig. 34). Despite slightly differing $K_2O/Na_2O$ ratios (Fig. 16) plagioclase-hosted melt inclusions from the tholeiitic andesite appear to be similar to those from the andesitic basalt, as evident by the same trace and REE patterns (Fig. 37). Plagioclase-hosted melt inclusions in the andesitic basalt and the tholeiitic

andesite both have a pronounced Ti anomaly, which can be attributed to earlier magnetite fractionation.
This observation can be seen as an argument against a common magmatic origin with respect to melt inclusion in the tholeiitic basalt, since those do not consistently show this anomaly as outlined above. In addition, as evident from Fig. 27A and Fig. 21A, the multi-element plots of MI from the tholeiitic basalt and the tholeiitic andesite differ especially for Ce and Sm,also questioning a common source magma. But, it has to be mentioned that the uncertainty on Sm concentrations are up to 80% with around 30% on average, which means that the negative spike in Fig. 27 should not be over interpreted since it would disappear if the uncertainty is considered.
Despite these differences, it is argued for a common magma trapped in amphibole and plagioclase-hosted MI. This magma at evolved least partly by fractional crystallization up to a dacitic-rhyolitic composition, recorded in plagioclase-hosted MI.
This interpretation is in accordance with modeling results from Waite et al. (1997) who suggested that fractional crystallization was active during magma evolution in Bingham. The evolved melt recorded in plagioclase and amphibole-hosted MI might represent the composition of the felsic magma of Hattori and Keith (2001) that, according to the authors, mixed in an upper crustal magma chamber with a more mafic magma to form ore related porphyry intrusion in Bingham.

In order to constrain the source of this evolving magma it is useful to look at the most mafic melt inclusions, since they should preserve a composition best reflecting source characteristics. From Fig. 21A, showing the composition of amphiboles hosted Si-MI from the tholeiitic basalt, we know that LILE are enriched compared to MORB. In addition HFSE are decoupled from LILE and Nb shows a pronounced negative spike. This pattern is a typical subduction zone feature, where the mobile components originate from slab derived fluids (Winter, 2010). The lower amount of HFSE is often attributed to the presence of residual titanate phases (Foley and Peccerillo, 1992). The clear calk-alkaline trend in Fig. 18 supports a subduction related genesis of these melts. From the constant HREE slope in Fig. 21B we can conclude that garnet was not present in the magmatic source, since it would fractionate Y and Yb leading to pronounced negative spikes. This observation can be taken to conclude, that the main source for the magmas is not located at deep mantle levels larger than 70km, since garnet occurs as a stable phase in these environments. The only way to produce a constant HREE slope in melts from a garnet bearing source would be a high degree of partial melting, exceeding 20% (Winter, 2010). However, in this case we would not expect such a strong decoupling of incompatible (LILE) and compatible elements since the differences in compatibility play a less important role during high degrees of partial melting.

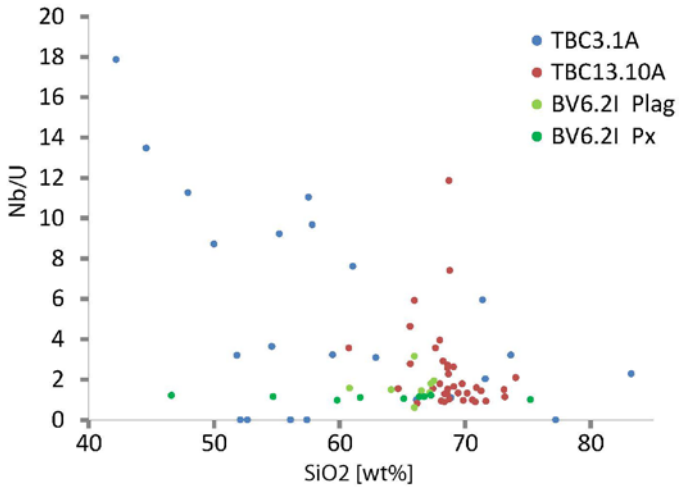


*Fig. 35: Nb/U ratio against $SiO_2$. Nb/U are both immobile and incompatible. The ratio indicates the amount of crustal contamination since U is dominantly present in the continental crust and Nb can be used as a source indicator. Increasing crustal contamination with ongoing evolution can be observed for the tholeiitic basalt TBC3.1A = tholeiitic basalt; TBC13.10A = tholeiitic andesite; BV6.2I = andesitic basalt*

If the magmatic origin is related to subduction, we have to assess the possibility of crustal contamination during magma rise through the continental crust. In Fig. 35 we can see that the Nb/U ratio decreases with increasing silicate content in amphibole hosted Si-MI from the tholeiitic basalt. Since Nb behaves incompatible and U is mainly present in the continental crust, we can derive increasing crustal contamination with ongoing evolution of amphibole-hosted melt inclusions in the tholeiitic basalt.

In Fig. 36 we can see a comparison of a multi element plot for mafic, amphibole hosted Si-MI from the tholeiitic basalt to volcanic rocks from the central volcanic zone (CVZ) of the Andes (average values from Thorpe et al. (1984)). Both have a similar pattern, although especially LILE and Ce in MI from Bingham show higher concentrations. In addition Zr is lower in the Bingham inclusions which might be attributed to the presence of zircons. The central volcanic zone in the Andes has the strongest decoupling of LILE and HFSE out of all volcanic zones in the Andes. It was suggested that this might point to a thickened continental crust in the CVZ compared to other volcanic zones in the Andes (Winter, 2010). If we transfer this argumentation to Bingham, this might imply that subduction related calk-alkaline magmas have penetrated through even thicker continental crust because the decoupling of LILE and HFSE is more pronounced in inclusions from Bingham. The other possibility to explain the CVZ pattern in Fig. 36 would be a lower degree of partial melting in metasomatized sub-continental lithospheric mantle (Pearce, 1983). Problematic with that argumentation is that such melts would have high content of Nb and Zr which is clearly not the case for the Bingham MI. So a thicker continental crust seems more likely indicating that assimilation has played a role during magma evolution in Bingham. A further argument for the assimilation of crustal material can be seen in the presence of paleoproterozoic zircon ages in the Bingham porphyry intrusions (Quadt et al., 2011).

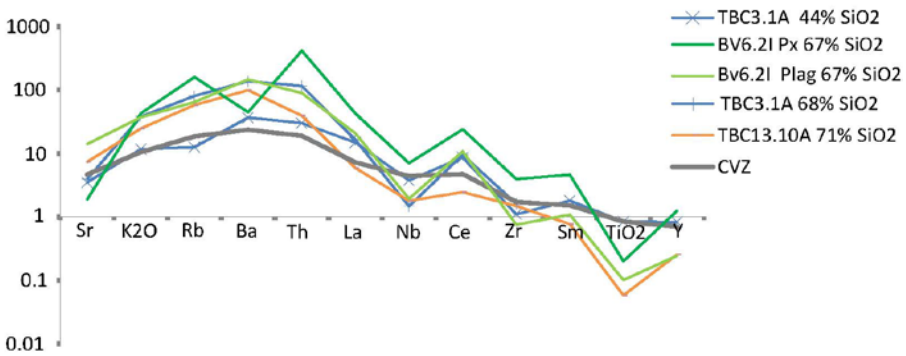


*Fig. 36 MORB normalized multi element plot of most mafic inclusions in amphiboles compared to average values form the central volcanic zone of the Andes. A correlation of the pattern is visible. Especially LILE are offset in their concentration. For comparison representative inclusions from Lark and the lava flow are shown. Notable difference is the Ba anomaly for the pyroxene hosted inclusions and their general higher concentration. Plagioclase hosted melt inclusions form the lava flow overlap nicely with amphibole hosted melt inclusions and plagioclase hosted MI from the lava flow, indicating a similar origin. Differences are lower Ce values in Lark plagioclase hosted MI and the missing Ti anomaly for amphibole hosted MI.*

Since lower and upper continental crust are chemically distinct, it might be possible to assess in which regions the majority of assimilation has taken place. In figure Fig. 37 the Rb/Ba ratio is used to assess the contribution of lower and upper crustal involvement. This ratio is applied due to three reasons. Frist, both elements behave incompatible so changes in the ratio should not arise due to fractional crystallization. Second, the upper and lower continental crust have a distinct Rb/Ba ratio. And third, both have similar Kds for amphiboles (same order of magnitude in basaltic and intermediate melts) for hornblends (Rollinson, 1993). From Fig. 37 we can see that for the basaltic amphibole-hosted Si-MI from the tholeiitic basalt the Rb/Ba ratio is rather low, in the range of 0.03, with two outliers. Compared to upper continental crust which has a Rb/Ba ratio of 0.15 (Taylor et al., 1981) this is considerably lower. The Rb/Ba ratio of lower continental crust is 0.015 (Weaver and Tarney, 1984) so a value of 0.03 might indicate a significant amount of lower crustal contamination.

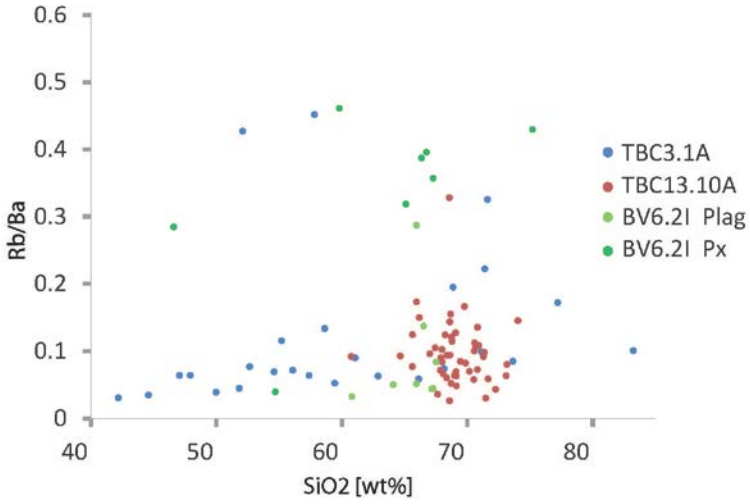


*Fig. 37: Ratio of Rb/Ba to test for crustal contamination. The ratio of Rb and Ba should not change during fluid alteration since they have similar Kds in hornblende. In addition they are not affected by fractional crystallization since both are incompatible. Low Rb/Ba values in basaltic amphibole- hosted MI form the tholeiitic basalt might indicate lower crustal contamination. See text for explanation..*

Taken together a scenario as follows can be imagined. Melts, associated with the subduction in the western cordilleran (Presnell, 1997) and derived from metasomatized mantle ponded at the crust-mantle boundary. Ongoing fractional crystallization lead to the formation of mafic cumulates. Assimilation of lower crustal material changed the magma composition until the magma was buoyant enough to rise further up into a mid-upper crustal magma chamber.
The contamination with lower crustal material might have led to early sulfide saturation, explaining the low Cu-content in the mafic amphibole hosted Si-MI from the tholeiitic basalt. The presence of sulfide melt inclusion in mafic cumulates (Fig. 10) and in amphiboles from the tholeiitic basalt is consistent with this interpretation. Sulfide exsolution might have led to the formation of sulfide rich cumulates in the lower crust.
A similar model, proposed for the central Andes, based on a more extensive geochemical and isotopic database, also postulates a scenario in which melts derived from metasomatized mantle ponded at the lower crust and underwent assimilation and fractional crystallization (Hildreth and Moorbath, 1988) before rising further up.

There are two arguments questioning that this interpretation is complete. First, there are no such felsic rocks in the area as inclusions recorded in the plagioclase from the tholeiitic andesite from Lark. This implies that the Bingham volcanic cannot be the results of a simple fractional crystallization trend, coupled with crustal assimilation (Audétat and Pettke, 2006). The majority of the rocks in the Bingham volcanic section are intermediate in composition, making a mafic magmatic component necessary to mix with the evolved magma. Second, assimilation and fractional crystallization should produce a certain pattern of MI composition with respect to position in the mineral (more primitive inclusions in the core, more evolved in growth zones). However, this is not observed. Thus, there is a need for another mafic magma that mixed with the evolved calc-alkaline magma explaining the dominance of intermediate volcanics.
The first evidence for magma mixing being present are sieve textured plagioclase and growth zones in amphiboles which have been described in the petrographic results (Fig. 7,Fig. 8,Fig. 9). Moreover, resorption textures in amphiboles and magmatic quartz, indicate that they have been out of equilibrium during magma evolution (Fig. 6 and Fig. 8), possibly due to a chemical change of magma composition after injection of a mafic magma. Maughan et al. (2002) suggests that the minette may represent this mafic magma input.

There is not much which can be stated here with a certain level of confidence about the pyroxene hosted MI in the andesitic basalt due to the reason mentioned before. The multi-element pattern in Fig. 37 is very similar to the other inclusions, implying that they are also related to the same magmatic system. This is also supported by similar REE patterns in Fig. 21, Fig. 24 and Fig. 27. In addition, the major oxide composition for inclusions from the andesitic basalt and the tholeiitic basalt overlap well for MgO, $TiO_2$ and MnO at a given $SiO_2$ content.

However, it is evident that they are the only inclusions with elevated Cu concentrations (Fig. 32B). Next to their elevated Cu content, high Rb and low Cs concentrations are probably reliable, based on the LA-ICPMS signal. Elevated K-values, especially compared to intermediate-MI from the tholeiitic basalt (Fig. 16) are also pretty reliable (Fig. 32A). In addition MI in pyroxenes from the andesitic basalt are distinguish by optical petrography from inclusions in plagioclase in the same sample (Fig. 11). Based on this we might conclude that the MI hosted in clinopyroxenes in the andesitic basalt are related to the same magmatic system as all other analyzed MI but possibly underwent a slightly different history.

Since this study deals with the magmatic evolution of a porphyry Cu forming system the main question which will be addresses here is why they have elevated Cu-contents. A possible scenario would be that the pyroxene hosted MI from the andesitic basalt have grown in a later magma batch. The later timing of this magma batch might be indicated by the higher K-values. As outlined by Müller et al. (1992) high K-magmas in subduction settings are often stratigraphically younger than less K-rich magmas, attributed to a slightly deeper source of the magma during late stage arc evolution. The deeper magma source for the case of Bingham might be related to the Eocene slap break off in the western cordilleran subduction zone (Presnell, 1997).

Ponding of the later magma batch at the lower crust hypothetically led to the dissolution of the previously formed sulfide cumulates and thus enriching the later stage melts in Cu, now recorded as the high Cu concentrations in pyroxene hosted MI from the andesitic basalt.

Thus, it can be imagined that the K and Cu rich characteristics of the pyroxene hosted Si-MI are inherited from a mafic parental magma which would be in accordance with suggestions of Maughan et al. (2002) who argued for a Cu-rich late stage mafic input at Bingham. This later stage mafic magma mixed in upper crustal levels with the evolved magma recorded in plagioclase-hosted Si-MI and lead to the observed petrographic indications for magma mixing.

### *5.3 Lessons from sulfide melt inclusion analysis*

As outlined before, a nice correlation with the function $y=Ax^n$ between sulfide melt inclusion composition and ID fluid composition was found (Fig. 30). In order to draw a conclusion from this correlation we have to think about the parameters that govern the transfer of metals from sulfide melt to a ID-fluid.

The major controls on the distribution of elements between a sulfide melt and a fluid phase are probably exerted by the mass factor o $R=\frac{m(sulfide\ melt)}{m(ID\ fluid)}$ and the distribution coefficient $Kd_{ID\ fluid}^{sulfide\ melt}$.

There are basically two options for the distribution coefficient Kd. Assuming that is similar for all metals, than the linear trend would possibly points to the fact the sulfide melt composition has an influence on the composition of the intermediate density fluids. If we assume the opposite, that the Kds are very different for all metals, we would expect an independency of the fluid composition and the sulfide melt composition. However, since we observe a dependency, we might conclude that also in this case the composition of the sulfide melt influenced the composition of the ID-fluid. Surely this does not tell us anything about the relative importance of this dependency. So, in any case, the correlation fits very well, implying that there is some relation between fluid and melt composition. This might be supported by the observations that the concentration ratio sulfide-melt/ID-fluid is

similar for Cu and Zn (Fig. 29). In this context we might conclude that the findings at least do not contradict recent view on the importance of a sulfide melt in pre-concentrating ore metals before they are released to a hydrothermal fluid (Wilkinson, 2013).
The obtained information might yield another important aspect. As mentioned the transfer of metals from the sulfide melt to the ID-fluid is likely to be governed by Kd and R. So if we could get a hold on R, we might learn about the partition behavior of certain ore metals between a sulfide melt and an ID-fluid.
According to Steinberger et al. (2013), a conservative estimate of the amount of fluid necessary to deposit the known mineralization at Bingham is 115Gt of fluid assuming a melt with a saturated water concentration of 5.7wt%. Assuming a 2000km$^3$ of silicate melt in an upper crustal magma chamber in around 4km depth with a temperature of 900°C (Steinberger et al., 2013) and sulfur concentration of around 500-1000ppm (based on our assumptions, an FeO content of 4% measured in Si-melt inclusions of trachytic composition in the tholeiitic basalt and experimental data from Carroll and Rutherford (1985)) we can estimate the approximate amount of available sulfide melt (assuming that all sulfur from the Si-melt contributes to the formation of a sulfide melt. Considering the values mentioned above the maximum amount of sulfide melt which can exsolve from the silicate melt in Bingham is around 2km$^3$. With a density of an assumed FeS melt of 4.86g/cm$^3$ this by far exceeds the weight of available fluid. Possibly, with such a rough estimate of R we might use the obtained correlation to get an idea about the Kd values for certain elements.
A last interesting fact is the similar concentration of Ag in the sulfide melt and the average grade of the ore mined up to today. Possibly this indicates that most of the Ag in Bingham was contributed by the sulfide melts. Up on destabilization this Ag content become available to the ID-ore fluid which is in accordance with findings of Keith et al. (1997) who suggested that Ag in the ore fluid mainly derived from dissolution of sulfide globules found in quenched latite dykes in the Bingham volcanics. If this is true, this would support the idea that the amount of sulfide melt exceeded the amount of ore fluid, since the concentration of Ag in the ore fluid is higher than in the sulfide melt (Fig. 29)

# 6 Conclusion – A genetic model for the Bingham Cu-porphyry system

A study on volcanic rocks contemporary to the mineralization at the large Bingham Cu-porphyry system revealed a complex stack of debris and lava flows of mostly dacitic to andesitic composition. Abundant orthopyroxenes rich mafic enclaves in lava flows are considered to be the results of fractional crystallization active during the magmatic history of the Bingham system. LA-ICPMS results of Si-melt inclusions from three different rocks sampled in the volcanic section support this interpretation. The enrichment and depletion pattern of major oxides and trace elements in amphibole-hosted Si-MI from the tholeiitic basalt indicate that fractional crystallization is active in the system. At comparable Si-content the composition of plagioclase-hosted Si-melt inclusions from the tholeiitic andesite and the andesitic basalt overlap nicely with the composition of Si-MI from the tholeiitic basalt. Together with the similar REE and trace element pattern this suggests that plagioclase was a later crystallizing phase in the same melt that was trapped in amphiboles from the tholeiitic basalt. Trace element concentration in this melt are typical for a calc-alkaline melt, revealing a strong subduction related imprint. Magma genesis in this context might be related to subduction in the western cordilleran during the Cretaceous. Chondrite like HREE depict that magma genesis was in regions shallower than 70km, the stability depth of garnet in the mantle. The high content of LILE is possibly due to a derivation of the magma from a metasomatized mantle source. The rising magmas might have ponded at the lower crust leading to a considerable degree of assimilation, expressed by a

low Rb/Ba ratio in the most mafic amphibole hosted MI from the tholeiitic basalt. During ponding of the magmas at the lower crustal boundary the formation of orthopyroxenes and phlogopite bearing mafic cumulates might have happened. Hypothetically the assimilation of lower crustal material might have triggered an early sulfide saturation explaining lower Cu-contents of around 20-70ppm in the MI from the tholeiitic basalt. Observed sulfide inclusion in orthopyroxenes form the mafic cumulates possibly support this idea.

Elevated and systematically with $SiO_2$ varying Nb/U ratios in this melt indicate ongoing crustal contamination during magma rise through a thickened continental crust. After evolving to a dacitic to rhyoliltic magma, mixing with a more mafic magma must have taken place in order to explain the dominance of intermediate volcanic rocks at Bingham. Petrographic observations of sieve textures plagioclase, zoned amphiboles and resorbed quartz and amphibole phenocrysts can be seen as an indication towards magma mixing.

High Cu and K-concentrations were detected in clinopyroxene hosted MI from the andesitic basalt. A similar compositional signature compared to the other Si-MI indicate that these Cu-rich melt are associated to the same magmatic system. However, certain trace elements like Cs and Rb, have different values in the clinopyroxene-hosted melt inclusions. Elevated K-concentrations in pyroxene-hosted MI from the andesitic basalt compared to basaltic-intermediate Si-MI from the tholeiitic basalt and tholeiitic andesite, possibly indicate a later stage magmatic input. The high Cu-concentrations possibly originate from dissolution of the previously formed mafic cumulates at the lower crust. Clinopyroxene hosted MI might inherit the signature of the mafic parental magma that mixed with the evolved rhyolitic magma recorded in plagioclase hosted MI.

Amphibole-hosted sulfide melt inclusions show high Cu-concentrations of around 2-4wt%. A correlation between the elemental composition of the sulfide melt and intermediate density fluid from the deep center at Bingham was shown, possibly indicating an influence of the sulfide melt composition on the ore fluid composition. The concentration ratio sulfide-melt/ID-fluid is similar for Cu and Zn, which are both enriched in the sulfide melt. Mo, Ag, Au, As and Pb are all enriched in the fluid. However, Ag concentrations in the sulfide match the average Ag-grade of the ore mined up to today very well. This possibly indicates that the amount of sulfide melt exceeded the amount available ore fluid in Bingham.

# 7 Outlook

There are several question which arise from this study.

In the first place the mechanisms of post entrapment modification in amphibole-hosted melt inclusions are not considered in this thesis. A first approach towards this problems would to determine which elements were affected by an compositional modification after melt entrapment. Element concentration maps of the host amphibole around depleted inclusions might yield valuable information about the elements that diffused (in?) and out of the inclusions. In addition heating experiments of inclusions in amphiboles might help to understand the modification mechanisms.

Further effort should be put into petrographic work, especially constraining the composition of the host minerals would be very helpful to better understand the wide concentration range in amphibole-hosted melt inclusions. Possibly this would help to reveal a certain pattern between melt inclusion composition and the host-composition. Especially the Al-content in the hornblends might yield interesting information about the formation depth of the minerals.

A great room for improvement is associated with the choice of the processing parameters for melt inclusion quantification. As outlined, a constant internal standard for the amphibole-hosted melt

inclusion is probably not correct and additional effort should be put into a thorough determination of a proper internal standard, possibly by EMPA-analysis of exposed melt inclusions. Additional support should be brought up for the assumptions that amphibole-hosted MI, considered in this thesis, are really unmodified.
The quantification of pyroxene hosted MI should also be reconsidered. Elevated Cu-concentrations might be due to post entrapment diffusion of Cu into the inclusions. Possibly this could be revealed by Cu-depletion in the host-clinopyroxene around the melt inclusion. Processing should be done in several ways in order to exclude concentrations shift due to systematic error during quantification.
In order to support the story presented here, it would be very interesting to study the composition of melt inclusions hosted in orthopyroxenes in the mafic cumulates. If their composition is similar to the most primitive inclusions analyzed here, this might yield real support for the hypothesis that their formation took place at the crust-mantle boundary and was associated with a sulfide saturation.

# 8 Acknowledgement

I want to thank Professor Dr. Christoph A. Heinrich for giving me the possibility to write this thesis. Dr. Philipp Weis, Katerina Schlöglova and Szandra Fekete are greatfully thanked for the assistance and company during field work in Bingham. The staff of Kennecott Copper is thanked for their support during field work and the permission to work on the mine site. The effort of Remy Lüchinger for thin section preparation is highly acknowledged. The input of Katerina Schlöglova for sample preparation and cleaning was very valuable. Dr. Markus Wälle is kindly acknowledged for his help during laser ablation and his time to discuss the quantification procedure with SILLS, which was a significant part of this thesis. Dr. Philipp Weis is thanked for his helpful comments on an early version of this thesis.
Special thanks go to my family for their support in the last two year. Their confidence is the basis of this work. My friends and girlfriend helped and trusted me in every situation which enabled me to finish this thesis. Their patience during writing is very much appreciated.
Finally, Professor Dr. Christoph A. Heinrich, Dr. Philipp Weis and Professor Dr. Olivier Bachmann are thanked for their helpful suggestions and supervision of this thesis.

# 9 References


Anderson, A. T., DAVIS, A. M., and LU, F., 2000, Evolution of Bishop Tuff rhyolitic magma based on melt and magnetite inclusions and zoned phenocrysts: Journal of Petrology, v. 41, p. 449-473.

Audétat, A., and Lowenstern, J. B., 2014, Melt Inclusions, *in* K.K., H. H. D. a. T., ed., Treatise on Geochemistry, 13, p. 143-173.

Audétat, A., and Pettke, T., 2006, Evolution of a porphyry-Cu mineralized magma system at Santa Rita, New Mexico (USA): Journal of Petrology, v. 47, p. 2021-2046.

Audétat, A., and Simon, A. C., 2012, Magmatic Controls on Porphyry Copper Genesis, *in* Hedenquist, J. W., Harris, M., and Camus, F., eds., Geology and Genesis of Major Copper Deposits and Districts of the World, 16. Special Publication, Society of Economic Geologists, p. 553-572.

Barton, P. B., and Skinner, B. J., 1979, Sulfide mineral stabilities, *in* Barnes, H. L., ed., Geochemistry of hydrothermal ore deposits: New York, Wiley-Interscience, p. 278-403.

Blundy, J., Cashman, K. V., and Berlo, K., 2008, Evolving magma storage conditions beneath Mount St. Helens inferred from chemical variations in melt inclusions from the 1980-1986 and current (2004-2006) eruptions: US Geological Survey professional paper, p. 755-790.

Carroll, M., and Rutherford, M., 1985, Sulfide and sulfate saturation in hydrous silicate melts: Journal of Geophysical Research: Solid Earth (1978–2012), v. 90, p. C601-C612.

Core, D. P., Kesler, S. E., and Essene, E. J., 2006, Unusually Cu-rich magmas associated with giant porphyry copper deposits: Evidence from Bingham, Utah: Geology, v. 34, p. 41-44.

Danyushevsky, L., Della-Pasqua, F., and Sokolov, S., 2000, Re-equilibration of melt inclusions trapped by magnesian olivine phenocrysts from subduction-related magmas: petrological implications: Contributions to Mineralogy and Petrology, v. 138, p. 68-83.

Deino, A., and Keith, J. D., 1997, Ages of Volcanic and Intrusive Rocks in the Bingham Mining District, Utah, *in* John, D. A., and Ballantyne, G. H., eds., Geology and Ore Deposits of the Oquirrh and Wasatch Mountains, Utah, 29. Guidebook Series, Society of Economic Geologists.

Foley, S., and Peccerillo, A., 1992, Potassic and ultrapotassic magmas and their origin: Lithos, v. 28, p. 181-185.

Gruen, G., Heinrich, C. A., and Schroeder, K., 2010, The Bingham Canyon porphyry Cu-Mo-Au deposit. II. Vein geometry and ore shell formation by pressure-driven rock extension: Economic Geology, v. 105, p. 69-90.

Guillong, M., and Heinrich, C. A., 2007, Sensitivity enhancement in laser ablation ICP-MS using small amounts of hydrogen in the carrier gas: Journal of Analytical Atomic Spectrometry, v. 22, p. 1488-1494.

Halter, W. E., Heinrich, C. A., and Pettke, T., 2004a, Laser-ablation ICP-MS analysis of silicate and sulfide melt inclusions in an andesitic complex II: evidence for magma mixing and magma chamber evolution: Contributions to Mineralogy and Petrology, v. 147, p. 397-412.

Halter, W. E., Heinrich, C. A., and Pettke, T., 2005, Magma evolution and the formation of porphyry Cu–Au ore fluids: evidence from silicate and sulfide melt inclusions: Mineralium Deposita, v. 39, p. 845-863.

Halter, W. E., Pettke, T., and Heinrich, C. A., 2002a, The origin of Cu/Au ratios in porphyry-type ore deposits: Science, v. 296, p. 1844-1846.

Halter, W. E., Pettke, T., and Heinrich, C. A., 2004b, Laser-ablation ICP-MS analysis of silicate and sulfide melt inclusions in an andesitic complex I: analytical approach and data evaluation: Contributions to Mineralogy and Petrology, v. 147, p. 385-396.

Halter, W. E., Pettke, T., Heinrich, C. A., and Rothen-Rutishauser, B., 2002b, Major to trace element analysis of melt inclusions by laser-ablation ICP-MS: methods of quantification: Chemical Geology, v. 183, p. 63-86.

Haskin, L. A., Haskin, M. A., and Frey, F. A., 1968, Relative and absolute terrestial abundances of rare earth, *in* Ahrens, L. H., ed., Origin and disstribution of the elements, 1: Oxford, Pergamon.

Hattori, K. H., and Keith, J. D., 2001, Contribution of mafic melt to porphyry copper mineralization: evidence from Mount Pinatubo, Philippines, and Bingham Canyon, Utah, USA: Mineralium Deposita, v. 36, p. 799-806.

Hedenquist, J. W., and Lowenstern, J. B., 1994, The role of magmas in the formation of hydrothermal ore deposits: Nature, v. 370, p. 519-527.

Heinrich, C., Pettke, T., Halter, W., Aigner-Torres, M., Audétat, A., Günther, D., Hattendorf, B., Bleiner, D., Guillong, M., and Horn, I., 2003, Quantitative multi-element analysis of minerals, fluid and melt inclusions by laser-ablation inductively-coupled-plasma mass-spectrometry: Geochimica et Cosmochimica Acta, v. 67, p. 3473-3497.

Hildreth, W., and Moorbath, S., 1988, Crustal contributions to arc magmatism in the Andes of central Chile: Contributions to mineralogy and petrology, v. 98, p. 455-489.

Irvine, T., and Baragar, W., 1971, A guide to the chemical classification of the common volcanic rocks: Canadian journal of earth sciences, v. 8, p. 523-548.

Kamenetsky, V., Métrich, N., and Cioni, R., 1995, Potassic primary melts of Vulsini (Roman Province): evidence from mineralogy and melt inclusions: Contributions to Mineralogy and Petrology, v. 120, p. 186-196.

Kamenetsky, V. S., and Danyushevsky, L. V., 2005, Letter: Metals in quartz-hosted melt inclusions: Natural facts and experimental artifacts: American Mineralogist, v. 90, p. 1674-1678.

Keith, J., Whitney, J., Hattori, K., Ballantyne, G., Christiansen, E., Barr, D., Cannan, T., and Hook, C., 1997, The role of magmatic sulfides and mafic alkaline magmas in the Bingham and Tintic mining districts, Utah: Journal of Petrology, v. 38, p. 1679-1690.

Kent, A. J., 2008, Melt inclusions in basaltic and related volcanic rocks: Reviews in Mineralogy and Geochemistry, v. 69, p. 273-331.

Kuno, H., 1968, Differentiation of basalt magmas, *in* H, H. H., and A, P., eds., Basalt: The Polervaart treatise on rocks of basaltic composition, 2: New York, Interscience, p. 623-688.

Landtwing, M. R., Furrer, C., Redmond, P. B., Pettke, T., Guillong, M., and Heinrich, C. A., 2010, The Bingham Canyon porphyry Cu-Mo-Au deposit. III. Zoned copper-gold ore deposition by magmatic vapor expansion: Economic Geology, v. 105, p. 91-118.

Lowell, J. D., and Guilbert, J. M., 1970, Lateral and vertical alteration-mineralization zoning in porphyry ore deposits: Economic Geology, v. 65, p. 373-408.

Maughan, D. T., Keith, J. D., Christiansen, E. H., Pulsipher, T., Hattori, K., and Evans, N. J., 2002, Contributions from mafic alkaline magmas to the Bingham porphyry Cu–Au–Mo deposit, Utah, USA: Mineralium Deposita, v. 37, p. 14-37.

Middlemost, E. A., 1975, The basalt clan: Earth-Science Reviews, v. 11, p. 337-364.

Moore, G., and Carmichael, I., 1998, The hydrous phase equilibria (to 3 kbar) of an andesite and basaltic andesite from western Mexico: constraints on water content and conditions of phenocryst growth: Contributions to Mineralogy and Petrology, v. 130, p. 304-319.

Moore, W. J., 1973, A Summary of Radiometric Ages of Igneous Rocks in the Oquirrh Mountains, North-Central Utah: Economic Geology, v. 68, p. 97-101.

Müller, D.-G. D., Rock, N., and Groves, D., 1992, Geochemical discrimination between shoshonitic and potassic volcanic rocks in different tectonic settings: a pilot study: Mineralogy and Petrology, v. 46, p. 259-289.

Nakamura, N., 1974, Determination of REE, Ba, Fe, Mg, Na and K in carbonaceous and ordinary chondrites: Geochimica et Cosmochimica Acta, v. 38, p. 757-775.

Parry, W., Wilson, P. N., Moser, D., and Heizler, M. T., 2001, U-Pb dating of Zircon and 40Ar/39Ar dating of Biotite at Bingham, Utah: Economic Geology, v. 96, p. 1671-1683.

Pearce, J. A., 1982, Trace element characteristics of lavas from destructive plate boundaries: Andesites, p. 525-548.

Pearce, J. A., 1983, Role of sub-continental lithosphere in magma genesis at active continental margins, *in* C.J, H., and M.J, N., eds., Continental basalts and mantle xenolith: Nantwich, Shiva, p. 230-249.

Pettke, T., Halter, W. E., Webster, J. D., Aigner-Torres, M., and Heinrich, C. A., 2004, Accurate quantification of melt inclusion chemistry by LA-ICPMS: a comparison with EMP and SIMS and advantages and possible limitations of these methods: Lithos, v. 78, p. 333-361.

Porter, J. P., Schroeder, K., and Austin, G., 2012, Geology of the Bingham Canyon Porphyry Cu-Mo-Au Deposit, Utah, *in* Hedenquist, J. W., Harris, M., and Camus, F., eds., Geology and Genesis of Major Copper Deposits and Districts of the World, 16. Special Publication, Society of Economic Geologists, p. 127 - 146.

Presnell, R., and Parry, W. T., 1995, Evidence of Jurassic tectonism from the Barneys Canyon gold deposit, Oquirrh Mountains, Utah: Geological Society of America Special Papers, v. 299, p. 313-326.

Presnell, R. D., 1997, Structural control on the Plutonism and Metallogeny in the Wasatch and Oquirrh Mountains, Utah, *in* John, D. A., and Ballantyne, G. H., eds., Geology and Ore Deposits of the Oquirrh and Wasatch Mountains, Utah, 29. Guidebook Series, Society of Economic Geologists, p. 1 - 9.

Quadt, A. v., Erni, M., Martinek, K., Moll, M., Peytcheva, I., and Heinrich, C. A., 2011, Zircon crystallization and the lifetimes of ore-forming magmatic hydrothermal systems: Geology, v. 39, p. 731-734.

Redmond, P., Einaudi, M., Inan, E., Landtwing, M., and Heinrich, C., 2004, Copper deposition by fluid cooling in intrusion-centered systems: new insights from the Bingham porphyry ore deposit, Utah: Geology, v. 32, p. 217-220.

Reubi, O., and Blundy, J., 2008, Assimilation of plutonic roots, formation of high-K 'exotic'melt inclusions and genesis of andesitic magmas at Volcán de Colima, Mexico: Journal of Petrology, v. 49, p. 2221-2243.

Richards, J. P., 2014, The oxidation state, and sulfur and Cu contents of arc magmas: implications for metallogeny: Lithos.

Rollinson, H. R., 1993, Using geochemical data: evaluation, presentation, interpretation, Longman Group.

Seo, J. H., Guillong, M., and Heinrich, C. A., 2009, The role of sulfur in the formation of magmatic–hydrothermal copper–gold deposits: Earth and Planetary Science Letters, v. 282, p. 323-328.

Seo, J. H., Guillong, M., and Heinrich, C. A., 2012, Separation of molybdenum and copper in porphyry deposits: The roles of sulfur, redox, and pH in ore mineral deposition at Bingham Canyon: Economic Geology, v. 107, p. 333-356.

Sillitoe, R. H., 2010, Porphyry copper systems: Economic Geology, v. 105, p. 3-41.

Spandler, C., O'Neill, H. S. C., and Kamenetsky, V., 2007, Survival times of anomalous melt inclusions from element diffusion in olivine and chromite: Nature, v. 447, p. 303-306.

Stavast, W. J., Keith, J. D., Christiansen, E. H., Dorais, M. J., Tingey, D., Larocque, A., and Evans, N., 2006, The fate of magmatic sulfides during intrusion or eruption, Bingham and Tintic districts, Utah: Economic Geology, v. 101, p. 329-345.

Steinberger, I., Hinks, D., Driesner, T., and Heinrich, C. A., 2013, Source Plutons Driving Porphyry Copper Ore Formation: Combining Geomagnetic Data, Thermal Constraints, and Chemical Mass Balance to Quantify the Magma Chamber Beneath the Bingham Canyon Deposit: Economic Geology, v. 108, p. 605-624.

Taylor, S., McLennan, S., Armstrong, R., and Tarney, J., 1981, The composition and evolution of the continental crust: rare earth element evidence from sedimentary rocks [and discussion]: Philosophical Transactions of the Royal Society of London A: Mathematical, Physical and Engineering Sciences, v. 301, p. 381-399.

Thorpe, R., Francis, P., O'Callaghan, L., Hutchison, R., and Turner, J., 1984, Relative Roles of Source Composition, Fractional Crystallization and Crustal Contamination in the Petrogenesis of Andean Volcanic Rocks [and Discussion]: Philosophical Transactions of the Royal Society of London A: Mathematical, Physical and Engineering Sciences, v. 310, p. 675-692.

Ulrich, T., Guenther, D., and Heinrich, C., 1999, Gold concentrations of magmatic brines and the metal budget of porphyry copper deposits: Nature, v. 399, p. 676-679.

Waite, K. A., Keith, J. D., Christiansen, E. H., Whitney, J. A., Hattori, K., Tingey, D. G., and Hook, C. J., 1997, Petrogenesis of the Volcanic and Intrusive Rocks Associated with the Bingham Canyon Porphyry Cu-Au-Mo Deposit, Utah, *in* John, D. A., and Ballantyne, G. H., eds., Geology and Ore Deposits of the Oquirrh and Wasatch Mountains, Utah, 29. Guidebook Series, Society of Economic Geologists.

Weaver, B. L., and Tarney, J., 1984, Empirical approach to estimating the composition of the continental crust.
Wilkinson, J. J., 2013, Triggers for the formation of porphyry ore deposits in magmatic arcs: Nature Geoscience, v. 6, p. 917-925.
Winter, J. D., 2010, Subduction related igneous acitvity, Part II - Continental Arcs, *in* Folchetti, N., ed., Principles of Igenous and Metamorphic Petrology: New Jersey, Pearson Education Inc, p. 352-377.
Zajacz, Z., and Halter, W., 2007, LA-ICPMS analyses of silicate melt inclusions in co-precipitated minerals: quantification, data analysis and mineral/melt partitioning: Geochimica et cosmochimica acta, v. 71, p. 1021-1040.
Zajacz, Z., Hanley, J. J., Heinrich, C. A., Halter, W. E., and Guillong, M., 2009, Diffusive reequilibration of quartz-hosted silicate melt and fluid inclusions: Are all metal concentrations unmodified?: Geochimica et Cosmochimica Acta, v. 73, p. 3013-3027.

# 10 Appendix

LA-ICPMS analyses of amphibole-hosted Si-MI in **tholeiitic basalt**, Bingham canyon volcanic suite. Element concentrations and uncertainty

Table 1.1

| Melt inclusions | 15jn01a04 | | 15jn01a05 | | 15jn01a07 | | 15jn01a08 | | 15jn01a10 | | 15jn01a12 | | 15jn01b03 | | 15jn01b04 | | 15jn01c03 | | 15jn01c06 | | 15jn01c07 | |
|---|---|---|---|---|---|---|---|---|---|---|---|---|---|---|---|---|---|---|---|---|---|---|
| SiO2 | 57.41 | 1% | 52.66 | 1% | 56.27 | 1% | 59.96 | 1% | 63.87 | 1% | 53.96 | 0% | 372.82 | 6% | 55.42 | 1% | 233.84 | 5% | 64.96 | 5% | 52.10 | 4% |
| TiO2 | 0.89 | 2% | 1.12 | 1% | 1.68 | 1% | 1.26 | 1% | 0.78 | 2% | 0.82 | 1% | <2.42 | | 1.02 | 2% | <1.45 | | <0.18 | | 1.16 | 7% |
| Al2O3 | 14.13 | 0% | 14.19 | 0% | 10.02 | 0% | 8.03 | 0% | 7.01 | 0% | 14.95 | 0% | 13.84 | 10% | 11.00 | 0% | 16.84 | 5% | 14.67 | 1% | 14.61 | 1% |
| FeO | 6.30 | 1% | 7.47 | 1% | 8.55 | 1% | 8.40 | 1% | 8.79 | 1% | 6.69 | 1% | <11.04 | | 10.23 | 1% | <6.02 | | <1.17 | | 5.69 | 7% |
| MnO | 0.12 | 1% | 0.12 | 1% | 0.10 | 1% | 0.14 | 1% | 0.16 | 1% | 0.15 | 1% | <0.23 | | 0.18 | 1% | <0.12 | | <0.02 | | 0.17 | 5% |
| MgO | 6.19 | 0% | 7.65 | 0% | 9.51 | 0% | 9.73 | 0% | 8.01 | 0% | 6.15 | 0% | <3.06 | | 8.82 | 0% | <2.05 | | 5.06 | 3% | 8.68 | 1% |
| CaO | 2.70 | 5% | 6.63 | 1% | 7.73 | 1% | 6.41 | 2% | 5.45 | 2% | 5.67 | 1% | <16.83 | | 6.36 | 2% | <10.59 | | 10.52 | 9% | 9.62 | 7% |
| Na2O | 2.18 | 0% | 2.54 | 0% | 1.26 | 0% | 1.25 | 0% | 1.26 | 0% | 2.20 | 0% | <0.69 | | 1.48 | 0% | <0.44 | | 2.11 | 2% | 2.37 | 1% |
| K2O | 6.08 | 0% | 3.62 | 0% | 0.88 | 0% | 0.82 | 0% | 0.68 | 1% | 5.39 | 0% | 14.35 | 2% | 1.49 | 0% | 9.94 | 2% | 5.50 | 1% | 1.60 | 2% |
| Total | 100.00 | 0% | 100.00 | 0% | 100.00 | 0% | 100.00 | 0% | 100.00 | 0% | 100.00 | 0% | 405.01 | 0% | 100.00 | 0% | 264.62 | 0% | 106.82 | 0% | 100.00 | 0% |
| mass factor | 0.41 | 0% | 0.93 | 0% | 0.89 | 0% | 0.90 | 0% | 0.90 | 0% | 0.94 | 0% | 0.03 | 0% | 0.65 | 0% | 0.03 | 0% | 0.19 | 0% | 0.27 | 0% |
| P3 | | | | | | | | | | | | | | | | | | | | | | |
| Sc | | | | | | | | | | | | | | | | | | | | | | |
| V5 | 177.09 | 3% | 228.22 | 2% | 315.62 | 2% | 263.81 | 2% | 172.89 | 3% | 163.64 | 2% | <855.21 | | 249.67 | 3% | <484.46 | | <102.10 | | 164.55 | 17% |
| Cr | 204.39 | 13% | 316.26 | 6% | 482.52 | 6% | 574.22 | 5% | 316.40 | 11% | 151.86 | 8% | <5346.70 | | 585.88 | 6% | <2485.48 | | <492.14 | | <427.48 | |
| Co | | | | | | | | | | | | | | | | | | | | | | |
| Ni | 75.42 | 11% | 72.32 | 8% | 89.03 | 9% | 78.43 | 9% | 65.17 | 13% | 54.46 | 8% | <1109.19 | | 77.02 | 11% | <788.31 | | <129.74 | | <139.26 | |
| Cu | <2.13 | | <1.33 | | <1.83 | | <1.69 | | <2.08 | | <1.07 | | <96.52 | | <1.93 | | <71.38 | | <14.17 | | 2.75 | 67% |
| Rb | 148.94 | 1% | 81.41 | 2% | 4.77 | 11% | 4.09 | 11% | 2.65 | 19% | 237.05 | 1% | 1445.80 | 4% | 58.53 | 3% | 1606.39 | 3% | 162.02 | 5% | 63.29 | 8% |
| Sr | 224.64 | 2% | 381.96 | 1% | 263.24 | 1% | 191.61 | 1% | 147.84 | 2% | 264.30 | 1% | <459.65 | | 104.14 | 3% | 1432.40 | 9% | 169.48 | 15% | 268.97 | 7% |
| Y8 | 26.44 | 5% | 31.43 | 3% | 23.11 | 4% | 23.06 | 4% | 37.30 | 4% | 27.37 | 3% | <291.72 | | 102.26 | 2% | <97.79 | | <18.39 | | 107.79 | 7% |
| Zr | | | | | | | | | | | | | | | | | | | | | | |
| Nb | | | | | | | | | | | | | | | | | | | | | | |
| Ba | 2342.82 | 1% | 1059.96 | 1% | 302.71 | 3% | 159.92 | 4% | 183.38 | 5% | 1590.84 | 1% | 1271.39 | 40% | 234.91 | 4% | 956.05 | 32% | 3359.00 | 2% | 148.22 | 25% |
| Cs | 1.04 | 8% | 0.47 | 19% | <0.08 | | <0.04 | | <0.13 | | 2.18 | 7% | 20.46 | 23% | 0.92 | 15% | 39.05 | 13% | 5.44 | 14% | 2.39 | 27% |
| La | 21.30 | 6% | 31.25 | 3% | 21.12 | 4% | 16.29 | 4% | 24.17 | 5% | 26.38 | 2% | <147.59 | | 32.45 | 4% | <73.78 | | <12.82 | | 69.04 | 9% |
| Ce | 62.51 | 3% | 97.98 | 1% | 66.20 | 2% | 53.56 | 2% | 84.50 | 3% | 77.47 | 1% | <291.05 | | 123.53 | 2% | <132.06 | | <23.05 | | 222.99 | 5% |
| Nd | | | | | | | | | | | | | | | | | | | | | | |
| Sm | | | | | | | | | | | | | | | | | | | | | | |
| Yb | | | | | | | | | | | | | | | | | | | | | | |
| Pb | 17.46 | 3% | 12.03 | 5% | 4.27 | 11% | 2.99 | 13% | 1.38 | 27% | 14.11 | 4% | <57.68 | | 2.40 | 21% | 356.94 | 8% | 59.21 | 10% | 30.41 | 13% |
| Th | 8.85 | 3% | 10.06 | 4% | 2.73 | 11% | 13.98 | 4% | 10.66 | 7% | 5.85 | 5% | <15.76 | | 0.64 | 26% | 66.66 | 11% | 19.18 | 10% | 8.36 | 17% |
| U2 | 2.35 | 6% | 2.03 | 10% | 1.02 | 17% | 1.66 | 12% | 0.50 | 31% | 1.19 | 11% | 5.48 | 56% | <0.16 | | 5.01 | 29% | 6.14 | 16% | 2.15 | 34% |
| Ho | | | | | | | | | | | | | | | | | | | | | | |
| B1 | 60.64 | 23% | 71.42 | 17% | <53.73 | | <46.32 | | <61.74 | | 41.09 | 28% | <2577.00 | | <44.96 | | <2179.42 | | -18.37<I<503.28 | | <337.40 | |



Major oxide concentrations in wt%
Trace element concentrations in ppm

continued on next page

LA-ICPMS analyses of amphibole-hosted Si-MI in **tholeiitic basalt**, Bingham canyon volcanic suite. Element concentrations and uncertainty

Table 1.2

| Melt inclusions | 15jn01c08 | | 15jn01c09 | | 15jn01c10 | | 15jn01c12 | | 15jn01c13 | | 15jn08b08 | | 15jn08b09 | | 15jn08b11 | | 15jn08b12 | | 15jn08b13 | |
|---|---|---|---|---|---|---|---|---|---|---|---|---|---|---|---|---|---|---|---|---|
| SiO2 | 56.09 | 1% | 68.64 | 5% | 50.95 | 1% | 77.23 | 1% | 42.32 | 2% | 63.55 | 5% | 47.08 | 2% | 54.61 | 1% | 50.22 | 1% | 61.68 | 1% |
| TiO2 | 0.57 | 3% | <0.32 | | 0.98 | 2% | <0.05 | | 2.43 | 2% | 1.55 | 8% | 0.87 | 4% | 0.77 | 2% | 1.14 | 1% | 0.82 | 2% |
| Al2O3 | 14.60 | 0% | 14.52 | 2% | 14.47 | 0% | 14.40 | 0% | 15.04 | 0% | 14.08 | 1% | 14.22 | 1% | 14.11 | 0% | 14.95 | 0% | 10.00 | 0% |
| FeO | 7.55 | 1% | 3.54 | 22% | 7.92 | 1% | 1.56 | 6% | 13.15 | 2% | 8.03 | 8% | 7.98 | 2% | 6.32 | 2% | 9.43 | 1% | 7.99 | 1% |
| MnO | 0.14 | 1% | 0.21 | 7% | 0.15 | 1% | 0.02 | 8% | 0.11 | 3% | 0.08 | 15% | 0.19 | 2% | 0.12 | 2% | 0.13 | 1% | 0.13 | 1% |
| MgO | 4.47 | 1% | 6.91 | 3% | 8.22 | 0% | 1.06 | 3% | 13.53 | 0% | 3.51 | 6% | 11.32 | 0% | 8.40 | 0% | 9.97 | 0% | 7.72 | 0% |
| CaO | 4.31 | 3% | 3.53 | 31% | 7.52 | 2% | <0.39 | | 1.44 | 19% | 2.46 | 39% | 10.21 | 3% | 6.64 | 3% | 6.36 | 1% | 5.62 | 2% |
| Na2O | 3.27 | 0% | <0.11 | | 2.53 | 0% | 0.35 | 2% | 1.53 | 1% | 1.33 | 3% | 1.94 | 1% | 2.63 | 0% | 1.19 | 0% | 1.11 | 0% |
| K2O | 5.01 | 0% | <0.09 | | 3.26 | 0% | 1.59 | 0% | 6.45 | 0% | 1.40 | 2% | 2.19 | 1% | 2.41 | 0% | 2.59 | 0% | 0.93 | 1% |
| Total | 100.00 | 0% | 101.36 | 0% | 100.00 | 0% | 100.21 | 0% | 100.00 | 0% | 100.00 | 0% | 100.00 | 0% | 100.00 | 0% | 100.00 | 0% | 100.00 | 0% |
| mass factor | 0.36 | 0% | 0.18 | 0% | 0.74 | 0% | 0.58 | 0% | 0.45 | 0% | 0.14 | 0% | 0.43 | 0% | 0.59 | 0% | 0.81 | 0% | 0.90 | 0% |
| P3 | | | | | | | | | | | <284.95 | | <78.04 | | 213.69 | 14% | 51.72 | 19% | <56.72 | |
| Sc | | | | | | | | | | | <34.22 | | 43.61 | 9% | 41.26 | 7% | 20.61 | 5% | 20.26 | 8% |
| V5 | 169.72 | 3% | <114.83 | | 166.30 | 4% | <18.16 | | 273.17 | 5% | 268.78 | 16% | 227.84 | 5% | 156.49 | 5% | 241.14 | 2% | 182.07 | 3% |
| Cr | 538.97 | 6% | <643.61 | | 681.71 | 8% | <88.40 | | 1088.26 | 11% | <361.65 | | 285.10 | 16% | 202.43 | 17% | 90.90 | 13% | 177.79 | 13% |
| Co | | | | | | | | | | | <42.66 | | 37.38 | 14% | 34.33 | 11% | 37.10 | 5% | 34.48 | 7% |
| Ni | 30.64 | 40% | <191.02 | | 30.73 | 30% | <21.10 | | 216.35 | 11% | <147.74 | | 110.31 | 17% | 114.82 | 14% | 98.85 | 7% | 78.28 | 11% |
| Cu | <1.19 | | <18.54 | | <2.80 | | <3.39 | | 4.51 | 35% | <12.95 | | <3.35 | | <3.07 | | 1.58 | 31% | <2.49 | |
| Rb | 129.36 | 1% | <8.76 | | 99.27 | 3% | 49.51 | 4% | 190.40 | 2% | 22.78 | 21% | 75.72 | 5% | 69.23 | 3% | 149.72 | 1% | 18.55 | 6% |
| Sr | 491.97 | 1% | <72.89 | | 397.19 | 1% | 663.17 | 1% | 205.78 | 4% | 585.81 | 4% | 303.35 | 3% | 332.40 | 1% | 213.97 | 1% | 136.17 | 2% |
| Y8 | 24.16 | 5% | <23.83 | | 27.64 | 5% | <3.62 | | 8.04 | 32% | <26.94 | | 36.50 | 8% | 54.51 | 4% | 18.39 | 4% | 23.40 | 5% |
| Zr | | | | | | | | | | | 578.13 | 4% | 63.40 | 11% | 243.79 | 2% | 78.48 | 3% | 143.73 | 3% |
| Nb | | | | | | | | | | | 15.99 | 41% | 10.06 | 18% | 11.50 | 11% | 9.86 | 6% | 11.21 | 8% |
| Ba | 1815.61 | 1% | <178.34 | | 1187.91 | 2% | 288.00 | 5% | 6916.88 | 1% | 597.61 | 10% | 1188.16 | 3% | 1002.73 | 2% | 363.20 | 2% | 195.66 | 4% |
| Cs | 0.76 | 11% | 0.63 | 51% | 0.48 | 28% | 0.52 | 28% | 1.06 | 21% | 0.23 | 75% | 0.89 | 30% | 1.54 | 14% | 1.48 | 9% | 0.25 | 36% |
| La | 35.51 | 3% | 28.02 | 33% | 26.22 | 5% | 11.79 | 11% | 6.91 | 27% | 33.96 | 21% | 23.51 | 9% | 32.54 | 4% | 18.76 | 3% | 16.83 | 5% |
| Ce | 81.32 | 2% | <36.22 | | 72.80 | 3% | 17.54 | 12% | 17.73 | 19% | 89.49 | 14% | 61.35 | 6% | 89.88 | 3% | 70.71 | 2% | 59.44 | 3% |
| Nd | | | | | | | | | | | <54.94 | | 46.30 | 14% | 70.70 | 7% | 41.29 | 5% | 34.83 | 8% |
| Sm | | | | | | | | | | | <31.34 | | 13.06 | 26% | 10.53 | 23% | 6.87 | 14% | 7.28 | 18% |
| Yb | | | | | | | | | | | <15.14 | | <3.62 | | 6.61 | 22% | 1.64 | 27% | 3.34 | 25% |
| Pb | 9.54 | 6% | <8.56 | | 10.51 | 9% | 7.24 | 12% | 4.56 | 24% | <5.98 | | 7.47 | 19% | 25.96 | 5% | 2.77 | 11% | 2.99 | 15% |
| Th | 8.36 | 4% | 15.47 | 17% | 4.87 | 10% | 11.80 | 6% | <0.55 | | 32.62 | 8% | <1.95 | | 13.46 | 5% | 1.42 | 11% | 13.50 | 5% |
| U2 | 1.17 | 9% | 6.36 | 23% | 1.46 | 17% | 4.57 | 10% | 0.45 | 32% | 4.07 | 20% | <0.86 | | 3.16 | 10% | 0.36 | 20% | 0.45 | 26% |
| Ho | | | | | | | | | | | <4.19 | | <1.05 | | 2.77 | 14% | 0.91 | 15% | 1.04 | 18% |
| B1 | 42.37 | 27% | <486.55 | | <83.91 | | <87.29 | | <105.94 | | <313.62 | | <87.15 | | <83.36 | | <28.95 | | <69.97 | |



Major oxide concentrations in wt%
Trace element concentrations in ppm

continued on next page

LA-ICPMS analyses of amphibole-hosted Si-MI in **tholeiitic basalt**, Bingham canyon volcanic suite. Element concentrations and uncertainty

Table 1.3

| Melt inclusions | 15jn08b15 | | 15jn08b16 | | 15jn08b18 | | 15jn08b19 | | 15jn08b20 | | 15jn08b21 | | 15jn08b23 | | 15jn08b24 | | 15jn08b26 | | 15jn08b28 | | 15jn08b29 | |
|---|---|---|---|---|---|---|---|---|---|---|---|---|---|---|---|---|---|---|---|---|---|---|
| SiO2 | 49.71 | 1% | 48.01 | 1% | 56.94 | 2% | 114.19 | 5% | 55.89 | 1% | 57.25 | 1% | 67.22 | 2% | 226.73 | 2% | 55.37 | 1% | 148.34 | 4% | 55.21 | 1% |
| TiO2 | 0.79 | 2% | 1.03 | 1% | 1.48 | 4% | <0.19 | | 0.25 | 4% | 0.19 | 4% | 0.08 | 36% | <0.47 | | 0.49 | 2% | 4.25 | 6% | 0.71 | 1% |
| Al2O3 | 7.01 | 0% | 8.02 | 0% | 8.99 | 1% | 13.99 | 2% | 4.01 | 0% | 3.01 | 0% | 14.09 | 0% | 10.91 | 3% | 14.98 | 0% | 14.12 | 3% | 14.18 | 0% |
| FeO | 9.83 | 1% | 9.66 | 1% | 10.26 | 3% | <1.12 | | 8.50 | 1% | 6.53 | 1% | 2.38 | 7% | <2.35 | | 5.93 | 1% | <2.78 | | 7.02 | 1% |
| MnO | 0.19 | 1% | 0.21 | 1% | 0.17 | 3% | <0.02 | | 0.28 | 1% | 0.22 | 1% | 0.10 | 3% | <0.04 | | 0.11 | 1% | <0.05 | | 0.13 | 1% |
| MgO | 12.29 | 0% | 13.23 | 0% | 9.95 | 1% | <0.29 | | 12.56 | 0% | 13.58 | 0% | 1.29 | 4% | <0.71 | | 6.11 | 0% | <0.84 | | 7.65 | 0% |
| CaO | 13.68 | 1% | 13.63 | 1% | 5.98 | 6% | <1.36 | | 13.35 | 1% | 14.25 | 1% | <0.69 | | <3.58 | | 4.49 | 2% | <4.09 | | 5.71 | 1% |
| Na2O | 1.45 | 0% | 1.40 | 0% | 1.35 | 1% | 1.82 | 3% | 0.88 | 1% | 0.76 | 1% | 3.25 | 0% | 17.56 | 0% | 2.45 | 0% | <0.18 | | 2.73 | 0% |
| K2O | 1.04 | 0% | 0.81 | 1% | 0.88 | 2% | 12.37 | 1% | 0.29 | 1% | 0.20 | 1% | 7.96 | 0% | 19.17 | 0% | 6.07 | 0% | <0.18 | | 2.65 | 0% |
| Total | 100.00 | 0% | 100.00 | 0% | 100.00 | 0% | 146.37 | 0% | 100.00 | 0% | 100.00 | 0% | 100.37 | 0% | 278.37 | 0% | 100.00 | 0% | 170.72 | 0% | 100.00 | 0% |
| mass factor | 0.80 | 0% | 0.77 | 0% | 0.48 | 0% | 0.16 | 0% | 0.84 | 0% | 0.86 | 0% | 0.45 | 0% | 0.08 | 0% | 0.73 | 0% | 0.06 | 0% | 0.88 | 0% |
| P3 | 93.25 | 21% | 82.46 | 18% | <196.25 | | -621.00<I<236.13 | | <88.38 | | <63.97 | | <177.46 | | <599.31 | | 104.71 | 13% | <489.23 | | 64.32 | 21% |
| Sc | 35.58 | 5% | 40.60 | 4% | 22.20 | 24% | 34.16 | 58% | 27.03 | 8% | 24.80 | 7% | <10.16 | | <60.91 | | 12.77 | 9% | 93.19 | 29% | 20.02 | 6% |
| V5 | 251.95 | 2% | 304.90 | 2% | 284.26 | 6% | <74.18 | | 106.31 | 4% | 87.21 | 4% | <30.77 | | <183.88 | | 117.67 | 3% | <171.77 | | 153.05 | 2% |
| Cr | 289.12 | 8% | 425.51 | 6% | 293.64 | 23% | 582.95 | 82% | 2122.21 | 3% | 1088.66 | 5% | <184.49 | | <864.60 | | 278.14 | 8% | <1247.40 | | 440.70 | 5% |
| Co | 48.74 | 5% | 47.87 | 5% | 43.58 | 19% | <32.18 | | 32.88 | 8% | 37.94 | 7% | <13.35 | | <73.50 | | 25.08 | 7% | <88.77 | | 29.13 | 6% |
| Ni | 103.36 | 8% | 86.04 | 9% | 92.85 | 28% | <101.99 | | 127.78 | 9% | 138.30 | 8% | <41.82 | | <194.37 | | 58.37 | 10% | <302.57 | | 70.03 | 9% |
| Cu | 3.19 | 34% | 2.78 | 29% | <8.13 | | <11.77 | | <4.39 | | <3.03 | | <7.99 | | 39.74 | 31% | <1.61 | | <23.81 | | <1.85 | |
| Rb | 10.54 | 7% | 5.80 | 10% | <3.71 | | 454.84 | 3% | <1.34 | | <0.92 | | 238.76 | 2% | 780.34 | 2% | 223.10 | 1% | <17.85 | | 101.77 | 2% |
| Sr | 176.55 | 2% | 192.23 | 2% | 198.40 | 5% | <40.63 | | 99.30 | 3% | 137.59 | 2% | 318.97 | 2% | 914.67 | 5% | 327.91 | 1% | 464.10 | 11% | 416.65 | 1% |
| Y8 | 11.88 | 7% | 12.79 | 6% | 12.59 | 26% | <14.06 | | 9.85 | 9% | 11.26 | 7% | <6.01 | | <32.16 | | 9.22 | 7% | 67.64 | 26% | 17.01 | 5% |
| Zr | 46.76 | 5% | 32.21 | 6% | 131.14 | 8% | 36.84 | 74% | 35.84 | 7% | 32.12 | 6% | 124.58 | 5% | 609.61 | 6% | 72.78 | 3% | 764.93 | 6% | 103.67 | 2% |
| Nb | 1.82 | 22% | 2.58 | 16% | 30.80 | 11% | <12.63 | | 4.85 | 13% | 3.01 | 14% | 5.93 | 31% | <20.53 | | 6.49 | 8% | 84.48 | 16% | 8.64 | 7% |
| Ba | 212.52 | 3% | 189.70 | 4% | 323.85 | 9% | 3954.72 | 3% | 30.59 | 13% | 17.18 | 16% | 2771.24 | 1% | 2773.47 | 4% | 1998.07 | 1% | 833.78 | 15% | 881.64 | 1% |
| Cs | 0.19 | 38% | 0.12 | 39% | <0.30 | | 1.67 | 24% | <0.19 | | <0.05 | | 1.92 | 16% | 23.90 | 9% | 1.35 | 9% | <0.60 | | 0.51 | 18% |
| La | 14.02 | 5% | 10.49 | 6% | 28.81 | 10% | <11.86 | | 8.66 | 9% | 10.23 | 6% | <5.19 | | 48.52 | 22% | 19.34 | 4% | 106.81 | 15% | 20.58 | 3% |
| Ce | 34.67 | 3% | 33.29 | 3% | 79.89 | 7% | <22.10 | | 35.22 | 4% | 38.04 | 3% | <8.79 | | <44.48 | | 43.43 | 3% | 284.83 | 10% | 64.84 | 2% |
| Nd | 28.38 | 8% | 26.19 | 8% | 45.60 | 21% | <41.70 | | 23.67 | 11% | 23.21 | 9% | <16.48 | | <87.47 | | 20.46 | 9% | 312.94 | 15% | 40.98 | 5% |
| Sm | 5.63 | 19% | 5.34 | 20% | <9.81 | | <22.04 | | 3.41 | 30% | 4.56 | 21% | <7.58 | | <43.89 | | 3.67 | 23% | 85.85 | 28% | 9.05 | 12% |
| Yb | <1.13 | | 1.16 | 42% | <5.51 | | <9.68 | | 0.82 | 56% | <0.77 | | <3.52 | | <20.60 | | <0.99 | | <18.76 | | 1.25 | 34% |
| Pb | 3.58 | 12% | 2.36 | 14% | <2.72 | | 40.14 | 16% | 1.72 | 23% | 1.25 | 24% | 26.30 | 7% | 243.96 | 4% | 12.86 | 5% | <13.94 | | 6.69 | 7% |
| Th | 1.41 | 14% | 0.58 | 21% | 4.47 | 17% | 32.04 | 6% | <0.26 | | <0.14 | | 11.98 | 7% | 116.00 | 4% | 6.68 | 5% | 27.24 | 11% | 3.93 | 7% |
| U2 | 0.19 | 38% | 0.16 | 41% | 3.21 | 18% | 8.83 | 20% | <0.11 | | 0.16 | 44% | 3.74 | 12% | 32.28 | 8% | 2.32 | 7% | 18.77 | 10% | 0.94 | 13% |
| Ho | 0.34 | 35% | 0.53 | 25% | <1.08 | | <2.06 | | <0.32 | | 0.34 | 33% | <0.97 | | <5.18 | | 0.36 | 30% | <6.23 | | 0.75 | 17% |
| B1 | <65.94 | | <49.84 | | <203.73 | | <295.59 | | <113.52 | | <83.73 | | <235.74 | | <665.07 | | <42.82 | | -90.40<I<682.45 | | 40.85 | 40% |



Major oxide concentrations in wt%
Trace element concentrations in ppm

continued on next page

LA-ICPMS analyses of amphibole-hosted Si-MI in **tholeiitic basalt**, Bingham canyon volcanic suite. Element concentrations and uncertainty

Table 1.4

| Melt inclusions | 15jn08d03 | | 15jn08d05 | | 15jn08d06 | | 15jn08d07 | | 15jn08d08 | | 15jn08d09 | | 15jn08d10 | | 15jn08d11 | | 15jn09a04.xl | | 15jn09a05.xl | 15jn09a06.xl | |
|---|---|---|---|---|---|---|---|---|---|---|---|---|---|---|---|---|---|---|---|---|---|
| SiO2 | 55.02 | 1% | 53.37 | 1% | 60.44 | 1% | 62.53 | 1% | 71.15 | 4% | 66.02 | 2% | 55.15 | 1% | 51.04 | 0% | 64.47 | 2% | 55.31 | 46.94 | 1% |
| TiO2 | 0.66 | 3% | 0.92 | 2% | 0.51 | 3% | 0.80 | 2% | <0.20 | | 0.85 | 4% | 0.39 | 4% | 0.59 | 1% | 0.26 | 17% | 0.93 | 0.91 | 1% |
| Al2O3 | 14.86 | 0% | 14.98 | 0% | 8.03 | 0% | 8.07 | 0% | 14.19 | 1% | 9.13 | 1% | 4.11 | 1% | 6.16 | 0% | 12.01 | 1% | 9.01 | 9.01 | 0% |
| FeO | 6.50 | 1% | 8.99 | 1% | 10.81 | 1% | 8.49 | 1% | 3.28 | 11% | 5.77 | 3% | 8.73 | 1% | 9.21 | 1% | 6.37 | 4% | 11.08 | 11.23 | 1% |
| MnO | 0.13 | 1% | 0.19 | 1% | 0.27 | 1% | 0.16 | 1% | 0.03 | 26% | 0.11 | 3% | 0.25 | 1% | 0.22 | 0% | 0.11 | 4% | 0.17 | 0.22 | 1% |
| MgO | 7.35 | 0% | 9.41 | 0% | 9.90 | 0% | 8.34 | 0% | <0.32 | | 7.02 | 1% | 11.89 | 0% | 14.85 | 0% | 6.69 | 1% | 9.72 | 11.68 | 0% |
| CaO | 5.04 | 3% | 5.89 | 3% | 4.10 | 3% | 5.68 | 2% | <1.57 | | 5.99 | 5% | 14.17 | 2% | 12.09 | 1% | 3.60 | 10% | 7.31 | 13.34 | 1% |
| Na2O | 2.77 | 0% | 1.43 | 1% | 1.22 | 1% | 1.22 | 0% | 3.71 | 1% | 0.70 | 2% | 0.99 | 1% | 1.20 | 0% | 0.80 | 2% | 1.51 | 1.46 | 0% |
| K2O | 3.67 | 0% | 0.84 | 1% | 0.73 | 1% | 0.72 | 1% | 6.29 | 1% | 0.43 | 3% | 0.32 | 1% | 0.64 | 0% | 1.68 | 1% | 0.96 | 1.20 | 0% |
| Total | 100.00 | 0% | 100.00 | 0% | 100.00 | 0% | 100.00 | 0% | 102.65 | 0% | 100.00 | 0% | 100.00 | 0% | 100.00 | 0% | 100.00 | 0% | 100.00 | 100.00 | 0% |
| mass factor | 0.56 | 0% | 0.95 | 0% | 0.89 | 0% | 0.83 | 0% | 0.39 | 0% | 0.50 | 0% | 0.78 | 0% | 0.68 | 0% | 0.42 | 0% | 0.94 | 1.00 | 0% |
| P3 | 60.61 | 27% | <99.15 | | <97.51 | | <51.16 | | <367.57 | | <133.33 | | <107.77 | | 26.21 | 25% | <203.39 | | 120.65 | 75.83 | 25% |
| Sc | 19.40 | 9% | 24.00 | 10% | 12.64 | 15% | 19.11 | 8% | <22.94 | | 17.29 | 23% | 48.02 | 7% | 39.78 | 3% | <12.97 | | 31.23 | 36.47 | 4% |
| V5 | 130.65 | 4% | 197.67 | 4% | 173.76 | 4% | 180.61 | 3% | <68.60 | | 148.27 | 9% | 174.36 | 4% | 190.50 | 2% | 157.11 | 11% | 242.73 | 263.31 | 2% |
| Cr | 187.09 | 10% | 184.33 | 17% | 152.72 | 19% | 234.07 | 10% | <321.62 | | 288.09 | 20% | 2282.79 | 4% | 1376.39 | 2% | <192.71 | | 245.97 | 674.41 | 4% |
| Co | 27.84 | 9% | 37.19 | 9% | 54.03 | 7% | 39.45 | 7% | <31.69 | | 16.51 | 38% | 38.54 | 10% | 45.93 | 3% | 29.19 | 27% | 49.08 | 42.33 | 5% |
| Ni | 53.18 | 13% | 57.22 | 17% | 138.81 | 10% | 82.11 | 11% | <88.61 | | <42.87 | | 125.54 | 12% | 149.40 | 4% | <72.96 | | 104.50 | 120.64 | 7% |
| Cu | 0.83 | 67% | <4.30 | | <3.86 | | <2.12 | | <15.17 | | <5.38 | | <4.50 | | 0.93 | 38% | <7.57 | | <3.75 | <1.91 | |
| Rb | 102.31 | 1% | 5.08 | 16% | 13.74 | 9% | 2.75 | 17% | 190.83 | 5% | 3.01 | 41% | <1.37 | | 2.70 | 9% | 187.18 | 3% | 3.10 | 8.78 | 7% |
| Sr | 342.59 | 1% | 132.83 | 3% | 64.05 | 4% | 129.55 | 2% | 453.00 | 4% | 139.30 | 5% | 76.47 | 4% | 81.91 | 1% | <30.43 | | 204.08 | 259.49 | 1% |
| Y8 | 22.94 | 5% | 32.01 | 5% | 18.95 | 8% | 18.28 | 6% | <17.29 | | 23.86 | 10% | 13.01 | 10% | 22.28 | 3% | 13.35 | 24% | 19.04 | 21.19 | 4% |
| Zr | 99.85 | 3% | 90.10 | 5% | 40.40 | 7% | 46.61 | 5% | 155.35 | 10% | 182.31 | 4% | 18.93 | 11% | 18.91 | 4% | 260.79 | 5% | 83.54 | 73.46 | 3% |
| Nb | 10.62 | 7% | 10.91 | 10% | 8.14 | 12% | 9.84 | 8% | <10.64 | | 17.14 | 11% | 3.97 | 20% | 6.30 | 6% | <5.31 | | 8.48 | 5.00 | 9% |
| Ba | 1362.75 | 1% | 171.82 | 6% | 158.57 | 6% | 166.00 | 5% | 1929.96 | 4% | 179.04 | 11% | 28.31 | 16% | 78.38 | 3% | <77.48 | | 229.82 | 310.48 | 2% |
| Cs | 0.78 | 8% | 0.28 | 45% | 1.39 | 19% | 0.21 | 37% | 6.21 | 20% | <0.15 | | <0.22 | | <0.03 | | 2.50 | 20% | 0.20 | <0.07 | |
| La | 34.29 | 2% | 24.30 | 5% | 18.46 | 7% | 24.27 | 4% | 49.97 | 12% | 23.81 | 9% | 9.24 | 10% | 12.48 | 3% | 12.57 | 20% | 19.30 | 21.28 | 3% |
| Ce | 88.29 | 2% | 81.42 | 3% | 67.86 | 3% | 71.26 | 2% | 43.90 | 20% | 64.66 | 5% | 30.73 | 5% | 39.39 | 2% | 43.54 | 10% | 62.98 | 65.75 | 2% |
| Nd | 47.33 | 6% | 49.28 | 8% | 44.85 | 9% | 41.28 | 7% | <45.25 | | 33.50 | 19% | 23.54 | 14% | 36.77 | 4% | <22.24 | | 51.16 | 42.79 | 5% |
| Sm | 9.62 | 15% | 10.12 | 20% | 8.86 | 22% | 7.72 | 18% | <23.04 | | <6.13 | | 4.27 | 39% | 8.28 | 10% | 12.04 | 39% | 10.09 | 10.12 | 12% |
| Yb | 1.74 | 42% | 1.78 | 50% | 1.40 | 57% | 1.78 | 38% | <10.07 | | 2.77 | 62% | 1.73 | 49% | 1.70 | 20% | <4.91 | | 1.37 | 2.23 | 25% |
| Pb | 12.05 | 4% | 4.87 | 17% | 2.28 | 24% | 2.84 | 16% | 58.81 | 10% | <2.14 | | 1.04 | 44% | 1.75 | 12% | <3.47 | | 2.09 | 3.29 | 12% |
| Th | 6.54 | 3% | 1.14 | 26% | 5.15 | 11% | 2.48 | 12% | 28.69 | 11% | 16.76 | 7% | 0.46 | 38% | 0.17 | 26% | 23.91 | 7% | 0.72 | 1.08 | 15% |
| U2 | 1.26 | 8% | <0.13 | | <0.18 | | 0.13 | 57% | 6.50 | 21% | 3.62 | 14% | <0.14 | | 0.09 | 32% | 2.96 | 19% | <0.20 | 0.14 | 38% |
| Ho | 0.85 | 23% | 1.25 | 23% | 0.88 | 28% | 0.45 | 33% | <2.81 | | <0.82 | | 1.18 | 24% | 0.96 | 11% | 1.41 | 42% | 0.87 | 0.80 | 17% |
| B1 | 21.01 | 61% | <99.94 | | <89.98 | | <46.74 | | <318.60 | | <123.81 | | <106.65 | | 20.10 | 34% | <205.41 | | <110.50 | <50.21 | |



Major oxide concentrations in wt%
Trace element concentrations in ppm

continued on next page

LA-ICPMS analyses of amphibole-hosted Si-MI in **tholeiitic basalt**, Bingham canyon volcanic suite. Element concentrations and uncertainty

Table 1.5

| Melt inclusions | 15jn09c03 | | 15jn09c06 | | 15jn09d03.xl | | 15jn09d04.xl | | 15jn09d06.xl | | 15jn09d07.xl | | 15jn09d08.xl | | 15jn09d09.xl | | 15jn09d10.xl | | 15jn09d11.xl | | 15jn09d12.xl | |
|---|---|---|---|---|---|---|---|---|---|---|---|---|---|---|---|---|---|---|---|---|---|---|
| SiO2 | 61.07 | 2% | 54.87 | 1% | 59.45 | 1% | 42.19 | 3% | 60.59 | 1% | 57.83 | 1% | 68.89 | 1% | 58.65 | 1% | 45.78 | 2% | 54.19 | 0.63% | 71.42 | 3.00% |
| TiO2 | 0.77 | 6% | 1.21 | 1% | 0.60 | 5% | 3.61 | 2% | 0.51 | 6% | 0.84 | 2% | 0.13 | 17% | 0.68 | 4% | 2.28 | 2% | 0.89 | 1.25% | 2.39 | 3.46% |
| Al2O3 | 14.16 | 1% | 12.40 | 0% | 14.08 | 0% | 14.14 | 0% | 12.10 | 0% | 14.23 | 0% | 14.18 | 0% | 14.18 | 0% | 12.01 | 0% | 16.02 | 0.16% | 14.08 | 0.82% |
| FeO | 4.91 | 5% | 8.47 | 1% | 5.44 | 3% | 11.37 | 2% | 7.13 | 2% | 7.73 | 1% | 1.43 | 8% | 7.85 | 2% | 13.65 | 1% | 7.47 | 0.77% | 2.74 | 15.47% |
| MnO | 0.13 | 3% | 0.13 | 1% | 0.12 | 3% | 0.24 | 2% | 0.09 | 3% | 0.14 | 1% | 0.04 | 6% | 0.15 | 2% | 0.19 | 2% | 0.12 | 0.86% | 0.07 | 10.19% |
| MgO | 5.16 | 1% | 9.62 | 0% | 4.50 | 1% | 12.83 | 0% | 5.67 | 1% | 7.99 | 0% | 0.56 | 5% | 6.85 | 1% | 12.04 | 0% | 8.53 | 0.21% | 1.19 | 9.43% |
| CaO | 2.60 | 12% | 6.38 | 2% | 4.42 | 5% | 7.09 | 4% | 2.43 | 9% | 4.95 | 2% | 0.74 | 22% | 5.03 | 4% | 2.99 | 7% | 5.36 | 1.50% | 1.26 | 47.51% |
| Na2O | 2.80 | 1% | 1.23 | 0% | 3.35 | 0% | 0.50 | 3% | 3.57 | 0% | 1.06 | 0% | 3.53 | 0% | 1.37 | 1% | 1.37 | 1% | 0.94 | 0.36% | 0.33 | 7.88% |
| K2O | 4.40 | 0% | 1.68 | 0% | 4.04 | 0% | 4.03 | 0% | 3.92 | 0% | 1.23 | 0% | 6.50 | 0% | 1.24 | 1% | 5.68 | 0% | 2.48 | 0.24% | 2.52 | 1.08% |
| Total | 100.00 | 0% | 100.00 | 0% | 100.00 | 0% | 100.00 | 0% | 100.00 | 0% | 100.00 | 0% | 100.00 | 0% | 100.00 | 0% | 100.00 | 0% | 100.00 | 0.00% | 100.00 | 0.00% |
| mass factor | 0.38 | 0% | 0.69 | 0% | 0.54 | 0% | 0.49 | 0% | 0.45 | 0% | 0.77 | 0% | 0.65 | 0% | 0.58 | 0% | 0.55 | 0% | 0.93 | 0.00% | 0.27 | 0.00% |
| P3 | <141.66 | | 53.20 | 23% | 360.64 | 17% | <159.10 | | 1170.22 | 5% | 87.43 | 20% | 192.03 | 23% | 40.15 | 43% | <92.96 | | 80.66 | 15.60% | 316.14 | 38.48% |
| Sc | <9.26 | | 21.80 | 6% | 12.00 | 27% | 13.76 | 28% | <7.81 | | 20.90 | 8% | <6.49 | | 19.12 | 19% | 21.11 | 18% | 27.33 | 4.66% | 32.56 | 27.85% |
| V5 | 157.45 | 10% | 266.94 | 2% | 107.93 | 10% | 291.50 | 5% | 150.17 | 8% | 175.66 | 3% | <20.59 | | 162.78 | 6% | 446.14 | 3% | 236.08 | 1.78% | 341.81 | 9.27% |
| Cr | <92.20 | | 56.39 | 18% | <112.14 | | 4129.82 | 4% | 113.30 | 34% | 127.59 | 15% | <96.44 | | 132.32 | 28% | <72.85 | | 145.48 | 10.29% | <282.62 | |
| Co | <14.44 | | 32.40 | 6% | 21.75 | 22% | 38.27 | 18% | 58.18 | 9% | 28.57 | 8% | <9.05 | | 29.86 | 16% | 76.86 | 7% | 30.69 | 5.66% | <23.54 | |
| Ni | <36.48 | | 31.92 | 14% | <30.17 | | 124.85 | 19% | 142.26 | 13% | 60.46 | 12% | <26.60 | | 71.39 | 20% | 108.49 | 15% | 65.25 | 8.75% | <87.16 | |
| Cu | 2.32 | 52% | <0.77 | | 4.20 | 39% | <6.73 | | 60.24 | 6% | <1.53 | | <4.93 | | <4.88 | | <3.40 | | <1.32 | | 30.49 | 20.07% |
| Rb | 103.77 | 3% | 26.74 | 4% | 101.55 | 3% | 155.30 | 3% | 89.97 | 3% | 82.03 | 2% | 288.60 | 2% | 34.27 | 6% | 116.63 | 3% | 203.19 | 1.28% | 255.23 | 2.91% |
| Sr | 330.33 | 3% | 200.36 | 1% | 438.32 | 2% | 157.76 | 5% | 671.01 | 1% | 123.82 | 2% | 262.17 | 2% | 159.61 | 4% | 107.49 | 5% | 112.01 | 1.63% | 447.88 | 3.34% |
| Y8 | 18.97 | 15% | 25.28 | 4% | 18.62 | 14% | 32.55 | 9% | <4.40 | | 34.04 | 4% | <3.67 | | 32.85 | 9% | <4.23 | | 16.62 | 4.27% | 47.43 | 13.41% |
| Zr | 111.05 | 7% | 132.68 | 2% | 172.04 | 4% | 66.84 | 9% | 117.71 | 5% | 177.98 | 2% | 153.07 | 4% | 84.05 | 6% | 31.45 | 12% | 80.27 | 2.69% | 480.93 | 2.99% |
| Nb | 8.70 | 21% | 9.55 | 7% | 10.82 | 16% | 31.53 | 8% | 8.93 | 13% | 12.62 | 7% | 6.09 | 21% | 12.13 | 15% | 3.81 | 27% | 12.43 | 5.36% | 23.53 | 19.16% |
| Ba | 1156.86 | 3% | 756.49 | 1% | 1950.32 | 2% | 5144.73 | 1% | 1841.02 | 1% | 181.60 | 4% | 1480.66 | 2% | 256.75 | 6% | 3452.60 | 1% | 225.06 | 2.59% | 1148.37 | 3.67% |
| Cs | 0.53 | 31% | 0.13 | 37% | 2.48 | 14% | 0.67 | 43% | 2.81 | 11% | 1.23 | 14% | 4.33 | 11% | 2.26 | 15% | 1.20 | 19% | 2.15 | 8.65% | 5.06 | 13.49% |
| La | 17.15 | 13% | 19.05 | 4% | 40.00 | 6% | 45.57 | 5% | 46.55 | 4% | 25.28 | 4% | 51.32 | 4% | 29.82 | 8% | <2.80 | | 10.65 | 4.61% | 157.30 | 3.42% |
| Ce | 44.75 | 9% | 58.02 | 2% | 76.13 | 5% | 117.64 | 4% | 61.09 | 4% | 91.60 | 2% | 62.22 | 4% | 99.09 | 4% | 7.21 | 29% | 35.15 | 2.54% | 252.26 | 3.38% |
| Nd | <15.12 | | 39.60 | 6% | 33.12 | 19% | 69.35 | 10% | 16.81 | 25% | 67.25 | 5% | <9.58 | | 66.83 | 11% | <10.36 | | 26.90 | 6.46% | 108.34 | 13.54% |
| Sm | <8.34 | | 6.48 | 18% | <7.61 | | 13.41 | 27% | <4.92 | | 11.88 | 14% | <5.00 | | 11.49 | 32% | <4.21 | | 5.84 | 15.10% | 17.09 | 44.73% |
| Yb | <3.52 | | 2.23 | 25% | <3.50 | | <3.31 | | <2.91 | | 3.15 | 24% | <2.26 | | 4.44 | 44% | <2.35 | | 2.22 | 22.04% | <6.37 | |
| Pb | 15.51 | 11% | 1.44 | 28% | 38.05 | 5% | 11.10 | 15% | 18.44 | 7% | 3.51 | 13% | 48.61 | 5% | 4.31 | 20% | 4.46 | 18% | 3.59 | 10.11% | 4.34 | 44.82% |
| Th | 8.35 | 9% | 10.75 | 4% | 14.25 | 6% | <0.49 | | 13.48 | 5% | 13.31 | 4% | 27.64 | 5% | 1.44 | 23% | 0.93 | 26% | 3.19 | 7.62% | 34.06 | 5.16% |
| U2 | 1.14 | 27% | 0.45 | 20% | 3.36 | 12% | 1.77 | 22% | 1.63 | 16% | 1.31 | 14% | 5.58 | 10% | 0.18 | 60% | <0.15 | | 0.75 | 15.62% | 3.96 | 17.07% |
| Ho | 1.07 | 39% | 0.99 | 16% | 1.28 | 34% | 1.63 | 28% | <0.70 | | 1.57 | 14% | <0.49 | | 1.04 | 44% | 0.59 | 47% | 0.78 | 15.37% | <1.86 | |
| B1 | 28.92 | 74% | <23.43 | | 40.86 | 37% | <130.81 | | <56.91 | | 42.22 | 32% | <93.09 | | <93.24 | | <75.02 | | <22.55 | | <131.25 | |



Major oxide concentrations in wt%
Trace element concentrations in ppm

continued on next page

LA-ICPMS analyses of amphibole-hosted Si-MI in **tholeiitic basalt**, Bingham canyon volcanic suite. Element concentrations and uncertainty

Table 1.6

| Melt inclusions | 15jn09d 13 | | 15jn09d 14 | | 15jn09d 15 | | 15jn09g 03 | | 15jn09g 04 | | 15jn09g 05 | | 15jn09g 06. | | 15jn09g 07. | | 15jn09g08 | | 15jn09g 09. | | 15jn09g 10 |
|---|---|---|---|---|---|---|---|---|---|---|---|---|---|---|---|---|---|---|---|---|---|
| SiO2 | 74.18 | 1.56% | 56.17 | 1.62% | 64.15 | 2.03% | 62.90 | 3.61% | 83.25 | 2.26% | 57.53 | 2.59% | 66.14 | 2.60% | 58.73 | 1.27% | 44.54 | 3.89% | 60.75 | 2.38% | 51.82 |
| TiO2 | <0.09 | | 1.03 | 2.93% | 0.65 | 5.74% | 0.75 | 10.07% | <0.16 | | 0.74 | 6.00% | 0.33 | 10.37% | 0.57 | 3.22% | 2.99 | 2.88% | 0.21 | 13.61% | 2.24 |
| Al2O3 | 11.07 | 0.54% | 9.05 | 0.48% | 10.06 | 0.60% | 14.07 | 0.91% | 14.11 | 0.87% | 14.08 | 0.56% | 14.11 | 0.54% | 15.96 | 0.29% | 12.22 | 0.97% | 11.01 | 0.53% | 14.19 |
| FeO | 2.40 | 7.00% | 10.24 | 1.55% | 8.46 | 2.41% | 4.84 | 9.78% | <0.82 | | 4.87 | 5.02% | 1.35 | 16.25% | 7.30 | 1.57% | 16.41 | 2.60% | 14.46 | 1.55% | 9.19 |
| MnO | 0.06 | 5.23% | 0.16 | 1.76% | 0.12 | 3.13% | <0.02 | | 0.12 | 5.51% | 0.15 | 3.01% | 0.07 | 6.41% | 0.14 | 1.61% | 0.09 | 8.21% | 0.05 | 6.17% | 0.02 |
| MgO | 1.04 | 4.22% | 9.65 | 0.45% | 6.06 | 0.85% | 4.06 | 3.01% | <0.23 | | 6.91 | 0.97% | 2.63 | 1.99% | 5.67 | 0.48% | 11.97 | 0.93% | 0.76 | 4.77% | 8.60 |
| CaO | <0.65 | | 7.06 | 3.23% | 3.83 | 7.33% | 3.24 | 18.27% | <1.17 | | 5.72 | 6.04% | 2.80 | 10.48% | 4.62 | 3.28% | <1.31 | | 2.08 | 11.43% | <0.89 |
| Na2O | 4.06 | 0.40% | 1.61 | 0.64% | 1.45 | 0.89% | 2.92 | 1.09% | 4.53 | 0.64% | 1.83 | 0.96% | 2.89 | 0.67% | 0.98 | 0.68% | 0.83 | 2.71% | 3.04 | 0.51% | 2.01 |
| K2O | 3.70 | 0.46% | 1.02 | 0.89% | 1.22 | 1.07% | 3.19 | 0.82% | 6.78 | 0.42% | 4.17 | 0.54% | 5.70 | 0.45% | 2.03 | 0.48% | 12.40 | 0.29% | 3.65 | 0.49% | 8.53 |
| Total | 100.52 | 0.00% | 100.00 | 0.00% | 100.00 | 0.00% | 99.98 | 0.00% | 112.79 | 0.00% | 100.00 | 0.00% | 100.00 | 0.00% | 100.00 | 0.00% | 105.45 | 0.00% | 100.00 | 0.00% | 100.61 |
| mass factor | 0.55 | 0.00% | 0.79 | 0.00% | 0.61 | 0.00% | 0.28 | 0.00% | 0.23 | 0.00% | 0.53 | 0.00% | 0.64 | 0.00% | 0.86 | 0.00% | 0.26 | 0.00% | 0.65 | 0.00% | 0.55 |
| P3 | <173.46 | | <138.58 | | <205.46 | | <309.53 | | <202.08 | | <239.98 | | <326.33 | | <110.23 | | 7953.67 | 2.51% | <280.10 | | 1622.27 |
| Sc | <10.01 | | 28.11 | 12.09% | 18.99 | 23.26% | <25.38 | | <19.29 | | 26.59 | 17.66% | <11.73 | | 13.14 | 16.00% | <19.40 | | <9.71 | | <13.35 |
| V5 | <32.08 | | 248.42 | 4.43% | 212.27 | 7.00% | 180.19 | 19.63% | <58.98 | | 96.65 | 16.76% | 61.93 | 24.18% | 151.46 | 4.71% | 346.08 | 7.90% | 63.43 | 18.27% | 310.59 |
| Cr | <146.21 | | 194.35 | 24.97% | 511.24 | 15.90% | <266.14 | | <218.22 | | <205.04 | | 204.50 | 34.31% | 307.94 | 15.46% | 304.21 | 32.60% | <205.88 | | <281.80 |
| Co | <12.60 | | 42.59 | 11.56% | 50.94 | 13.51% | <22.07 | | <23.22 | | <17.46 | | <14.12 | | 24.08 | 13.13% | 109.11 | 11.43% | 417.70 | 3.51% | 73.91 |
| Ni | <38.41 | | 123.01 | 14.42% | <42.13 | | 74.47 | 28.81% | 128.21 | 21.06% | <67.27 | | <44.15 | | 42.27 | 22.92% | 181.86 | 19.83% | 2442.07 | 3.21% | 123.64 |
| Cu | <7.39 | | <4.60 | | <7.69 | | <13.09 | | <7.71 | | <10.29 | | 6.88 | 44.00% | <4.25 | | <7.77 | | 8174.84 | 0.86% | 73.09 |
| Rb | 120.77 | 3.54% | 7.14 | 17.25% | 23.95 | 10.29% | 92.77 | 5.72% | 220.14 | 2.70% | 1096.87 | 1.43% | 160.83 | 4.02% | 79.29 | 3.72% | 423.55 | 2.07% | 101.94 | 4.39% | 152.78 |
| Sr | 443.66 | 2.35% | 179.15 | 3.36% | 425.21 | 2.42% | 459.55 | 2.53% | 802.68 | 2.26% | 263.30 | 4.08% | 474.07 | 2.51% | 647.95 | 1.22% | <35.48 | | 546.08 | 1.94% | 218.14 |
| Y8 | <5.18 | | 33.68 | 7.01% | <5.71 | | <12.95 | | 10.82 | 47.47% | 18.67 | 16.28% | <5.13 | | 13.18 | 10.48% | <14.78 | | <4.77 | | <7.33 |
| Zr | 172.36 | 4.51% | 51.71 | 8.52% | 58.92 | 10.31% | 192.80 | 6.15% | 266.52 | 4.89% | 158.53 | 6.26% | 145.20 | 6.57% | 168.25 | 3.56% | <31.13 | | 113.61 | 6.36% | 28.24 |
| Nb | 8.98 | 17.77% | 10.79 | 13.68% | 5.24 | 33.34% | 12.24 | 25.19% | 19.54 | 17.93% | 9.15 | 25.61% | 5.15 | 42.14% | 10.68 | 11.25% | 15.66 | 26.33% | 9.82 | 16.69% | 4.96 |
| Ba | 240.65 | 9.34% | 220.81 | 6.67% | 282.63 | 7.81% | 1480.73 | 2.88% | 2190.47 | 2.40% | 571.71 | 5.49% | 2756.54 | 2.03% | 462.09 | 3.35% | 12523.39 | 0.83% | 1343.09 | 2.64% | 3432.47 |
| Cs | 3.95 | 13.37% | <0.14 | | 0.43 | 54.36% | 2.99 | 20.38% | 5.47 | 11.46% | 1.90 | 23.57% | 3.20 | 19.41% | 1.01 | 23.53% | 2.46 | 19.05% | 3.03 | 17.77% | 2.16 |
| La | 25.76 | 8.09% | 27.10 | 6.90% | 13.18 | 16.46% | 23.28 | 15.59% | 146.27 | 3.31% | 18.08 | 14.97% | 48.99 | 7.33% | 27.78 | 5.53% | 47.79 | 11.44% | 47.28 | 5.58% | 11.72 |
| Ce | 52.09 | 6.56% | 84.22 | 3.88% | 41.05 | 9.25% | 62.54 | 9.31% | 225.43 | 3.22% | 53.93 | 8.73% | 94.97 | 5.50% | 63.76 | 3.72% | 69.10 | 13.07% | 77.08 | 4.71% | 17.94 |
| Nd | <13.65 | | 55.98 | 10.62% | 16.43 | 37.56% | 24.72 | 41.66% | 76.46 | 15.84% | 30.08 | 26.11% | 26.34 | 29.93% | 34.10 | 11.66% | <37.05 | | 33.34 | 17.70% | <18.05 |
| Sm | 8.66 | 36.38% | 18.08 | 19.06% | <7.49 | | <11.48 | | 12.94 | 48.29% | <8.94 | | <7.07 | | 5.45 | 33.61% | <17.10 | | <6.36 | | <9.58 |
| Yb | <3.53 | | 3.97 | 37.20% | <3.89 | | <11.30 | | <7.25 | | <4.38 | | <5.44 | | <1.54 | | <9.40 | | <3.26 | | <4.75 |
| Pb | 40.22 | 6.34% | 3.04 | 27.99% | 3.21 | 34.23% | 24.31 | 13.05% | 62.19 | 5.32% | <2.67 | | 37.82 | 8.99% | 16.05 | 8.58% | 6.18 | 35.22% | 41.61 | 6.95% | 11.24 |
| Th | 11.88 | 8.17% | 1.47 | 25.18% | 6.31 | 13.42% | 15.01 | 10.97% | 52.28 | 4.12% | 6.38 | 15.25% | 23.11 | 8.19% | 4.41 | 12.35% | 3.42 | 25.58% | 15.84 | 8.45% | 6.68 |
| U2 | 4.52 | 13.02% | <0.29 | | 1.20 | 29.98% | 3.97 | 18.63% | 8.58 | 9.60% | 0.83 | 47.85% | 5.25 | 15.78% | 0.93 | 25.54% | <0.79 | | 3.41 | 17.33% | 1.55 |
| Ho | <0.83 | | 1.01 | 33.50% | <0.71 | | <1.86 | | <1.77 | | <0.97 | | <1.05 | | 0.44 | 45.89% | <2.25 | | <0.78 | | <1.32 |
| B1 | <136.91 | | <97.31 | | <187.32 | | <299.18 | | 59.29 | 87.54% | <183.30 | | <252.90 | | <83.92 | | 163.33 | 46.95% | <228.32 | | <258.19 |



Major oxide concentrations in wt%
Trace element concentrations in ppm

continued on next page

LA-ICPMS analyses of amphibole-hosted Si-MI in **tholeiitic basalt**, Bingham canyon volcanic suite. Element concentrations and uncertainty

Table 1.7

| Melt inclusions | 15jn09g10 | | 15jn09g12 | | 15jn09g13 | | 15jn09g14 | | 15jn09 g15 | | 15jn09g16 | | 15jn09 g17 | | 15jn09g18 | | 15jn09g19 | | 15jn09g20 | | 15jn09g21 | |
|---|---|---|---|---|---|---|---|---|---|---|---|---|---|---|---|---|---|---|---|---|---|---|
| SiO2 | 51.82 | 3.42% | 60.49 | 1.11% | 907.88 | 7.87% | 50.00 | 2.88% | 49.50 | 0.92% | 68.17 | 2.98% | 44.59 | 1.19% | 73.65 | 2.79% | 71.62 | 2.34% | 74.55 | 2.47% | 47.92 | 2.51% |
| TiO2 | 2.24 | 2.83% | 0.92 | 2.10% | <5.29 | | 2.59 | 2.52% | 0.35 | 2.95% | 0.23 | 20.90% | 1.26 | 1.75% | 0.19 | 21.05% | <0.11 | | <0.16 | | 1.43 | 2.77% |
| Al2O3 | 14.19 | 0.61% | 8.09 | 0.37% | 14.55 | 28.69% | 14.11 | 0.70% | 5.03 | 0.40% | 14.15 | 0.68% | 14.19 | 0.28% | 14.06 | 0.61% | 13.98 | 0.56% | 9.93 | 1.04% | 14.10 | 0.43% |
| FeO | 9.19 | 2.95% | 10.56 | 1.09% | <35.78 | | 15.27 | 2.24% | 8.22 | 1.03% | 3.09 | 8.66% | 11.56 | 1.04% | 1.87 | 14.09% | 1.30 | 18.30% | 3.87 | 9.33% | 11.30 | 1.90% |
| MnO | 0.02 | 17.38% | 0.15 | 1.32% | <0.59 | | 0.11 | 5.29% | 0.21 | 0.87% | 0.04 | 10.77% | 0.17 | 1.19% | <0.01 | | <0.01 | | 0.02 | 39.73% | 0.15 | 2.35% |
| MgO | 8.60 | 0.80% | 7.27 | 0.37% | <8.76 | | 7.56 | 1.17% | 13.98 | 0.22% | 1.16 | 6.36% | 10.37 | 0.31% | <0.21 | | <0.17 | | <0.23 | | 10.00 | 0.56% |
| CaO | <0.89 | | 6.10 | 2.42% | <46.07 | | <1.01 | | 17.50 | 1.07% | <1.06 | | 10.06 | 1.74% | <1.17 | | <0.89 | | <1.20 | | 6.61 | 4.19% |
| Na2O | 2.01 | 0.89% | 1.33 | 0.49% | 22.45 | 4.21% | 1.07 | 1.72% | 0.88 | 0.51% | 4.22 | 0.58% | 2.06 | 0.39% | 4.19 | 0.54% | 4.68 | 0.45% | 3.37 | 0.72% | 1.63 | 0.79% |
| K2O | 8.53 | 0.38% | 1.10 | 0.60% | 87.63 | 1.13% | 8.22 | 0.31% | 0.33 | 1.00% | 4.57 | 0.57% | 1.75 | 0.46% | 5.34 | 0.48% | 4.53 | 0.44% | 5.23 | 0.47% | 2.85 | 0.54% |
| Total | 100.61 | 0.00% | 100.00 | 0.00% | 1036.51 | 0.00% | 102.93 | 0.00% | 100.00 | 0.00% | 99.63 | 0.00% | 100.00 | 0.00% | 103.31 | 0.00% | 100.12 | 0.00% | 100.97 | 0.00% | 100.00 | 0.00% |
| mass factor | 0.55 | 0.00% | 0.86 | 0.00% | 0.01 | 0.00% | 0.29 | 0.00% | 0.91 | 0.00% | 0.50 | 0.00% | 0.90 | 0.00% | 0.42 | 0.00% | 0.41 | 0.00% | 0.25 | 0.00% | 0.63 | 0.00% |
| P3 | 1622.27 | 9.01% | <100.37 | | <6739.09 | | <182.41 | | 46.33 | 35.32% | <383.47 | | 138.32 | 17.26% | 389.50 | 31.61% | 348.96 | 26.41% | <290.4 | | <188.8 | |
| Sc | <13.35 | | 22.58 | 9.37% | <634.82 | | <13.29 | | 28.65 | 6.24% | <15.58 | | 25.04 | 8.19% | <17.64 | | <14.30 | | <19.28 | | 33.97 | 12.86% |
| V5 | 310.59 | 6.58% | 211.19 | 3.29% | <2022.10 | | 267.93 | 7.36% | 144.27 | 3.24% | <47.37 | | 305.88 | 2.59% | 87.99 | 19.65% | 92.26 | 18.28% | 56.07 | 41.74% | 288.43 | 5.12% |
| Cr | <281.80 | | 1192.62 | 5.50% | <22328.8 | | 448.08 | 25.16% | 492.65 | 7.05% | <373.10 | | 125.35 | 18.63% | <334.49 | | 317.83 | 31.55% | 434.40 | 26.71% | 943.93 | 12.58% |
| Co | 73.91 | 13.23% | 39.67 | 8.24% | <1014.82 | | 59.61 | 16.63% | 35.47 | 7.25% | <20.60 | | 40.35 | 8.22% | <23.31 | | <18.13 | | 36.07 | 30.12% | 39.06 | 16.07% |
| Ni | 123.64 | 22.27% | 77.05 | 13.59% | <3190.52 | | 95.36 | 41.18% | 128.66 | 8.88% | <96.16 | | 67.49 | 14.38% | <94.41 | | <59.69 | | 119.86 | 31.15% | 99.12 | 23.59% |
| Cu | 73.09 | 12.99% | <4.22 | | 61.34 | 126.12% | 5.50 | 67.62% | <2.40 | | <16.18 | | <2.47 | | <17.53 | | <10.79 | | <10.21 | | 37.04 | 13.64% |
| Rb | 152.78 | 4.40% | 30.20 | 5.43% | 4407.09 | 4.05% | 326.21 | 2.01% | 1.50 | 24.97% | 133.73 | 4.79% | 25.24 | 6.07% | 167.62 | 4.09% | 125.33 | 3.81% | 137.32 | 3.57% | 121.60 | 3.56% |
| Sr | 218.14 | 5.11% | 175.62 | 2.29% | 8633.86 | 6.47% | 27.23 | 42.75% | 223.72 | 1.61% | 663.49 | 2.42% | 418.98 | 1.39% | 502.11 | 2.74% | 522.09 | 2.11% | 293.49 | 4.54% | 277.41 | 2.78% |
| Y8 | <7.33 | | 25.98 | 5.73% | <400.62 | | <9.83 | | 10.87 | 7.48% | <7.54 | | 24.90 | 5.75% | <10.09 | | <10.11 | | <15.02 | | 22.28 | 9.57% |
| Zr | 28.24 | 23.12% | 155.57 | 3.23% | 1717.02 | 28.75% | 27.60 | 32.00% | 34.60 | 6.05% | 100.59 | 9.99% | 98.97 | 4.16% | 174.28 | 6.63% | 166.46 | 5.77% | 111.41 | 10.97% | 57.50 | 8.47% |
| Nb | 4.96 | 37.50% | 12.58 | 8.84% | <261.21 | | 23.71 | 12.89% | 1.70 | 23.33% | <5.37 | | 13.20 | 8.57% | 16.13 | 18.64% | 9.10 | 28.10% | 11.22 | 35.57% | 8.95 | 15.90% |
| Ba | 3432.47 | 1.99% | 245.74 | 4.28% | 52576.62 | 3.10% | 8439.03 | 0.86% | 95.56 | 5.97% | 1819.12 | 2.87% | 734.54 | 2.38% | 1976.37 | 2.56% | 385.20 | 6.02% | 1266.01 | 3.38% | 1904.4 | 1.94% |
| Cs | 2.16 | 26.30% | 0.31 | 38.23% | 133.43 | 14.77% | 2.76 | 15.57% | <0.05 | | 3.80 | 19.41% | 0.75 | 24.25% | 5.34 | 16.12% | 4.78 | 13.49% | 2.01 | 21.30% | 5.74 | 11.18% |
| La | 11.72 | 19.57% | 22.77 | 5.41% | <365.01 | | <7.30 | | 16.00 | 5.36% | 18.15 | 17.84% | 44.73 | 3.63% | 25.87 | 14.96% | 23.65 | 14.22% | 38.04 | 13.45% | 28.31 | 7.48% |
| Ce | 17.94 | 19.91% | 77.24 | 2.86% | <631.35 | | 23.65 | 24.49% | 59.36 | 2.70% | 35.52 | 15.16% | 86.60 | 2.60% | 74.18 | 8.77% | 25.63 | 21.43% | 45.77 | 19.25% | 79.97 | 4.55% |
| Nd | <18.05 | | 60.38 | 7.01% | <1172.03 | | <23.90 | | 42.67 | 6.94% | <24.65 | | 42.28 | 8.26% | <26.66 | | <24.46 | | 43.49 | 37.43% | 52.77 | 12.14% |
| Sm | <9.58 | | 10.93 | 17.99% | <531.27 | | <11.40 | | 9.46 | 15.73% | <11.23 | | 5.95 | 24.28% | <14.03 | | <13.19 | | <18.46 | | 11.11 | 30.44% |
| Yb | <4.75 | | 3.53 | 29.58% | <216.81 | | <4.97 | | <0.85 | | <6.08 | | 1.99 | 40.14% | <6.64 | | <5.84 | | <8.98 | | 1.48 | 52.42% |
| Pb | 11.24 | 19.73% | 2.22 | 22.72% | 1102.09 | 9.08% | 7.37 | 22.08% | 1.16 | 26.04% | 41.41 | 8.77% | 8.04 | 10.70% | 47.05 | 7.88% | 41.60 | 6.88% | 39.77 | 7.51% | 37.62 | 6.78% |
| Th | 6.68 | 16.51% | 6.65 | 8.73% | 759.69 | 6.85% | 0.91 | 44.07% | 0.23 | 40.88% | 9.32 | 13.64% | 6.04 | 9.34% | 29.24 | 7.35% | 20.53 | 7.21% | 23.31 | 6.63% | 8.94 | 10.10% |
| U2 | 1.55 | 31.15% | 0.82 | 23.31% | 143.98 | 15.53% | 2.72 | 16.15% | <0.08 | | 4.36 | 18.72% | 0.98 | 22.05% | 5.02 | 16.47% | 4.50 | 14.80% | 4.25 | 13.88% | 0.79 | 34.13% |
| Ho | <1.32 | | 0.93 | 24.87% | <56.95 | | <1.41 | | 0.24 | 44.94% | <1.34 | | 0.64 | 29.01% | <1.58 | | <1.54 | | <2.39 | | 0.99 | 37.84% |
| B1 | <258.19 | | <79.10 | | <5578.95 | | <151.32 | | <40.81 | | <360.03 | | 71.44 | 28.93% | <293.46 | | <220.52 | | <202.90 | | <130.99 | |



Major oxide concentrations in wt%
Trace element concentrations in ppm

LA-ICPMS analyses of plagioclase-hosted Si-MI in **tholeiitic andesite** form Lark, Bingham canyon volcanic suite. Element concentrations and uncertainty

Table 2.1

| Melt inclusions | 15jl13a04.xl | | 15jl13a05.xl | | 15jl13a07.xl | | 15jl13a08.xl | | 15jl13b03.xl | | 15jl13b06.xl | | 15jl13b08.xl | | 15jl13b09.xl | | 15jl13b10.xl | | 15jl13b11.xl | | 15jl13b12.xl | | 15jl13b13.xl | |
|---|---|---|---|---|---|---|---|---|---|---|---|---|---|---|---|---|---|---|---|---|---|---|---|---|
| SiO2 | 68.99 | 3% | 68.79 | 1% | 68.60 | 2% | 60.75 | 1% | 69.13 | 0% | 68.25 | 0% | 74.92 | 8% | 67.66 | 2% | 69.14 | 8% | 73.11 | 5% | 74.05 | 2% | 68.37 | 2% |
| TiO2 | <0.02 | | 0.06 | 4% | 0.11 | 7% | 0.31 | 2% | 0.04 | 2% | 0.08 | 2% | 0.21 | 13% | 0.02 | 18% | <0.05 | | 0.05 | 26% | 0.05 | 10% | 0.02 | 20% |
| Al2O3 | 15.76 | 1% | 15.16 | 0% | 15.62 | 1% | 15.69 | 0% | 15.72 | 0% | 15.65 | 0% | 15.66 | 3% | 15.75 | 0% | 15.83 | 2% | 15.85 | 1% | 15.83 | 1% | 15.98 | 1% |
| FeO | 0.20 | 20% | 0.61 | 2% | 0.40 | 9% | 4.46 | 1% | 0.43 | 2% | 1.09 | 1% | 0.62 | 32% | 0.48 | 6% | <0.28 | | <0.21 | | 0.20 | 14% | 0.15 | 18% |
| MnO | <0.00 | | 0.01 | 4% | 0.01 | 13% | 0.06 | 2% | 0.01 | 2% | 0.01 | 2% | 0.02 | 20% | <0.00 | | <0.01 | | <0.01 | | 0.00 | 20% | 0.00 | 19% |
| MgO | 0.01 | 22% | 0.08 | 2% | 0.03 | 8% | 1.91 | 0% | 0.03 | 1% | 0.18 | 1% | <0.04 | | 0.02 | 8% | <0.01 | | 0.01 | 29% | 0.01 | 14% | 0.01 | 17% |
| CaO | 2.64 | 13% | 2.11 | 4% | 1.96 | 14% | 3.33 | 6% | 2.25 | 2% | 2.20 | 2% | <2.22 | | 2.15 | 8% | 3.87 | 23% | <1.88 | | 1.33 | 18% | 3.12 | 8% |
| Na2O | 6.11 | 1% | 4.41 | 0% | 3.11 | 1% | 6.87 | 0% | 5.10 | 0% | 4.47 | 0% | <0.29 | | 6.26 | 0% | 4.09 | 2% | 1.97 | 4% | 1.68 | 2% | 6.52 | 0% |
| K2O | 2.29 | 1% | 4.77 | 0% | 6.18 | 0% | 2.63 | 0% | 3.29 | 0% | 4.07 | 0% | 14.22 | 0% | 3.66 | 0% | 2.85 | 2% | 3.30 | 1% | 2.84 | 0% | 1.82 | 1% |
| Total | 100.00 | 0% | 100.00 | 0% | 100.00 | 0% | 100.00 | 0% | 100.00 | 0% | 100.00 | 0% | 109.66 | 0% | 100.00 | 0% | 99.77 | 0% | 98.29 | 0% | 100.00 | 0% | 100.00 | 0% |
| mass factor | 0.48 | 0.00 | 0.56 | 0.00 | 0.32 | 0.00 | 0.29 | 0.00 | 0.69 | 0.00 | 0.76 | 0.00 | 0.11 | 0.00 | 0.55 | 0.00 | 0.29 | 0.00 | 0.21 | 0.00 | 0.27 | 0.00 | 0.45 | 0.00 |
| P3 | <497.24 | | <48.84 | | <205.14 | | 135.81 | 28% | 33.03 | 13% | 30.68 | 16% | <573.56 | | <203.83 | | <1037.73 | | <582.73 | | <237.82 | | 2687.62 | 4% |
| Sc | <16.36 | | 2.65 | 18% | <6.92 | | 20.60 | 8% | 1.35 | 13% | 4.98 | 6% | <21.03 | | <6.79 | | <31.59 | | <18.80 | | <7.50 | | <8.15 | |
| V5 | <32.40 | | 3.23 | 29% | <14.61 | | 19.80 | 11% | 1.58 | 21% | 4.07 | 11% | <51.42 | | <17.50 | | <96.66 | | <50.36 | | <21.53 | | <23.64 | |
| Cr | <371.74 | | <38.53 | | <137.69 | | <64.55 | | <12.02 | | <12.51 | | <548.82 | | <186.80 | | <1129.12 | | <613.89 | | <247.74 | | <218.92 | |
| Co | <5.70 | | <0.69 | | <3.27 | | 3.85 | 19% | <0.26 | | 0.44 | 30% | <14.28 | | <4.04 | | <20.43 | | <11.59 | | <4.96 | | <4.69 | |
| Ni | <31.93 | | <4.49 | | 2.70 | 67% | 6.64 | 38% | <1.18 | | <1.19 | | <38.72 | | <13.19 | | <81.20 | | <36.68 | | <18.24 | | <9.71 | |
| Cu | <13.15 | | 3.11 | 24% | 52.43 | 6% | 81.55 | 4% | 9.76 | 5% | 10.61 | 5% | 62.91 | 39% | <11.38 | | <53.41 | | <29.45 | | <10.82 | | 83.49 | 8% |
| Rb | 55.28 | 8% | 136.32 | 1% | 183.86 | 3% | 52.92 | 3% | 95.56 | 1% | 123.61 | 1% | 462.87 | 4% | 37.68 | 6% | 86.04 | 16% | 49.63 | 9% | 87.10 | 3% | 35.92 | 9% |
| Sr | 1265.79 | 3% | 774.65 | 1% | <78.53 | | 910.00 | 2% | 784.55 | 0% | 848.62 | 0% | 1141.51 | 10% | 1040.52 | 2% | 879.62 | 9% | 788.29 | 8% | 416.80 | 6% | 1138.12 | 2% |
| Y8 | <1.20 | | 0.28 | 36% | 11.22 | 10% | 6.40 | 8% | 6.03 | 3% | 3.36 | 5% | 26.16 | 14% | <0.77 | | <5.16 | | 6.33 | 30% | 1.36 | 24% | 6.83 | 16% |
| Zr | 9.97 | 23% | 31.38 | 4% | 113.66 | 5% | 197.10 | 2% | 38.24 | 2% | 44.00 | 2% | 97.66 | 15% | 4.49 | 24% | <10.81 | | 49.88 | 15% | 38.13 | 6% | 20.89 | 13% |
| Nb | 2.43 | 35% | 1.37 | 15% | 12.46 | 11% | 20.05 | 5% | 7.25 | 3% | 5.91 | 4% | 33.33 | 13% | 0.32 | 63% | <1.72 | | 4.32 | 36% | 1.78 | 23% | 1.27 | 42% |
| Ba | 869.50 | 5% | 1192.63 | 1% | 560.41 | 6% | 575.69 | 3% | 1382.42 | 1% | 995.63 | 1% | 3145.60 | 5% | 1058.01 | 3% | 1369.77 | 9% | 785.64 | 10% | 600.45 | 5% | 599.13 | 5% |
| Cs | <0.63 | | 2.87 | 7% | 7.40 | 9% | 1.13 | 14% | 3.42 | 3% | 2.69 | 4% | 14.80 | 15% | <0.10 | | <4.35 | | 3.54 | 27% | 3.93 | 9% | 1.16 | 28% |
| La | 7.91 | 18% | 3.98 | 8% | 51.96 | 4% | 40.94 | 4% | 12.47 | 2% | 7.08 | 3% | 50.73 | 13% | 8.66 | 10% | 20.85 | 22% | 17.50 | 19% | 4.90 | 21% | 14.82 | 9% |
| Ce | 8.22 | 18% | 4.75 | 8% | 84.69 | 3% | 62.73 | 3% | 23.27 | 1% | 12.70 | 2% | 134.56 | 6% | 12.57 | 8% | 9.03 | 42% | 22.56 | 16% | 5.41 | 20% | 30.25 | 6% |
| Nd | <4.91 | | <0.77 | | 36.93 | 11% | 18.99 | 10% | 8.62 | 5% | 4.12 | 8% | 34.61 | 33% | <3.57 | | <6.77 | | <10.79 | | <2.78 | | 12.63 | 21% |
| Sm | 2.98 | 60% | <0.37 | | 5.97 | 29% | 3.22 | 29% | 1.34 | 14% | 0.67 | 23% | <5.77 | | <1.94 | | <14.37 | | <6.36 | | <2.19 | | <2.33 | |
| Yb | <5.16 | | <0.25 | | <2.35 | | <0.60 | | 0.95 | 16% | 0.34 | 30% | 0.96 | 63% | <0.49 | | <13.64 | | <3.26 | | <1.93 | | <3.65 | |
| Pb | 33.74 | 11% | 22.66 | 5% | 35.15 | 9% | 5.65 | 40% | 36.23 | 2% | 21.45 | 2% | 84.19 | 17% | 31.74 | 7% | 77.25 | 15% | 52.41 | 15% | 61.17 | 5% | 41.03 | 8% |
| Th | 3.56 | 19% | 1.76 | 8% | 12.11 | 7% | 9.62 | 5% | 8.16 | 2% | 4.60 | 3% | 27.22 | 11% | 1.10 | 22% | <2.02 | | 8.81 | 17% | 1.53 | 15% | 2.78 | 17% |
| U2 | <0.56 | | 0.19 | 25% | 9.77 | 8% | 5.63 | 6% | 4.42 | 3% | 2.03 | 4% | 24.15 | 9% | 0.09 | 71% | <1.35 | | 2.90 | 28% | 0.85 | 19% | 1.44 | 23% |
| Ho | <0.22 | | <0.05 | | <0.22 | | 0.31 | 37% | 0.19 | 15% | 0.07 | 28% | 0.86 | 63% | <0.14 | | 0.64 | 105% | <0.53 | | <0.31 | | 0.30 | 59% |
| B1 | <539.01 | | 56.44 | 50% | <254.02 | | <97.98 | | 40.93 | 15% | 29.66 | 17% | <543.78 | | <179.49 | | <975.06 | | <539.46 | | <175.89 | | <208.24 | |



Major oxide concentrations in wt%
Trace element concentrations in ppm

continued on next page

LA-ICPMS analyses of plagioclase-hosted Si-MI in **tholeiitic andesite** form Lark, Bingham canyon volcanic suite. Element concentrations and uncertainty

Table 2.2

| Melt inclusions | 15jl13b14.xl | | 15jl13b15.xl | | 15jl13b16.xl | | 15jl13b17.xl | | 15jl13b18.xl | | 15jl13b20.xl | | 15jl13b22.xl | | 15jl13b24.xl | | 15jl13b25.xl | | 15jl13b26.xl | | 15jl13b28.xl | |
|---|---|---|---|---|---|---|---|---|---|---|---|---|---|---|---|---|---|---|---|---|---|---|
| SiO2 | 71.50 | 5% | 65.64 | 1% | 61.80 | 4% | 67.91 | 1% | 68.63 | 3% | 65.52 | 24% | 86.31 | 6% | 73.18 | 2% | 69.71 | 4% | <60.56 | | 67.45 | 2% |
| TiO2 | <0.03 | | 0.06 | 3% | 0.09 | 10% | 0.05 | 8% | 0.12 | 7% | 0.43 | 11% | 0.16 | 14% | 0.02 | 26% | <0.02 | | 0.25 | 40% | 0.07 | 7% |
| Al2O3 | 15.79 | 1% | 15.76 | 0% | 15.73 | 1% | 15.72 | 0% | 15.73 | 1% | 15.90 | 6% | 15.90 | 2% | 15.84 | 1% | 15.86 | 1% | 15.42 | 15% | 15.86 | 1% |
| FeO | 0.19 | 36% | 1.28 | 1% | 1.18 | 5% | 0.38 | 7% | 0.52 | 9% | 1.37 | 26% | 0.35 | 32% | 0.36 | 12% | 0.21 | 30% | 10.38 | 8% | 0.59 | 6% |
| MnO | <0.01 | | 0.02 | 2% | 0.02 | 9% | 0.00 | 29% | 0.01 | 12% | 0.02 | 63% | <0.01 | | 0.01 | 11% | <0.00 | | 0.06 | 40% | 0.01 | 8% |
| MgO | 0.01 | 39% | 0.36 | 1% | 0.24 | 2% | 0.01 | 14% | 0.03 | 7% | 0.06 | 24% | <0.01 | | 0.01 | 22% | 0.01 | 35% | 1.30 | 4% | 0.05 | 4% |
| CaO | 3.50 | 17% | 2.29 | 3% | <0.77 | | 1.90 | 9% | 1.99 | 16% | <4.01 | | <2.87 | | 2.15 | 15% | 2.71 | 20% | <12.25 | | 1.83 | 13% |
| Na2O | 3.49 | 2% | 5.81 | 0% | 5.07 | 1% | 5.70 | 0% | 4.38 | 1% | 2.71 | 13% | <0.32 | | 2.33 | 2% | 5.78 | 1% | 24.48 | 3% | 5.16 | 1% |
| K2O | 1.54 | 2% | 4.77 | 0% | 11.50 | 0% | 4.34 | 0% | 4.59 | 0% | 15.41 | 1% | 2.91 | 1% | 2.10 | 1% | 1.71 | 1% | 53.43 | 1% | 4.99 | 0% |
| Total | 100.01 | 0% | 100.00 | 0% | 99.61 | 0% | 100.00 | 0% | 100.00 | 0% | 105.42 | 0% | 109.64 | 0% | 100.00 | 0% | 99.99 | 0% | 109.32 | 0% | 100.00 | 0% |
| mass factor | 0.39 | 0.00 | 0.50 | 0.00 | 0.17 | 0.00 | 0.46 | 0.00 | 0.35 | 0.00 | 0.06 | 0.00 | 0.11 | 0.00 | 0.22 | 0.00 | 0.19 | 0.00 | 0.02 | 0.00 | 0.33 | 0.00 |
| P3 | <566.33 | | <37.62 | | - <176.63 | | <90.42 | | - <189.85 | | 3014.58 | 23% | 1146.36 | 27% | <231.28 | | <334.11 | | <2266.58 | | - <123.96 | |
| Sc | <19.25 | | 4.59 | 11% | <6.02 | | <3.10 | | <4.70 | | <30.66 | | <32.70 | | <7.11 | | <10.30 | | <90.76 | | <4.40 | |
| V5 | <56.23 | | 4.06 | 27% | <16.09 | | <8.26 | | <13.57 | | <94.28 | | <97.07 | | <23.83 | | <31.50 | | <259.18 | | <11.97 | |
| Cr | <647.79 | | <36.83 | | <165.65 | | <99.34 | | <135.86 | | <915.54 | | <999.82 | | <215.83 | | <325.53 | | <2932.29 | | <138.03 | |
| Co | <12.26 | | 2.64 | 15% | <3.55 | | <2.24 | | <3.85 | | <17.91 | | <28.89 | | <3.84 | | <6.99 | | <61.16 | | <2.65 | |
| Ni | <20.06 | | <3.90 | | 5.92 | 63% | <8.61 | | <12.98 | | <86.90 | | <22.84 | | <15.33 | | <20.22 | | <264.02 | | <15.71 | |
| Cu | <28.88 | | 17.71 | 6% | <18.53 | | <5.21 | | 57.87 | 7% | <102.63 | | <57.87 | | 21.36 | 26% | <22.17 | | <156.06 | | 6.30 | 23% |
| Rb | 28.74 | 24% | 133.99 | 1% | 359.60 | 2% | 119.29 | 2% | 135.55 | 4% | 574.97 | 5% | 134.60 | 8% | 69.85 | 5% | 33.84 | 12% | 570.31 | 10% | 159.16 | 2% |
| Sr | 1293.74 | 4% | 852.71 | 1% | <85.05 | | 854.88 | 2% | 630.20 | 5% | <421.57 | | 588.98 | 16% | 1004.36 | 3% | 1101.06 | 5% | <1261.37 | | 868.38 | 3% |
| Y8 | <2.64 | | 1.09 | 14% | 1.33 | 21% | <0.65 | | 6.70 | 13% | 34.26 | 17% | 10.08 | 24% | 3.55 | 21% | 2.92 | 37% | 23.06 | 38% | 8.97 | 9% |
| Zr | 12.09 | 39% | 48.39 | 3% | 64.69 | 5% | 23.18 | 6% | 163.55 | 4% | 331.07 | 6% | 296.19 | 6% | 33.11 | 9% | 11.11 | 23% | 115.47 | 23% | 53.83 | 5% |
| Nb | <2.99 | | 4.66 | 6% | 8.66 | 11% | <0.75 | | 8.87 | 13% | 36.66 | 15% | 15.82 | 22% | 3.52 | 23% | 5.55 | 26% | <14.26 | | 10.18 | 9% |
| Ba | 969.07 | 8% | 1077.28 | 1% | 4216.63 | 2% | 1328.52 | 2% | 946.72 | 5% | 2192.77 | 16% | 2238.39 | 6% | 873.88 | 5% | 1107.21 | 7% | 9945.98 | 8% | 1520.52 | 2% |
| Cs | 1.07 | 60% | 3.32 | 5% | 8.28 | 8% | 4.31 | 7% | 4.78 | 13% | 24.18 | 13% | <3.00 | | 2.85 | 16% | 1.74 | 27% | <5.92 | | 5.68 | 8% |
| La | 10.67 | 27% | 8.79 | 5% | 18.50 | 13% | 5.66 | 13% | 31.71 | 7% | 154.78 | 9% | 57.86 | 9% | 8.28 | 19% | <7.30 | | 57.94 | 53% | 16.96 | 7% |
| Ce | 8.75 | 31% | 13.16 | 4% | 20.22 | 11% | 4.97 | 18% | 50.57 | 5% | 247.71 | 6% | 77.11 | 8% | 10.65 | 16% | <8.02 | | <61.56 | | 26.37 | 5% |
| Nd | <10.34 | | 2.88 | 17% | <4.05 | | 0.76 | 727% | 16.37 | 17% | 52.27 | 17% | 19.10 | 34% | <5.29 | | <8.97 | | 68.65 | 58% | 7.48 | 25% |
| Sm | <7.13 | | 0.44 | 39% | <3.20 | | <0.72 | | - <2.76 | | - <21.48 | | <14.07 | | <3.00 | | <5.56 | | <27.16 | | <1.83 | |
| Yb | <2.05 | | 0.17 | 60% | <1.38 | | <1.54 | | -0.54<I<1.71 | | 6.18 | 101% | <9.72 | | <2.50 | | <5.39 | | <28.85 | | 1.55 | 53% |
| Pb | 63.24 | 13% | 34.30 | 3% | 24.11 | 26% | 22.05 | 12% | 18.89 | 21% | <45.96 | | 174.08 | 7% | 64.26 | 6% | 34.67 | 16% | <134.72 | | 28.78 | 9% |
| Th | 2.70 | 38% | 3.66 | 5% | 4.76 | 9% | 2.30 | 9% | 12.78 | 7% | 47.69 | 8% | 14.03 | 14% | 5.19 | 11% | 3.65 | 19% | 57.41 | 13% | 11.62 | 5% |
| U2 | 1.71 | 45% | 1.68 | 7% | 0.89 | 26% | 0.70 | 37% | 5.87 | 9% | 19.91 | 14% | 4.73 | 22% | 3.11 | 14% | 1.62 | 26% | <6.56 | | 6.61 | 7% |
| Ho | 0.83 | 72% | <0.08 | | <0.29 | | <0.16 | | -0.15<I<0.21 | | <1.89 | | <0.51 | | <0.22 | | <0.71 | | <8.55 | | 0.22 | 48% |
| B1 | <607.18 | | <31.81 | | <177.68 | | <99.52 | | <113.33 | | <1019.52 | | <939.54 | | <206.26 | | <330.32 | | <2603.01 | | <129.77 | |



Major oxide concentrations in wt%
Trace element concentrations in ppm

continued on next page

LA-ICPMS analyses of plagioclase-hosted Si-MI in **tholeiitic andesite** form Lark, Bingham canyon volcanic suite. Element concentrations and uncertainty

Table 2.3

| Melt inclusions | 15jl13b41.xl | | 15jl13b42.xl | | 15jl13b43.xl | | 15jl13b44.xl | | 15jl13c03.xl | | 15jl13c04.xl | | 15jl13c05.xl | | 15jl13c06.xl | | 15jl13c07.xl | | 15jl13c08.xl | | 15jl13c09.xl | | 15jl13c10.xl | |
|---|---|---|---|---|---|---|---|---|---|---|---|---|---|---|---|---|---|---|---|---|---|---|---|---|
| SiO2 | 70.82 | 2% | 69.88 | 1% | 61.20 | 3% | 71.67 | 2% | 66.18 | 7% | 70.92 | 3% | 68.00 | 2% | 63.06 | 9% | 68.11 | 2% | 69.16 | 6% | 70.53 | 2% | 67.87 | 3% |
| TiO2 | 0.02 | 25% | 0.02 | 7% | 0.09 | 6% | 0.09 | 8% | 0.06 | 15% | 0.02 | 32% | 0.08 | 7% | 0.10 | 13% | 0.16 | 6% | <0.04 | | 0.03 | 21% | 0.04 | 19% |
| Al2O3 | 15.80 | 1% | 15.65 | 0% | 15.85 | 1% | 15.87 | 1% | 15.74 | 1% | 15.84 | 1% | 15.78 | 1% | 15.75 | 2% | 15.87 | 1% | 15.86 | 2% | 15.82 | 1% | 15.74 | 1% |
| FeO | 0.45 | 8% | 0.50 | 3% | 2.78 | 2% | 0.25 | 12% | 0.36 | 28% | 0.21 | 20% | 0.92 | 4% | 0.93 | 14% | 2.35 | 3% | 0.46 | 23% | 0.50 | 9% | 0.32 | 13% |
| MnO | 0.02 | 7% | 0.00 | 7% | 0.05 | 2% | 0.01 | 14% | 0.01 | 41% | 0.00 | 31% | 0.01 | 6% | 0.01 | 51% | 0.02 | 7% | <0.01 | | 0.00 | 29% | <0.00 | |
| MgO | 0.08 | 4% | 0.00 | 8% | 1.62 | 0% | 0.01 | 21% | 0.02 | 19% | <0.00 | | 0.04 | 4% | 0.05 | 10% | 0.10 | 4% | <0.01 | | <0.01 | | 0.01 | 26% |
| CaO | 2.00 | 12% | 1.74 | 3% | <0.69 | | 1.10 | 25% | 2.89 | 25% | 2.50 | 13% | 1.53 | 14% | <1.38 | | 3.59 | 10% | <2.22 | | 1.85 | 16% | 1.75 | 19% |
| Na2O | 3.59 | 1% | 4.73 | 0% | 8.50 | 1% | 3.29 | 1% | 3.78 | 2% | 2.92 | 1% | 4.64 | 1% | 6.39 | 2% | 1.52 | 3% | 5.02 | 2% | 4.20 | 1% | 6.78 | 1% |
| K2O | 3.23 | 0% | 3.47 | 0% | 8.64 | 0% | 3.72 | 0% | 6.95 | 1% | 3.59 | 1% | 4.99 | 0% | 8.54 | 1% | 4.28 | 0% | 5.60 | 1% | 3.09 | 1% | 3.48 | 1% |
| Total | 100.00 | 0% | 100.00 | 0% | 102.75 | 0% | 100.00 | 0% | 99.97 | 0% | 100.00 | 0% | 100.00 | 0% | 98.82 | 0% | 100.00 | 0% | 100.10 | 0% | 100.00 | 0% | 99.99 | 0% |
| mass factor | 0.42 | 0.00 | 0.92 | 0.00 | 0.14 | 0.00 | 0.26 | 0.00 | 0.30 | 0.00 | 0.30 | 0.00 | 0.39 | 0.00 | 0.19 | 0.00 | 0.22 | 0.00 | 0.29 | 0.00 | 0.41 | 0.00 | 0.36 | 0.00 |
| P3 | <259.93 | | <58.59 | | 94.44 | 47% | <177.07 | | <371.14 | | <279.40 | | <92.89 | | <331.27 | | <257.22 | | <814.09 | | <238.97 | | <176.52 | |
| Sc | <8.81 | | <1.69 | | 4.39 | 13% | <5.65 | | <10.94 | | <9.20 | | <3.39 | | <13.79 | | <7.87 | | <29.18 | | <6.75 | | <4.78 | |
| V5 | <26.97 | | <6.23 | | <8.11 | | <19.29 | | <36.50 | | <25.60 | | <9.28 | | <35.07 | | 28.58 | 23% | <77.05 | | <23.31 | | <16.44 | |
| Cr | <311.18 | | <58.89 | | <101.04 | | <232.77 | | <389.07 | | <316.94 | | <97.55 | | <412.75 | | <256.66 | | <912.35 | | <295.14 | | <190.96 | |
| Co | <6.52 | | 1.05 | 34% | 3.27 | 17% | <2.89 | | <7.81 | | <5.72 | | <1.29 | | <7.76 | | 5.03 | 43% | <15.59 | | <5.92 | | <2.84 | |
| Ni | <16.77 | | 1.32 | 54% | <6.26 | | <11.87 | | <44.10 | | <13.20 | | <9.37 | | <30.27 | | 17.43 | 36% | <85.89 | | <11.33 | | <11.62 | |
| Cu | <14.68 | | <4.28 | | 69.36 | 6% | <12.31 | | <27.45 | | <19.62 | | 2.35 | 25% | <23.61 | | <15.47 | | <51.31 | | 47.17 | 15% | <9.32 | |
| Rb | 91.60 | 4% | 95.72 | 2% | 234.85 | 1% | 116.38 | 3% | 215.92 | 5% | 113.02 | 5% | 139.54 | 3% | 316.35 | 4% | 118.63 | 4% | 72.18 | 14% | 71.73 | 6% | 89.49 | 5% |
| Sr | 958.63 | 2% | 831.57 | 1% | 202.24 | 23% | 885.85 | 3% | 880.04 | 7% | 1238.66 | 3% | 580.24 | 4% | 393.75 | 25% | 495.68 | 7% | 565.95 | 12% | 1046.02 | 3% | 1071.55 | 3% |
| Y8 | <0.97 | | 1.34 | 14% | 9.32 | 6% | 7.71 | 11% | 9.21 | 25% | 3.47 | 27% | 9.44 | 10% | 4.75 | 33% | 15.14 | 10% | 29.63 | 17% | <0.88 | | I<0.50 | |
| Zr | 8.93 | 17% | 24.25 | 5% | 125.38 | 2% | 133.88 | 4% | 69.51 | 9% | 36.45 | 10% | 66.04 | 5% | 46.96 | 11% | 165.27 | 4% | 6.04 | 57% | 5.28 | 33% | 14.48 | 16% |
| Nb | 0.54 | 53% | 1.41 | 17% | 8.55 | 7% | 6.29 | 14% | 6.07 | 18% | 4.09 | 24% | 16.01 | 8% | 7.64 | 26% | 22.68 | 9% | <2.83 | | 1.64 | 39% | <1.47 | |
| Ba | 1266.96 | 3% | 1168.23 | 1% | 2532.87 | 2% | 1992.38 | 2% | 1442.66 | 6% | 1042.66 | 4% | 1668.68 | 2% | 1659.97 | 7% | 1809.44 | 3% | 1501.03 | 7% | 1245.13 | 3% | 1254.68 | 4% |
| Cs | 3.35 | 14% | 4.18 | 5% | 5.52 | 6% | 4.66 | 10% | 8.42 | 15% | 4.65 | 14% | 5.76 | 9% | 4.62 | 15% | 0.67 | 40% | <0.59 | | 4.29 | 15% | 4.10 | 14% |
| La | 10.30 | 12% | 8.93 | 4% | 20.22 | 13% | 17.68 | 10% | 15.55 | 18% | 15.71 | 11% | 27.35 | 6% | 33.25 | 15% | 93.95 | 3% | 48.77 | 12% | 5.57 | 27% | <1.86 | |
| Ce | 9.80 | 13% | 10.78 | 4% | 31.18 | 9% | 24.53 | 8% | 25.42 | 14% | 17.83 | 10% | 58.49 | 3% | 48.19 | 12% | 170.11 | 2% | 36.42 | 15% | 7.41 | 21% | 2.73 | 57% |
| Nd | <2.37 | | 3.91 | 14% | 16.25 | 19% | 8.03 | 28% | 3.38 | 25% | <4.02 | | 24.47 | 11% | 15.25 | 39% | 59.46 | 9% | 77.56 | 18% | <3.70 | | <3.02 | |
| Sm | <0.90 | | <1.21 | | 2.46 | 48% | 2.54 | 44% | <4.89 | | <4.60 | | 2.61 | 33% | <7.39 | | 6.25 | 31% | 7.18 | 69% | <2.82 | | <3.43 | |
| Yb | <5.78 | | <0.57 | | 1.75 | 30% | <2.60 | | <7.19 | | <2.86 | | <0.81 | | <5.23 | | <4.55 | | <10.94 | | <4.04 | | <2.49 | |
| Pb | 54.22 | 6% | 34.32 | 3% | 16.59 | 28% | 62.23 | 5% | 33.03 | 25% | 70.18 | 6% | 23.05 | 12% | <16.58 | | 56.18 | 7% | 45.03 | 19% | 41.34 | 9% | 21.44 | 21% |
| Th | <0.39 | | 1.59 | 9% | 13.02 | 4% | 7.90 | 8% | 12.46 | 12% | 4.46 | 14% | 17.56 | 5% | 11.61 | 11% | 51.51 | 4% | 80.53 | 7% | 0.65 | 40% | -0.06<I<0.80 | |
| U2 | <0.18 | | 1.47 | 9% | 8.42 | 4% | 6.85 | 8% | 7.54 | 14% | 2.58 | 18% | 9.00 | 7% | 4.39 | 15% | 24.52 | 5% | 1.04 | 60% | <0.22 | | 0.48 | 59% |
| Ho | 0.18 | 63% | <0.13 | | 0.24 | 32% | <0.30 | | <0.76 | | <0.78 | | 0.22 | 54% | <1.14 | | 0.33 | 49% | <0.66 | | <0.44 | | <0.40 | |
| B1 | <261.96 | | <49.85 | | <94.33 | | <214.38 | | <387.28 | | <246.40 | | 3.83 | 178% | <364.78 | | <231.03 | | <808.38 | | <245.92 | | <166.90 | |



Major oxide concentrations in wt%
Trace element concentrations in ppm

continued on next page

LA-ICPMS analyses of plagioclase-hosted Si-MI in **tholeiitic andesite** form Lark, Bingham canyon volcanic suite. Element concentrations and uncertainty

Table 2.4

| Melt inclusions | 15jl13c11.xl | | 15jl13c13.xl | | 15jl13c14.xl | | 15jl13c15.xl | | 15jl13c16.xl | | 15jl13c17.xl | | 15jl13c20.xl | | 15jl13c22.xl | | 15jl13c23.xl | | 15jl13c25.xl | | 15jl13c26.xl | | 15jl13c27.xl | | 15jl13c31.xl | |
|---|---|---|---|---|---|---|---|---|---|---|---|---|---|---|---|---|---|---|---|---|---|---|---|---|---|---|
| SiO2 | 72.28 | 5% | 70.83 | 2% | 69.10 | 0% | 70.59 | 1% | 67.04 | 2% | 69.47 | 0% | 68.69 | 5% | 68.95 | 16% | 59.20 | 3% | 70.56 | 2% | 64.31 | 6% | 71.38 | 4% | 71.27 | 9% |
| TiO2 | <0.03 | | 0.04 | 15% | 0.05 | 2% | 0.03 | 7% | 0.04 | 17% | 0.06 | 2% | 0.11 | 10% | 0.19 | 15% | 0.10 | 6% | 0.03 | 18% | 0.22 | 6% | 0.04 | 19% | <0.05 | |
| Al2O3 | 15.81 | 1% | 15.75 | 0% | 15.74 | 0% | 15.79 | 0% | 15.80 | 1% | 15.74 | 0% | 15.75 | 1% | 15.68 | 4% | 15.79 | 1% | 15.81 | 1% | 15.69 | 2% | 15.87 | 1% | 15.88 | 2% |
| FeO | 0.22 | 33% | 0.24 | 13% | 0.49 | 1% | 0.30 | 5% | 1.71 | 4% | 0.58 | 1% | 0.43 | 17% | 1.17 | 20% | 1.51 | 3% | 0.38 | 11% | 1.95 | 5% | 0.32 | 16% | 0.38 | 36% |
| MnO | <0.01 | | 0.00 | 30% | 0.01 | 2% | 0.01 | 6% | 0.02 | 6% | 0.02 | 1% | 0.01 | 37% | 0.02 | 33% | 0.02 | 4% | 0.00 | 23% | 0.02 | 14% | 0.01 | 29% | <0.01 | |
| MgO | 0.01 | 40% | 0.01 | 14% | 0.04 | 1% | 0.01 | 8% | 0.48 | 2% | 0.06 | 1% | 0.03 | 12% | 0.08 | 12% | 0.52 | 1% | 0.01 | 16% | 0.07 | 6% | 0.01 | 21% | 0.03 | 23% |
| CaO | 2.16 | 25% | 1.72 | 12% | 1.52 | 2% | 1.31 | 8% | 2.41 | 10% | 2.07 | 2% | 1.44 | 36% | <2.31 | | 1.55 | 22% | 1.82 | 14% | <1.18 | | <1.14 | | <3.03 | |
| Na2O | 2.88 | 2% | 4.27 | 1% | 4.96 | 0% | 3.27 | 0% | 6.50 | 0% | 4.49 | 0% | 2.27 | 3% | <0.32 | | 3.83 | 1% | 3.27 | 1% | <0.17 | | 3.54 | 1% | 7.28 | 2% |
| K2O | 2.65 | 1% | 3.13 | 1% | 4.11 | 0% | 4.69 | 0% | 2.01 | 1% | 3.51 | 0% | 7.27 | 0% | 15.97 | 1% | 13.48 | 0% | 4.13 | 0% | 16.41 | 0% | 3.88 | 1% | 4.27 | 1% |
| Total | 100.00 | 0% | 100.00 | 0% | 100.00 | 0% | 100.00 | 0% | 100.00 | 0% | 100.00 | 0% | 99.99 | 0% | 106.05 | 0% | 100.00 | 0% | 100.00 | 0% | 102.67 | 0% | 99.05 | 0% | 103.12 | 0% |
| mass factor | 0.27 | 0.00 | 0.59 | 0.00 | 0.57 | 0.00 | 0.36 | 0.00 | 0.52 | 0.00 | 0.58 | 0.00 | 0.25 | 0.00 | 0.10 | 0.00 | 0.13 | 0.00 | 0.37 | 0.00 | 0.12 | 0.00 | 0.28 | 0.00 | 0.16 | 0.00 |
| P3 | <587.38 | | <232.37 | | 33.54 | 10% | <81.30 | | <276.67 | | 39.91 | 10% | <254.31 | | <981.46 | | 586.65 | 8% | <222.54 | | <435.96 | | <431.53 | | <1087.30 | |
| Sc | <18.15 | | <7.89 | | 1.21 | 10% | <2.42 | | <8.83 | | 0.89 | 16% | <8.91 | | <19.39 | | 7.30 | 23% | <6.43 | | <6.98 | | <15.78 | | <34.73 | |
| V5 | <57.42 | | <26.10 | | 1.71 | 15% | <6.69 | | <28.49 | | 2.67 | 12% | <27.07 | | <63.01 | | <9.33 | | <23.35 | | <25.40 | | <48.82 | | <117.85 | |
| Cr | <706.28 | | <272.78 | | <10.53 | | <80.96 | | <323.82 | | <12.62 | | <329.06 | | <698.43 | | <108.69 | | <276.77 | | <263.61 | | <451.09 | | <1271.03 | |
| Co | <18.82 | | <5.18 | | 0.31 | 33% | <1.19 | | <7.11 | | <0.23 | | <5.79 | | <14.99 | | <2.26 | | <4.38 | | <4.49 | | <9.22 | | <18.40 | |
| Ni | <48.61 | | <6.19 | | 0.48 | 54% | <6.42 | | 14.31 | 47% | <0.77 | | <25.24 | | <73.38 | | <7.53 | | <13.51 | | <16.23 | | <14.44 | | <86.65 | |
| Cu | <39.55 | | <14.93 | | 2.93 | 9% | 22.29 | 9% | 43.17 | 17% | 9.57 | 4% | <24.44 | | 33.60 | 25% | 18.67 | 12% | <15.96 | | <17.22 | | <31.40 | | <73.28 | |
| Rb | 89.49 | 9% | 94.76 | 5% | 115.02 | 1% | 140.55 | 2% | 44.50 | 9% | 107.22 | 1% | 233.81 | 4% | 565.79 | 4% | 451.62 | 1% | 133.95 | 4% | 1161.33 | 1% | 127.48 | 6% | 93.46 | 16% |
| Sr | 815.62 | 6% | 716.81 | 3% | 679.99 | 1% | 484.45 | 2% | 728.00 | 3% | 729.51 | 1% | 100.92 | 55% | <250.58 | | 280.11 | 14% | 657.54 | 4% | <133.17 | | 555.29 | 7% | <324.69 | |
| Y8 | <1.87 | | 4.45 | 21% | 3.50 | 3% | 3.02 | 10% | 1.74 | 38% | 7.98 | 2% | 4.53 | 17% | 15.86 | 22% | 9.82 | 8% | <0.70 | | 13.39 | 11% | <1.40 | | 3.27 | 59% |
| Zr | 3.80 | 60% | 46.18 | 9% | 33.34 | 1% | 45.16 | 4% | 21.44 | 14% | 46.96 | 1% | 95.27 | 7% | 438.09 | 5% | 157.52 | 3% | 15.68 | 16% | 126.65 | 5% | 7.06 | 28% | 81.53 | 16% |
| Nb | <2.98 | | 2.79 | 27% | 3.95 | 3% | 2.09 | 13% | <0.99 | | 7.15 | 3% | 15.25 | 12% | 35.13 | 12% | 12.50 | 7% | <1.13 | | 9.30 | 15% | 3.89 | 26% | 9.05 | 38% |
| Ba | 2086.11 | 4% | 701.11 | 4% | 904.12 | 1% | 1254.27 | 1% | 463.63 | 6% | 1268.47 | 1% | 1512.09 | 5% | 2115.44 | 9% | 3118.77 | 2% | 1338.60 | 3% | 2678.43 | 4% | 1303.85 | 4% | 2128.33 | 7% |
| Cs | 2.35 | 31% | 3.69 | 16% | 1.75 | 3% | 4.67 | 6% | 0.82 | 34% | 4.36 | 2% | 7.57 | 12% | 18.93 | 10% | 7.38 | 6% | 5.52 | 13% | 101.71 | 3% | 3.50 | 19% | <3.41 | |
| La | <4.63 | | 10.16 | 11% | 7.10 | 2% | 1.98 | 25% | 7.85 | 15% | 18.05 | 1% | 18.42 | 11% | 78.78 | 9% | 44.91 | 4% | 2.97 | 31% | 67.67 | 4% | 13.49 | 13% | <15.49 | |
| Ce | <4.87 | | 19.54 | 8% | 16.21 | 1% | 2.30 | 22% | 6.77 | 17% | 33.52 | 1% | 33.31 | 7% | 98.60 | 8% | 76.56 | 3% | 2.95 | 32% | 113.56 | 3% | 14.86 | 13% | <16.65 | |
| Nd | <10.08 | | 7.27 | 29% | 6.60 | 4% | <1.30 | | 8.30 | 29% | 13.14 | 3% | 18.50 | 21% | 28.77 | 22% | 27.56 | 10% | 3.25 | 51% | 42.61 | 11% | <5.23 | | <17.46 | |
| Sm | 2.77 | 80% | <2.73 | | 1.27 | 10% | <0.86 | | <4.14 | | 2.01 | 10% | <3.16 | | <10.07 | | 4.91 | 20% | <3.39 | | 6.49 | 33% | 4.15 | 45% | <19.16 | |
| Yb | <8.56 | | <2.54 | | 0.47 | 16% | <0.98 | | <2.94 | | 0.94 | 13% | <5.24 | | <9.02 | | <0.86 | | <2.36 | | <3.98 | | <4.49 | | 6.60 | 72% |
| Pb | 96.65 | 8% | 36.58 | 8% | 21.14 | 2% | 57.90 | 3% | 43.32 | 8% | 31.40 | 2% | 29.57 | 25% | 49.80 | 44% | 30.29 | 15% | 44.84 | 8% | 15.29 | 56% | 86.23 | 6% | 57.26 | 22% |
| Th | 0.21 | 109% | 8.76 | 10% | 4.81 | 2% | 6.09 | 5% | 6.05 | 13% | 9.54 | 2% | 13.88 | 8% | 32.18 | 9% | 16.77 | 5% | 0.48 | 43% | 36.81 | 5% | 3.10 | 19% | 7.32 | 26% |
| U2 | <0.21 | | 3.17 | 16% | 1.51 | 3% | 2.12 | 7% | <0.52 | | 5.40 | 2% | 6.73 | 13% | 15.61 | 13% | 6.44 | 6% | <0.12 | | 3.10 | 14% | <0.58 | | 2.58 | 41% |
| Ho | <1.00 | | <0.41 | | 0.11 | 13% | <0.11 | | <0.46 | | 0.29 | 10% | <0.50 | | 0.74 | 105% | 0.35 | 30% | <0.38 | | <0.55 | | <0.72 | | <1.71 | |
| B1 | <645.66 | | <237.16 | | 21.49 | 20% | <85.62 | | <268.01 | | 38.31 | 13% | <264.65 | | <553.73 | | <109.30 | | <236.76 | | <261.01 | | <478.60 | | <1060.02 | |



Major oxide concentrations in wt%
Trace element concentrations in ppm

continued on next page

LA-ICPMS analyses of plagioclase-hosted Si-MI in **tholeiitic andesite** form Lark, Bingham canyon volcanic suite. Element concentrations and uncertainty

Table 2.5

| Melt inclusions | 15jl13c32.xl | | 15jl13c33.xl | | 15jl13c35.xl | | 15jl13c36.xl | | 15jl13c37.xl | | 15jl13c38.xl | | 15jl13c39.xl | | 15jl13c40.xl | | 15jl13c41.xl | | 15jl13c42.xl | | 15jl13b33.xl | |
|---|---|---|---|---|---|---|---|---|---|---|---|---|---|---|---|---|---|---|---|---|---|---|
| SiO2 | 70.19 | 2% | 69.79 | 1% | 68.63 | 1% | 68.00 | 1% | 78.29 | 5.45% | 65.63 | 1.43% | 68.73 | 1.57% | 68.39 | 2.77% | 70.68 | 2.13% | 71.30 | 1.74% | 65.96 | 5.90% |
| TiO2 | 0.03 | 17% | 0.07 | 6% | 0.02 | 12% | 0.06 | 4% | 0.04 | 32.70% | 0.06 | 7.78% | 0.05 | 10.78% | 0.11 | 8.35% | 0.02 | 26.47% | 0.06 | 9.38% | 0.25 | 10.42% |
| Al2O3 | 15.83 | 1% | 15.67 | 0% | 15.79 | 0% | 15.81 | 0% | 15.82 | 2.23% | 15.80 | 0.47% | 15.71 | 0.40% | 15.79 | 0.85% | 15.75 | 0.52% | 15.78 | 0.59% | 15.92 | 1.68% |
| FeO | 0.28 | 12% | 0.51 | 4% | 0.40 | 5% | 0.54 | 3% | <0.29 | | 2.04 | 2.42% | 0.69 | 5.33% | 0.69 | 7.65% | 0.18 | 16.30% | 0.29 | 11.02% | 1.04 | 10.51% |
| MnO | 0.01 | 15% | 0.01 | 6% | 0.01 | 8% | 0.01 | 4% | 0.02 | 11.29% | 0.03 | 3.47% | 0.02 | 5.18% | 0.01 | 20.13% | <0.00 | | 0.00 | 25.22% | 0.02 | 14.55% |
| MgO | 0.01 | 15% | 0.02 | 5% | 0.04 | 3% | 0.07 | 2% | 0.02 | 25.60% | 0.57 | 1.07% | 0.26 | 1.98% | 0.03 | 8.21% | 0.00 | 31.73% | 0.01 | 12.48% | 0.08 | 7.74% |
| CaO | 3.02 | 8% | 1.86 | 5% | 2.61 | 5% | 1.33 | 8% | 3.86 | 24.55% | 2.44 | 8.10% | 2.88 | 6.28% | 1.88 | 19.32% | 2.24 | 10.29% | 1.26 | 18.85% | 1.95 | 41.17% |
| Na2O | 4.70 | 1% | 4.07 | 0% | 6.30 | 0% | 6.20 | 0% | <0.32 | | 6.72 | 0.37% | 4.45 | 0.43% | 5.36 | 0.78% | 4.81 | 0.57% | 3.54 | 0.83% | 6.72 | 1.14% |
| K2O | 1.94 | 1% | 4.01 | 0% | 2.20 | 0% | 3.98 | 0% | 7.48 | 0.63% | 2.70 | 0.40% | 3.21 | 0.41% | 3.74 | 0.52% | 2.31 | 0.61% | 3.75 | 0.40% | 4.06 | 0.79% |
| Total | 100.00 | 0% | 100.00 | 0% | 100.00 | 0% | 100.00 | 0% | 109.53 | 0.00% | 100.00 | 0.00% | 100.00 | 0.00% | 100.00 | 0.00% | 100.00 | 0.00% | 100.00 | 0.00% | 100.00 | 0.00% |
| mass factor | 0.34 | 0.00 | 0.74 | 0.00 | 0.49 | 0.00 | 0.36 | 0.00 | 0.07 | 0.00 | 0.43 | 0.00 | 0.71 | 0.00 | 0.31 | 0.00 | 0.47 | 0.00 | 0.32 | 0.00 | 0.27 | 0.00 |
| P3 | <143.35 | | <65.72 | | <81.06 | | <48.40 | | <471.72 | | <117.90 | | <154.13 | | <204.52 | | <215.89 | | <163.93 | | <560.17 | |
| Sc | <4.68 | | <2.21 | | <2.76 | | 1.30 | 44% | <16.54 | | 3.57 | 35.55% | <5.20 | | <6.24 | | <7.10 | | <4.77 | | <15.43 | |
| V5 | <15.97 | | <7.16 | | <8.56 | | <5.21 | | <50.47 | | <12.01 | | <17.01 | | <22.49 | | <24.91 | | <15.61 | | <45.23 | |
| Cr | <168.10 | | <84.03 | | <87.95 | | <46.71 | | <583.79 | | <131.68 | | <198.76 | | <267.20 | | <298.66 | | <167.98 | | <560.54 | |
| Co | <3.98 | | <1.40 | | <1.61 | | <0.77 | | <9.81 | | <2.56 | | <2.29 | | <5.24 | | <5.24 | | <3.64 | | <9.64 | |
| Ni | <13.91 | | <6.85 | | <6.58 | | <3.80 | | <32.42 | | <7.52 | | <18.09 | | <23.18 | | <16.55 | | <9.64 | | <43.92 | |
| Cu | <10.01 | | 5.83 | 16% | 6.19 | 29% | 8.67 | 13% | <35.46 | | 34.37 | 10.61% | 15.37 | 24.30% | 41.63 | 15.14% | <15.98 | | <10.16 | | <23.99 | |
| Rb | 46.81 | 6% | 125.21 | 2% | 56.74 | 3% | 114.84 | 1% | 350.60 | 3.49% | 69.16 | 4.09% | 49.43 | 4.30% | 106.76 | 4.75% | 70.72 | 6.15% | 118.82 | 3.47% | 115.30 | 7.84% |
| Sr | 1036.84 | 3% | 757.78 | 1% | 1083.53 | 1% | 770.04 | 1% | <283.20 | | 947.85 | 2.16% | 948.20 | 1.82% | 838.15 | 4.82% | 787.91 | 2.85% | 603.65 | 4.14% | 898.08 | 9.06% |
| Y8 | 2.85 | 22% | 6.31 | 10% | 0.54 | 39% | 1.77 | 11% | 4.03 | 31.31% | 0.83 | 45.32% | 0.27 | 71.63% | <2.96 | | <0.79 | | 8.23 | 12.12% | 4.47 | 40.58% |
| Zr | 16.63 | 13% | 48.79 | 5% | 24.90 | 6% | 47.69 | 3% | 4.57 | 39.04% | 45.29 | 6.20% | 23.42 | 11.05% | 55.68 | 11.88% | 11.86 | 18.05% | 42.00 | 7.43% | 181.61 | 7.24% |
| Nb | 2.48 | 26% | 8.45 | 9% | 1.44 | 21% | 8.39 | 5% | <2.01 | | 4.60 | 14.61% | 2.67 | 24.29% | 14.82 | 11.64% | 0.59 | 57.89% | 7.71 | 13.17% | 12.42 | 25.22% |
| Ba | 671.15 | 5% | 753.09 | 2% | 604.46 | 3% | 1120.46 | 1% | 4179.34 | 3.23% | 900.07 | 2.88% | 952.52 | 2.79% | 1139.57 | 4.49% | 670.10 | 4.64% | 1296.29 | 2.78% | 666.41 | 12.08% |
| Cs | 2.83 | 16% | 4.70 | 8% | 1.23 | 15% | 3.64 | 5% | 8.80 | 13.69% | 1.22 | 18.81% | 3.96 | 13.33% | 6.92 | 10.23% | 2.23 | 19.65% | 4.27 | 11.13% | 5.42 | 21.72% |
| La | 9.53 | 13% | 12.52 | 6% | 1.73 | 24% | 6.52 | 7% | 59.32 | 8.06% | 7.06 | 12.86% | 3.52 | 21.97% | 36.13 | 6.49% | 4.98 | 19.29% | 10.20 | 11.26% | 54.62 | 10.38% |
| Ce | 13.13 | 10% | 23.27 | 4% | 2.86 | 17% | 9.67 | 5% | 88.09 | 6.21% | 11.43 | 9.35% | 5.04 | 16.52% | 71.29 | 4.19% | 5.72 | 17.56% | 19.43 | 7.46% | 83.94 | 8.12% |
| Nd | 3.92 | 42% | 7.14 | 16% | <1.69 | | 4.50 | 15% | 22.75 | 26.43% | 4.97 | 27.78% | <1.46 | | 26.43 | 16.48% | 3.19 | 45.56% | 11.09 | 19.44% | 24.44 | 32.52% |
| Sm | <1.05 | | 0.96 | 48% | <1.46 | | <0.80 | | <6.38 | | <1.77 | | 1.37 | 71.63% | 5.48 | 32.60% | <3.69 | | <2.17 | | 4.97 | 56.89% |
| Yb | <2.13 | | <0.97 | | 0.28 | 80% | <0.39 | | <6.88 | | 0.28 | 105.95% | <2.02 | | <2.85 | | <2.49 | | <1.52 | | <6.86 | |
| Pb | 48.93 | 7% | 27.92 | 5% | 32.90 | 5% | 48.13 | 3% | 200.36 | 6.18% | 27.43 | 8.06% | 31.30 | 7.31% | 20.05 | 22.23% | 36.02 | 8.25% | 45.86 | 6.82% | 37.03 | 21.05% |
| Th | 3.86 | 13% | 7.41 | 6% | 0.80 | 17% | 3.78 | 5% | 14.45 | 10.62% | 1.21 | 18.44% | <0.30 | | 8.43 | 13.15% | 0.46 | 47.26% | 8.51 | 8.11% | 12.24 | 13.61% |
| U2 | 1.88 | 18% | 4.74 | 7% | 0.53 | 20% | 2.13 | 6% | 0.57 | 50.40% | 0.99 | 19.02% | 0.23 | 51.66% | 11.63 | 8.91% | <0.56 | | 5.41 | 9.51% | 2.10 | 43.95% |
| Ho | 0.44 | 41% | 0.30 | 33% | <0.13 | | <0.14 | | <1.34 | | <0.19 | | <0.39 | | <0.56 | | 0.22 | 69.60% | <0.33 | | <1.31 | |
| B1 | <168.51 | | <70.59 | | <83.42 | | <44.86 | | <609.41 | | <122.43 | | <159.48 | | <248.52 | | <224.80 | | <159.03 | | <491.81 | |



Major oxide concentrations in wt%
Trace element concentrations in ppm

continued on next page

LA-ICPMS analyses of plagioclase-hosted Si-MI in **tholeiitic andesite** form Lark, Bingham canyon volcanic suite. Element concentrations and uncertainty

Table 2.6

| Melt inclusions | 15jl13b35.xl | | 15jl13b38.xl | |
|---|---|---|---|---|
| SiO2 | 64.67 | 3.90% | 68.76 | 4.22% |
| TiO2 | 0.10 | 11.39% | <0.02 | |
| Al2O3 | 15.88 | 1.03% | 15.91 | 0.93% |
| FeO | 1.60 | 4.73% | 0.30 | 20.30% |
| MnO | 0.03 | 6.05% | <0.01 | |
| MgO | 0.12 | 4.07% | 0.02 | 16.42% |
| CaO | 3.43 | 13.98% | 3.13 | 16.36% |
| Na2O | 4.39 | 1.11% | 5.34 | 0.85% |
| K2O | 5.78 | 0.44% | 2.53 | 0.89% |
| Total | 100.00 | 0.00% | 99.98 | 0.00% |
| mass factor | 0.30 | 0.00 | 0.42 | 0.00 |
| P3 | <279.30 | | <525.30 | |
| Sc | <9.05 | | <18.64 | |
| V5 | <27.72 | | <52.26 | |
| Cr | <277.37 | | <623.76 | |
| Co | <4.64 | | <14.39 | |
| Ni | <24.58 | | <25.03 | |
| Cu | 53.91 | 14.57% | <34.27 | |
| Rb | 163.30 | 4.47% | 76.68 | 9.72% |
| Sr | 1055.11 | 4.70% | 901.27 | 5.20% |
| Y8 | 15.31 | 10.87% | 2.79 | 50.18% |
| Zr | 80.20 | 7.13% | 26.10 | 18.56% |
| Nb | 11.61 | 14.75% | 3.63 | 36.33% |
| Ba | 1763.29 | 3.41% | 634.95 | 7.68% |
| Cs | 4.01 | 16.97% | 2.54 | 30.54% |
| La | 89.55 | 4.19% | 12.80 | 22.52% |
| Ce | 161.72 | 2.97% | 12.77 | 24.08% |
| Nd | 39.67 | 14.73% | <8.51 | |
| Sm | 8.21 | 33.96% | <5.99 | |
| Yb | <3.15 | | <13.05 | |
| Pb | 61.00 | 8.51% | 42.02 | 11.89% |
| Th | 27.47 | 5.84% | 4.32 | 21.83% |
| U2 | 7.55 | 10.23% | 3.57 | 22.90% |
| Ho | <0.51 | | <0.51 | |
| B1 | <262.50 | | <595.14 | |



Major oxide concentrations in wt%
Trace element concentrations in ppm

LA-ICPMS analyses of Si-MI in **andesitic basalt** from lava flow, Bingham canyon volcanic suite. Element concentrations and uncertainty

Table 3.1

| Host | cpx | | cpx | | cpx | | cpx | | cpx | | cpx | | plag | | plag | | plag | | plag | | plag | |
|---|---|---|---|---|---|---|---|---|---|---|---|---|---|---|---|---|---|---|---|---|---|---|
| Melt inclusions | 15jl21a03.xl | 0% | 15jl21a06.xl | 0% | 15jl21a07.xl | 0% | 15jl21a08.xl | 0% | 15jl21a09.xl | 0% | 15jl21a11.xl | 0% | 15jl21a12.xl | 0% | 15jl21a13.xl | 0% | 15jl21a14.xl | 0% | 15jl21b03.xl | 0% | 15jl21b04.xl | 0% |
| SiO2 | 72.72 | 3% | 35.13 | 26% | 60.85 | 5% | 61.66 | 8% | 56.54 | 7% | 54.83 | 5% | <18.88 | | 65.96 | 2% | 60.80 | 2% | 65.97 | 1% | <33.93 | |
| TiO2 | 0.99 | 5% | 2.06 | 11% | 0.52 | 10% | 3.53 | 2% | 6.36 | 1% | 0.12 | 43% | 0.66 | 12% | 0.09 | 9% | 0.12 | 7% | 0.03 | 11% | 0.81 | 13% |
| Al2O3 | 15.69 | 0% | 15.63 | 2% | 15.66 | 1% | 12.92 | 1% | 13.87 | 1% | 16.34 | 0% | 16.13 | 7% | 16.24 | 1% | 17.60 | 1% | 16.36 | 0% | 15.45 | 10% |
| FeO | 18.44 | 2% | <3.63 | | 4.59 | 11% | 36.04 | 2% | 29.80 | 2% | <0.85 | | 0.90 | 56% | 0.36 | 12% | 0.69 | 8% | 0.34 | 7% | 9.43 | 8% |
| MnO | 0.32 | 4% | <0.09 | | 0.21 | 7% | 1.44 | 2% | 0.93 | 2% | <0.02 | | 0.02 | 68% | <0.00 | | 0.00 | 23% | <0.00 | | 0.03 | 32% |
| MgO | <0.36 | | 12.79 | 5% | <0.50 | | <0.49 | | <0.44 | | <0.32 | | 0.08 | 38% | 0.01 | 19% | 0.04 | 8% | 0.02 | 8% | 0.95 | 5% |
| CaO | <2.33 | | 28.75 | 15% | 10.62 | 14% | <2.68 | | <2.75 | | 28.69 | 4% | 7.50 | 47% | <0.62 | | 2.82 | 12% | 1.94 | 7% | <8.49 | |
| Na2O | 4.92 | 0% | 1.41 | 7% | 3.65 | 1% | 4.23 | 1% | 3.49 | 1% | 3.81 | 1% | 27.12 | 1% | 3.62 | 1% | 6.69 | 1% | 4.74 | 0% | <1.03 | |
| K2O | 4.75 | 0% | 2.69 | 1% | 7.12 | 0% | 6.10 | 0% | 6.40 | 0% | 7.42 | 0% | 30.88 | 1% | 10.86 | 0% | 7.23 | 0% | 6.60 | 0% | 90.83 | 0% |
| Total | 121.83 | 0% | 102.47 | 0% | 107.22 | 0% | 129.92 | 0% | 121.39 | 0% | 115.21 | 0% | 87.28 | 0% | 101.15 | 0% | 100.00 | 0% | 100.00 | 0% | 121.49 | 0% |
| mass factor | 0.09 | 0% | 0.04 | 0% | 0.11 | 0% | 0.04 | 0% | 0.06 | 0% | 0.13 | 0% | 0.04 | 0% | 0.31 | 0% | 0.34 | 0% | 0.47 | 0% | 0.02 | 0% |
| P3 | <191.25 | | <900.79 | | <336.33 | | <169.85 | | 1015.45 | 13% | 81754.02 | 1% | <1317.87 | | <138.60 | | 2.24 | 97% | <80.12 | | <1294.56 | |
| Sc | 84.52 | 15% | <94.49 | | 135.68 | 11% | 565.38 | 5% | 423.61 | 5% | <30.35 | | <30.43 | | <4.08 | | <6.48 | | <2.70 | | 6.36 | 82% |
| V5 | 594.12 | 5% | 558.86 | 22% | 75.35 | 45% | 1271.15 | 4% | 1218.95 | 4% | <50.15 | | <81.20 | | <12.02 | | <18.21 | | <8.34 | | <111.66 | |
| Cr | <727.36 | | <1416.64 | | <1158.90 | | <841.78 | | <877.88 | | <351.29 | | <968.95 | | <130.33 | | <203.93 | | <83.70 | | <1125.01 | |
| Co | 100.74 | 18% | <133.23 | | <45.89 | | 67.66 | 49% | <37.37 | | <31.73 | | <14.66 | | <2.93 | | <4.57 | | 1.17 | 49% | <31.29 | |
| Ni | <233.39 | | 1115.72 | 25% | <372.16 | | <271.72 | | <281.77 | | <117.82 | | <68.52 | | <8.64 | | <13.01 | | 3.58 | 55% | <64.73 | |
| Cu | 174.60 | 6% | 176.61 | 18% | 280.22 | 6% | 230.12 | 7% | 192.87 | 7% | 291.53 | 4% | <55.27 | | 5.83 | 38% | <9.41 | | 112.22 | 4% | 311.72 | 11% |
| Rb | 236.62 | 2% | 51.79 | 9% | 336.70 | 3% | 291.74 | 2% | 267.35 | 2% | 349.43 | 2% | 425.03 | 9% | 160.58 | 3% | 89.70 | 5% | 79.33 | 3% | 2270.07 | 2% |
| Sr | <30.60 | | 246.23 | 17% | 85.27 | 27% | <35.41 | | <36.60 | | 790.77 | 2% | 1231.54 | 29% | 2147.67 | 1% | 1998.19 | 2% | 979.30 | 1% | <930.75 | |
| Y8 | 170.32 | 4% | 221.01 | 15% | 104.31 | 7% | 712.55 | 2% | 568.19 | 2% | 213.63 | 6% | 112.55 | 7% | 1.20 | 40% | 8.43 | 11% | 1.42 | 22% | 75.46 | 17% |
| Zr | 719.95 | 2% | 615.90 | 14% | 447.02 | 4% | 1036.53 | 2% | 1134.80 | 2% | 326.85 | 6% | 561.98 | 4% | 21.34 | 10% | 90.67 | 4% | 16.06 | 9% | 500.96 | 6% |
| Nb | 17.43 | 8% | 10.61 | 37% | 30.92 | 9% | 21.25 | 7% | 59.70 | 4% | 28.28 | 7% | 33.64 | 12% | 1.84 | 28% | 8.36 | 11% | 4.06 | 13% | 24.98 | 25% |
| Ba | 517.26 | 3% | 273.98 | 11% | 952.72 | 3% | 513.98 | 2% | 1209.30 | 2% | 688.40 | 3% | 5839.97 | 9% | 3136.10 | 2% | 2806.52 | 2% | 276.40 | 5% | 10519.94 | 7% |
| Cs | 11.71 | 6% | <2.81 | | 16.53 | 8% | 11.70 | 5% | 10.25 | 6% | 15.66 | 6% | 11.74 | 30% | 6.32 | 9% | 3.69 | 13% | 4.62 | 8% | 43.90 | 11% |
| La | 246.04 | 2% | 90.34 | 31% | 178.24 | 4% | 474.48 | 2% | 442.48 | 2% | 1838.54 | 1% | 213.98 | 17% | 12.53 | 23% | 46.93 | 8% | 24.64 | 6% | 329.81 | 15% |
| Ce | 699.15 | 1% | 184.26 | 29% | 406.27 | 3% | 1500.65 | 1% | 1320.07 | 1% | 3631.49 | 1% | 251.04 | 14% | 9.30 | 33% | 65.73 | 6% | 28.79 | 5% | 340.70 | 15% |
| Nd | 443.97 | 4% | 337.92 | 27% | 232.17 | 9% | 1195.86 | 3% | 1026.19 | 3% | 1493.88 | 2% | 251.70 | 15% | <5.30 | | 26.27 | 15% | 5.09 | 24% | 251.99 | 22% |
| Sm | 88.70 | 11% | <90.84 | | 46.49 | 21% | 277.05 | 6% | 211.40 | 7% | 203.25 | 8% | <18.48 | | <2.06 | | <2.19 | | <1.28 | | 66.51 | 29% |
| Yb | 19.62 | 22% | <44.49 | | <8.11 | | 63.27 | 12% | 47.53 | 14% | 18.43 | 32% | 10.45 | 60% | <1.41 | | <1.84 | | <0.42 | | <10.63 | |
| Pb | 64.39 | 5% | 44.72 | 23% | 88.65 | 6% | 97.35 | 4% | 105.51 | 4% | 109.49 | 4% | <92.43 | | 74.00 | 7% | <11.46 | | 48.90 | 5% | <129.06 | |
| Th | 53.95 | 3% | 81.65 | 8% | 86.61 | 4% | 56.64 | 3% | 68.06 | 3% | 117.16 | 2% | 123.94 | 5% | 4.03 | 12% | 28.52 | 4% | 12.25 | 5% | 181.42 | 5% |
| U2 | 14.87 | 5% | 22.93 | 11% | 23.79 | 7% | 14.31 | 5% | 18.28 | 5% | 26.58 | 5% | 20.17 | 17% | 0.58 | 37% | 5.34 | 10% | 6.71 | 7% | 23.78 | 15% |
| Ho | 8.22 | 13% | <9.63 | | 2.07 | 52% | 31.00 | 6% | 25.30 | 7% | 8.05 | 22% | 3.47 | 34% | 0.14 | 51% | <0.29 | | <0.13 | | 5.63 | 36% |
| B1 | <187.65 | | <679.17 | | <276.37 | | <130.99 | | <188.10 | | <171.15 | | <803.45 | | <110.02 | | <152.24 | | <51.43 | | <709.91 | |



Major oxide concentrations in wt%
Trace element concentrations in ppm

continued on next page

LA-ICPMS analyses of Si-MI in **andesitic basalt** from lava flow, Bingham canyon volcanic suite. Element concentrations and uncertainty

Table3.2

| Host | plag | | plag | | plag | | plag | | plag | | plag | | plag | | plag | | cpx | | cpx | | cpx | |
|---|---|---|---|---|---|---|---|---|---|---|---|---|---|---|---|---|---|---|---|---|---|---|
| Melt inclusions | 15jl21b05.xl | 0% | 15jl21b07.xl | 0% | 15jl21b08.xl | 0% | 15jl21b10.xl | 0% | 15jl21b11.xl | 0% | 15jl21b12.xl | 0% | 15jl21b13.xl | 0% | 15jl21b14.xl | 0% | 15jl21b21.xl | 0% | 15jl21b22.xl | 0% | 15jl21b23.xl | 0% |
| SiO2 | 55.19 | 27% | 67.29 | 1% | 67.53 | 1% | 67.37 | 4% | 64.12 | 3% | 64.19 | 6% | 67.20 | 1% | 66.53 | 1% | <10.05 | | 82.96 | 6% | 68.00 | 14% |
| TiO2 | 0.64 | 11% | 0.15 | 3% | 0.13 | 5% | <0.03 | | 0.24 | 7% | 0.42 | 7% | 0.13 | 4% | 0.17 | 4% | 7.49 | 2% | 1.28 | 9% | <0.39 | |
| Al2O3 | 16.13 | 7% | 16.34 | 0% | 16.39 | 0% | 16.37 | 1% | 16.42 | 1% | 16.31 | 2% | 16.40 | 0% | 16.31 | 0% | 15.78 | 1% | 15.80 | 1% | 15.75 | 2% |
| FeO | 3.03 | 18% | 1.17 | 2% | 0.96 | 4% | <0.24 | | 1.81 | 6% | 2.49 | 7% | 0.87 | 4% | 0.73 | 4% | 101.92 | 1% | 45.82 | 2% | <3.21 | |
| MnO | <0.02 | | 0.00 | 6% | 0.00 | 13% | <0.00 | | 0.01 | 19% | 0.01 | 32% | 0.00 | 10% | 0.01 | 6% | <0.05 | | <0.06 | | <0.07 | |
| MgO | 0.12 | 29% | 0.09 | 2% | 0.06 | 4% | <0.01 | | 0.14 | 5% | 0.15 | 7% | 0.07 | 3% | 0.05 | 4% | <0.63 | | <0.76 | | <0.91 | |
| CaO | <6.25 | | 2.04 | 4% | 1.04 | 18% | <1.47 | | 6.08 | 8% | <2.10 | | 3.68 | 5% | 1.56 | 11% | <4.39 | | <5.63 | | 16.45 | 25% |
| Na2O | <0.75 | | 3.35 | 0% | 3.47 | 1% | 2.73 | 2% | <0.14 | | 0.58 | 20% | 3.96 | 1% | 4.44 | 0% | 2.81 | 2% | <0.11 | | 4.98 | 2% |
| K2O | 59.79 | 0% | 5.55 | 0% | 6.42 | 0% | 11.83 | 0% | 7.40 | 1% | 19.36 | 0% | 3.68 | 0% | 6.21 | 0% | 7.61 | 0% | 0.32 | 3% | 8.54 | 0% |
| Total | 138.89 | 0% | 100.00 | 0% | 100.00 | 0% | 102.30 | 0% | 100.22 | 0% | 107.52 | 0% | 100.00 | 0% | 100.00 | 0% | 139.60 | 0% | 150.17 | 0% | 117.72 | 0% |
| mass factor | 0.03 | 0% | 0.58 | 0% | 0.32 | 0% | 0.20 | 0% | 0.21 | 0% | 0.08 | 0% | 0.41 | 0% | 0.33 | 0% | 0.06 | 0% | 0.09 | 0% | 0.06 | 0% |
| P3 | 4590.55 | 12% | 68.10 | 19% | <75.87 | | <317.02 | | <279.81 | | <247.17 | | <55.38 | | <51.67 | | 1343.73 | 12% | <580.42 | | 2626.92 | 14% |
| Sc | <39.16 | | 3.00 | 19% | <2.55 | | <10.11 | | <8.60 | | <9.80 | | 2.44 | 37% | 4.29 | 20% | <60.28 | | <77.84 | | 193.18 | 26% |
| V5 | <103.63 | | 13.27 | 10% | 2.87 | 26% | <33.29 | | 19.99 | 28% | 33.97 | 24% | 3.35 | 16% | 12.20 | 16% | 4927.61 | 2% | 204.87 | 33% | <203.76 | |
| Cr | <1239.37 | | <33.61 | | <92.48 | | <296.03 | | <250.94 | | <253.66 | | <54.16 | | <55.11 | | 8751.41 | 6% | 1510.27 | 22% | <876.87 | |
| Co | <25.42 | | 1.31 | 31% | <1.82 | | 5.88 | 45% | <7.03 | | <7.03 | | 0.91 | 59% | 1.27 | 43% | 153.87 | 27% | 138.52 | 26% | <103.05 | |
| Ni | <73.34 | | 17.37 | 17% | 6.43 | 45% | <11.35 | | <20.21 | | 5.63 | 66% | 3.10 | 38% | <4.12 | | 663.24 | 25% | 780.08 | 20% | <469.66 | |
| Cu | <55.22 | | 13.52 | 10% | 18.95 | 11% | <22.76 | | <16.61 | | 70.81 | 19% | 17.51 | 13% | 313.97 | 2% | 764.01 | 4% | 857.07 | 5% | 350.77 | 12% |
| Rb | 846.60 | 4% | 129.24 | 2% | 120.43 | 3% | 75.96 | 9% | 246.74 | 4% | 474.54 | 3% | 99.13 | 3% | 143.40 | 2% | 372.96 | 3% | <9.14 | | 438.00 | 4% |
| Sr | 2232.48 | 15% | 1687.06 | 1% | 1190.96 | 2% | <150.24 | | 4395.08 | 1% | 545.17 | 20% | 1921.81 | 1% | 1096.31 | 2% | 248.94 | 10% | 90.90 | 25% | 385.76 | 11% |
| Y8 | 169.03 | 7% | 7.34 | 7% | 19.35 | 6% | 21.79 | 12% | 15.34 | 13% | 47.52 | 8% | 14.25 | 7% | 6.94 | 9% | <38.55 | | <50.02 | | <52.89 | |
| Zr | 245.90 | 9% | 67.77 | 3% | 76.05 | 4% | <7.87 | | 138.66 | 6% | 343.40 | 4% | 127.46 | 3% | 127.02 | 3% | 103.09 | 38% | <108.61 | | 531.44 | 15% |
| Nb | 26.39 | 21% | 6.77 | 8% | 7.08 | 10% | <2.16 | | 12.71 | 15% | 32.16 | 10% | 8.14 | 9% | 11.02 | 7% | 38.40 | 10% | 13.08 | 25% | 18.53 | 26% |
| Ba | 3606.70 | 16% | 2922.57 | 1% | 1440.43 | 3% | <253.41 | | 4944.67 | 2% | 780.89 | 23% | 2272.70 | 1% | 1046.53 | 3% | 970.66 | 3% | 355.83 | 9% | 612.64 | 7% |
| Cs | 17.11 | 16% | 3.49 | 7% | 3.02 | 11% | <0.94 | | 7.76 | 13% | 14.00 | 10% | 3.11 | 10% | 6.99 | 6% | 20.53 | 8% | 0.58 | 72% | 20.33 | 13% |
| La | 255.41 | 14% | 62.10 | 2% | 73.90 | 4% | <15.92 | | 184.89 | 4% | 227.18 | 6% | 88.54 | 3% | 73.50 | 3% | 48.71 | 29% | <33.39 | | 181.49 | 14% |
| Ce | 348.34 | 10% | 107.21 | 2% | 88.92 | 3% | <16.08 | | 237.29 | 3% | 301.11 | 4% | 111.34 | 2% | 117.42 | 2% | <50.41 | | <61.26 | | 287.25 | 16% |
| Nd | 148.11 | 29% | 33.09 | 6% | 46.75 | 7% | <15.45 | | 72.83 | 11% | 138.01 | 11% | 46.49 | 7% | 30.19 | 9% | <97.59 | | <122.34 | | 145.62 | 60% |
| Sm | 30.20 | 44% | 3.57 | 20% | 7.23 | 19% | 4.87 | 72% | 8.76 | 37% | 27.41 | 21% | 4.35 | 26% | 3.63 | 26% | <50.88 | | <62.73 | | <69.68 | |
| Yb | -3.30<l<14.66 | | 0.90 | 33% | 1.26 | 43% | <2.63 | | <2.87 | | 1.95 | 100% | 1.33 | 42% | 0.86 | 45% | <25.00 | | <27.70 | | <27.17 | |
| Pb | <96.96 | | 37.86 | 4% | 22.35 | 14% | <20.89 | | 76.54 | 11% | 37.94 | 40% | 34.29 | 8% | 48.20 | 6% | 76.61 | 8% | <10.18 | | 101.54 | 10% |
| Th | 62.23 | 9% | 17.95 | 3% | 24.62 | 4% | <2.18 | | 39.81 | 6% | 106.53 | 4% | 26.88 | 3% | 35.10 | 3% | 88.91 | 4% | 12.28 | 21% | 88.91 | 7% |
| U2 | 18.49 | 15% | 3.78 | 6% | 3.66 | 9% | <0.81 | | 8.52 | 12% | 20.36 | 8% | 6.12 | 7% | 7.67 | 5% | 23.29 | 8% | 11.87 | 16% | 24.14 | 10% |
| Ho | -0.26<l<3.69 | | 0.14 | 41% | 0.37 | 31% | 1.19 | 37% | 0.61 | 61% | 1.98 | 27% | 0.54 | 27% | 0.14 | 49% | <5.87 | | <7.91 | | <7.65 | |
| B1 | <789.71 | | <24.76 | | <53.66 | | <171.92 | | <158.90 | | <173.79 | | 2.56 | 72% | 8.63 | 43% | <278.31 | | <424.22 | | <366.88 | |



Major oxide concentrations in wt%
Trace element concentrations in ppm

continued on next page

LA-ICPMS analyses of Si-MI in **andesitic basalt** from lava flow, Bingham canyon volcanic suite. Element concentrations and uncertainty
Table 3.3

| Host | cpx | | cpx | | cpx | | cpx | | cpx | | cpx | | cpx | | cpx | | cpx | | cpx | | cpx | |
|---|---|---|---|---|---|---|---|---|---|---|---|---|---|---|---|---|---|---|---|---|---|---|
| Melt inclusions | 15jl21b24.xl | 0% | 15jl21b25.xl | 0% | 15jl21b26.xl | 0% | 15jl21b27.xl | 0% | 15jl21b28.xl | 0% | 15jl21b30.xl | 0% | 15jl21c03.xl | 0% | 15jl21c04.xl | 0% | 15jl21c05.xl | 0% | 15jl21c06.xl | 0% | 15jl21c07.xl | 0% |
| SiO2 | 60.92 | 8% | <21.32 | | 46.61 | 8% | <118.45 | | 26.88 | 18% | 58.75 | 6% | 169.61 | 6% | 74.53 | 4% | 66.76 | 3% | 82.80 | 3% | 40.15 | 15% |
| TiO2 | 0.62 | 16% | 0.98 | 20% | 1.05 | 7% | <2.36 | | <0.22 | | 0.42 | 16% | <0.46 | | <0.09 | | 0.21 | 17% | <0.07 | | 3.14 | 3% |
| Al2O3 | 15.74 | 1% | 18.61 | 1% | 15.75 | 1% | 21.67 | 5% | 16.06 | 1% | 15.67 | 1% | 15.65 | 1% | 15.68 | 1% | 15.69 | 0% | 15.68 | 0% | 15.64 | 1% |
| FeO | <1.35 | | <3.70 | | 1.11 | 55% | <23.69 | | <2.27 | | <1.43 | | 12.85 | 16% | <1.04 | | <0.63 | | <0.79 | | <1.58 | |
| MnO | <0.03 | | <0.09 | | 0.15 | 10% | <0.54 | | <0.05 | | <0.03 | | <0.14 | | <0.03 | | 0.08 | 14% | <0.02 | | <0.04 | |
| MgO | 5.50 | 5% | <1.14 | | 10.57 | 2% | 41.19 | 6% | 16.09 | 2% | 16.02 | 1% | <1.69 | | 2.98 | 6% | 1.89 | 7% | 2.21 | 7% | 1.03 | 45% |
| CaO | <2.97 | | 234.02 | 3% | 11.22 | 12% | 676.54 | 3% | 66.20 | 4% | 14.20 | 11% | <13.03 | | 12.52 | 11% | 4.36 | 21% | <2.02 | | 43.35 | 7% |
| Na2O | 3.70 | 1% | 5.65 | 2% | 2.98 | 1% | <0.97 | | 1.52 | 3% | 2.59 | 1% | 5.53 | 2% | 2.65 | 1% | 3.82 | 0% | 3.57 | 1% | 2.82 | 2% |
| K2O | 7.76 | 0% | 9.54 | 1% | 6.57 | 0% | 24.70 | 1% | 7.19 | 0% | 5.58 | 0% | 7.70 | 1% | 8.60 | 0% | 6.85 | 0% | 7.20 | 0% | 8.54 | 0% |
| Total | 98.26 | 0% | 272.80 | 0% | 100.00 | 0% | 768.10 | 0% | 137.94 | 0% | 117.22 | 0% | 215.33 | 0% | 120.97 | 0% | 103.66 | 0% | 115.46 | 0% | 118.68 | 0% |
| mass factor | 0.15 | 0% | 0.05 | 0% | 0.19 | 0% | 0.01 | 0% | 0.06 | 0% | 0.08 | 0% | 0.04 | 0% | 0.14 | 0% | 0.17 | 0% | 0.14 | 0% | 0.06 | 0% |
| P3 | <667.81 | | | 0% | <419.02 | | | 1% | 54565.03 | 1% | <418.79 | | <1550.82 | | <259.31 | | <214.92 | | 7.60 | 133% | 26.06 | 44% |
| Sc | 64.21 | 44% | 290.65 | 21% | 129.17 | 13% | <680.24 | | 160.61 | 20% | <41.49 | | 288.26 | 16% | <17.07 | | 24.18 | 44% | 72.74 | 12% | <35.05 | |
| V5 | <80.77 | | <202.54 | | <63.99 | | <1503.03 | | <131.81 | | <88.39 | | <325.88 | | <62.84 | | <36.18 | | <45.75 | | <79.50 | |
| Cr | <698.93 | | <2275.31 | | <428.88 | | <11225.36 | | <892.70 | | 5281.71 | 5% | <1987.69 | | <312.66 | | -164.76 | | <174.72 | | <362.49 | |
| Co | <46.10 | | <134.13 | | <39.10 | | <882.92 | | <83.64 | | <52.12 | | <166.97 | | <34.61 | | <24.27 | | <25.81 | | <53.40 | |
| Ni | <261.90 | | <1000.01 | | <206.86 | | <3422.92 | | <324.54 | | 834.19 | 14% | <554.71 | | <100.96 | | <76.12 | | 145.64 | 33% | <197.31 | |
| Cu | 244.47 | 9% | 446.10 | 19% | 386.21 | 5% | 766.49 | 23% | 356.47 | 6% | 314.51 | 5% | 131.98 | 30% | 292.21 | 7% | 356.96 | 3% | 421.33 | 3% | 343.69 | 7% |
| Rb | 392.09 | 3% | 475.72 | 5% | 284.03 | 4% | 926.40 | 8% | 380.11 | 3% | 276.08 | 3% | 400.66 | 7% | 371.81 | 3% | 359.18 | 2% | 307.36 | 2% | 403.44 | 3% |
| Sr | 265.17 | 10% | 6410.31 | 1% | 266.71 | 7% | 17770.41 | 2% | 855.01 | 3% | 565.82 | 3% | <131.95 | | 232.24 | 6% | 221.37 | 4% | 87.07 | 13% | 68.34 | 42% |
| Y8 | 69.87 | 23% | 2212.52 | 2% | 76.39 | 13% | 4962.12 | 5% | 253.62 | 8% | <26.55 | | <97.69 | | <16.62 | | 36.44 | 21% | <15.26 | | 178.09 | 11% |
| Zr | 408.61 | 7% | 650.22 | 8% | 259.57 | 8% | <822.62 | | 246.02 | 16% | <47.45 | | 511.25 | 12% | 323.45 | 6% | 401.85 | 3% | 373.08 | 4% | 515.60 | 6% |
| Nb | 24.67 | 13% | 23.62 | 24% | 19.72 | 15% | 111.05 | 27% | 24.03 | 13% | 17.26 | 10% | 30.86 | 23% | 30.69 | 10% | 25.32 | 6% | 27.82 | 7% | 238.14 | 3% |
| Ba | 977.21 | 4% | 919.08 | 9% | 997.97 | 4% | 5527.82 | 6% | 779.96 | 4% | 801.95 | 3% | 936.63 | 8% | 1749.82 | 3% | 907.89 | 2% | 1426.55 | 2% | 1139.45 | 3% |
| Cs | 16.51 | 9% | 15.28 | 15% | 16.16 | 9% | 39.22 | 26% | 16.18 | 9% | 14.15 | 7% | 24.60 | 16% | 16.39 | 9% | 16.92 | 5% | 12.50 | 7% | 18.13 | 8% |
| La | 134.00 | 10% | 13545.25 | 1% | 83.47 | 11% | 30898.73 | 1% | 1247.97 | 2% | <17.94 | | 88.67 | 33% | <13.99 | | 78.61 | 8% | 76.14 | 8% | 175.27 | 8% |
| Ce | 246.50 | 10% | 26077.69 | 0% | 160.34 | 10% | 59226.16 | 1% | 2366.29 | 1% | <32.98 | | 143.38 | 37% | <26.74 | | 99.64 | 11% | 48.99 | 23% | 492.33 | 5% |
| Nd | 148.93 | 27% | 10884.32 | 2% | 131.05 | 21% | 26650.76 | 3% | 946.26 | 6% | <64.70 | | <253.30 | | <46.43 | | 86.12 | 23% | <39.61 | | 302.50 | 14% |
| Sm | <33.54 | | 1558.27 | 5% | <23.64 | | 3859.94 | 9% | 143.12 | 20% | <33.52 | | <131.44 | | <22.43 | | <13.96 | | <20.14 | | 65.79 | 31% |
| Yb | 16.25 | 36% | 129.18 | 13% | 19.28 | 30% | 357.19 | 36% | <25.62 | | <16.94 | | <56.94 | | <11.07 | | <5.91 | | <8.24 | | 19.12 | 49% |
| Pb | 47.81 | 6% | 134.14 | 12% | 80.10 | 6% | 268.61 | 19% | 91.34 | 7% | 50.00 | 7% | 178.16 | 10% | 61.79 | 9% | 92.19 | 3% | 82.11 | 4% | 78.80 | 8% |
| Th | 79.48 | 5% | 568.21 | 3% | 62.22 | 5% | 1329.51 | 4% | 121.77 | 3% | 40.40 | 5% | 108.91 | 7% | 78.08 | 4% | 81.59 | 2% | 91.39 | 2% | 101.08 | 4% |
| U2 | 16.39 | 10% | 94.78 | 7% | 16.36 | 9% | 205.33 | 11% | 31.00 | 6% | 11.25 | 9% | 33.82 | 14% | 24.23 | 7% | 22.19 | 4% | 21.18 | 5% | 37.08 | 6% |
| Ho | <3.86 | | 78.40 | 10% | 4.65 | 28% | 192.60 | 17% | 11.51 | 28% | <4.11 | | <12.56 | | <2.65 | | 1.55 | 70% | <1.97 | | 11.30 | 22% |
| B1 | <229.70 | | <633.34 | | <206.23 | | <3851.84 | | <189.00 | | -50.31<I<127.64 | | <1344.30 | | <173.05 | | <108.49 | | -52.90<I<94.01 | | <222.96 | |



Major oxide concentrations in wt%
Trace element concentrations in ppm

continued on next page

LA-ICPMS analyses of Si-MI in **andesitic basalt** from lava flow, Bingham canyon volcanic suite. Element concentrations and uncertainty
Table 3.4

| Host | cpx | | cpx 15jl21c08. | | cpx 15jl21c09. | | cpx 15jl21c11. | | cpx 15jl21c12. | | cpx 15jl21c13. | | cpx | | cpx 15jl21c15. | | cpx | | cpx 15jl22a03 | | cpx 15jl22a04 | |
|---|---|---|---|---|---|---|---|---|---|---|---|---|---|---|---|---|---|---|---|---|---|---|
| Melt inclusions | 15jl21c08.xl | 0% | xl (copy) | 0% | xl | 0% | xl | 0% | xl | 0% | xl | 0% | 15jl21c14.xl | 0% | xl | 0% | 15jl21c16.xl | 0% | .xl | 0% | .xl | 0% |
| SiO2 | 64.26 | 7% | 76.34 | 14% | 67.29 | 2% | 30.93 | 8% | 65.13 | 2% | <10.75 | | 32.40 | 12% | 63.50 | 5% | 34.84 | 10% | 75.21468 | 1% | 66.37 | 2% |
| TiO2 | <0.13 | | <0.26 | | 0.30 | 7% | 1.39 | 4% | 0.55 | 5% | 5.68 | 2% | 2.51 | 4% | 0.48 | 14% | 1.12 | 6% | 0.257171 | 8% | 0.39 | 8% |
| Al2O3 | 15.65 | 1% | 15.60 | 1% | 15.71 | 0% | 15.69 | 0% | 15.79 | 0% | 15.63 | 1% | 15.68 | 1% | 15.74 | 1% | 15.74 | 1% | 15.76045 | 0% | 15.77 | 0% |
| FeO | <1.64 | | <3.39 | | <0.48 | | <0.82 | | 1.28 | 20% | 29.19 | 4% | 16.97 | 5% | <1.11 | | <1.40 | | <0.40 | | 2.36 | 13% |
| MnO | <0.04 | | <0.08 | | 0.06 | 11% | <0.02 | | <0.02 | | <0.06 | | 0.08 | 27% | <0.03 | | 0.19 | 9% | <0.01 | | 0.08 | 10% |
| MgO | 1.03 | 29% | <1.12 | | <0.16 | | 16.62 | 1% | 0.33 | 24% | 6.17 | 5% | 14.14 | 2% | 4.06 | 5% | 12.13 | 2% | <0.14 | | 0.70 | 13% |
| CaO | 23.03 | 9% | 40.05 | 12% | 5.18 | 10% | 29.35 | 4% | 2.98 | 18% | 20.59 | 11% | 6.91 | 27% | 3.94 | 37% | 33.10 | 4% | <0.94 | | <1.42 | |
| Na2O | 3.35 | 1% | 4.15 | 2% | 3.85 | 0% | 2.16 | 1% | 3.11 | 0% | 2.56 | 2% | 3.57 | 1% | 3.58 | 1% | 2.35 | 1% | 3.616954 | 0% | 3.67 | 0% |
| K2O | 8.96 | 0% | 14.54 | 0% | 6.44 | 0% | 5.06 | 0% | 6.86 | 0% | 6.68 | 0% | 3.74 | 0% | 7.71 | 0% | 5.30 | 0% | 6.98856 | 0% | 6.89 | 0% |
| Total | 120.28 | 0% | 154.67 | 0% | 102.83 | 0% | 105.19 | 0% | 100.02 | 0% | 90.49 | 0% | 100.00 | 0% | 103.01 | 0% | 108.77 | 0% | 105.8378 | 0% | 100.21 | 0% |
| mass factor | 0.09 | 0% | 0.04 | 0% | 0.18 | 0% | 0.13 | 0% | 0.20 | 0% | 0.05 | 0% | 0.06 | 0% | 0.14 | 0% | 0.12 | 0% | 0.268646 | 0% | 0.29 | 0% |
| P3 | <289.67 | | <679.41 | | 193.37 | 16% | <200.86 | | 123.40 | 27% | <828.95 | | <245.28 | | 43.34 | 69% | 3578.25 | 5% | 146.18 | 24% | 26.29 | 31% |
| Sc | <38.05 | | <79.64 | | <13.11 | | <24.15 | | <18.14 | | <64.33 | | <47.98 | | 40.41 | 47% | 205.60 | 10% | <12.26 | | <18.37 | |
| V5 | <89.77 | | <188.87 | | <25.61 | | <46.68 | | 208.46 | 8% | 2025.55 | 4% | 271.62 | 18% | <72.22 | | 249.85 | 17% | <23.47 | | <39.33 | |
| Cr | <262.84 | | <692.89 | | <84.17 | | 3983.18 | 4% | 1171.47 | 8% | 16792.23 | 3% | 14165.44 | 5% | <315.74 | | <428.37 | | <182.71 | | <280.99 | |
| Co | <57.12 | | <118.22 | | <16.27 | | <30.23 | | <22.74 | | <87.15 | | <65.68 | | <39.55 | | <50.70 | | <14.80 | | <21.92 | |
| Ni | <196.62 | | <407.51 | | <59.25 | | 1159.41 | 8% | 103.28 | 32% | <309.94 | | 275.10 | 41% | <134.46 | | <179.45 | | <56.99 | | <89.29 | |
| Cu | 159.70 | 11% | 628.16 | 7% | 439.87 | 2% | 27.65 | 43% | 218.22 | 4% | 168.38 | 12% | 105.05 | 14% | 398.87 | 5% | 213.27 | 8% | 215.0277 | 3% | 183.88 | 5% |
| Rb | 426.79 | 3% | 794.62 | 3% | 319.51 | 1% | 200.81 | 3% | 338.00 | 2% | 283.02 | 4% | 173.41 | 4% | 324.98 | 3% | 234.24 | 3% | 377.0688 | 1% | 382.34 | 2% |
| Sr | 612.49 | 4% | 1562.63 | 4% | 224.70 | 3% | 874.12 | 2% | 291.66 | 3% | 162.49 | 15% | 196.33 | 10% | 271.83 | 6% | 329.54 | 5% | 278.0005 | 2% | 279.83 | 3% |
| Y8 | <27.45 | | <56.77 | | 37.41 | 13% | <15.14 | | 18.97 | 26% | 65.84 | 30% | <31.46 | | 25.24 | 49% | 151.56 | 8% | <7.95 | | <11.23 | |
| Zr | 334.49 | 8% | 236.00 | 25% | 356.64 | 2% | 241.83 | 7% | 345.39 | 3% | 321.37 | 11% | 331.42 | 8% | 285.94 | 8% | 524.48 | 5% | 338.4775 | 3% | 323.22 | 4% |
| Nb | 26.05 | 11% | 38.97 | 12% | 24.66 | 5% | 24.48 | 7% | 20.96 | 7% | 33.07 | 10% | 16.08 | 12% | 22.47 | 10% | 18.33 | 11% | 22.86339 | 5% | 25.79 | 8% |
| Ba | 990.71 | 4% | 1395.72 | 5% | 895.11 | 2% | 1324.73 | 2% | 1061.21 | 2% | 681.02 | 4% | 699.05 | 4% | 1558.37 | 2% | 1087.74 | 3% | 878.0614 | 2% | 987.43 | 3% |
| Cs | 23.62 | 7% | 35.65 | 8% | 15.05 | 4% | 4.69 | 10% | 17.84 | 5% | 17.31 | 9% | 6.58 | 12% | 15.10 | 8% | 8.66 | 12% | 19.49 | 4% | 20.38 | 6% |
| La | <21.35 | | <44.19 | | 127.81 | 3% | 93.52 | 9% | 121.24 | 3% | <34.14 | | 43.40 | 24% | 22.97 | 39% | 224.93 | 4% | 95.76051 | 3% | 138.68 | 4% |
| Ce | <39.51 | | <81.67 | | 239.48 | 3% | <23.08 | | 231.05 | 3% | <60.53 | | <41.76 | | 106.35 | 16% | 476.09 | 4% | 148.0627 | 4% | 180.55 | 5% |
| Nd | <73.62 | | <152.37 | | 88.05 | 14% | <40.07 | | 65.28 | 19% | <111.08 | | <80.41 | | 116.71 | 26% | 333.42 | 10% | 40.12373 | 24% | <29.96 | |
| Sm | <34.02 | | <70.46 | | 15.26 | 40% | 26.36 | 43% | <14.49 | | <56.24 | | <40.62 | | <23.88 | | 61.60 | 26% | <10.42 | | <14.56 | |
| Yb | <14.55 | | <30.26 | | <5.13 | | <8.62 | | <6.49 | | <25.92 | | <16.82 | | <13.54 | | 27.53 | 22% | <4.85 | | <7.65 | |
| Pb | 79.38 | 7% | 138.89 | 8% | 82.92 | 3% | 47.98 | 6% | 85.19 | 3% | 81.86 | 8% | 34.64 | 13% | 90.60 | 5% | 54.68 | 9% | 83.41058 | 3% | 79.86 | 5% |
| Th | 83.60 | 4% | 112.97 | 5% | 83.16 | 2% | 57.06 | 3% | 87.54 | 2% | 69.45 | 5% | 32.82 | 6% | 49.50 | 4% | 61.11 | 4% | 59.6087 | 2% | 96.29 | 3% |
| U2 | 20.87 | 8% | 23.00 | 12% | 20.37 | 3% | 14.62 | 6% | 20.13 | 4% | 17.75 | 9% | 7.81 | 12% | <1.77 | | 15.74 | 9% | 22.99018 | 3% | 22.69 | 6% |
| Ho | <4.28 | | <8.87 | | <1.43 | | <2.24 | | <1.82 | | <6.50 | | <4.76 | | <2.99 | | 7.30 | 27% | <1.20 | | <1.56 | |
| B1 | 128.11 | | <363.79 | | 69.04 | 23% | <84.07 | | 22.40 | 31% | <222.60 | | <164.86 | | <123.63 | | -<I<125.71 | | 51.055 | 28% | <164.35 | |



Major oxide concentrations in wt%
Trace element concentrations in ppm

continued on next page

LA-ICPMS analyses of Si-MI in **andesitic basalt** from lava flow, Bingham canyon volcanic suite. Element concentrations and uncertainty

Table 3.5

| Host | cpx | | cpx | | cpx | | cpx | | cpx | | cpx | | cpx | | cpx | |
|---|---|---|---|---|---|---|---|---|---|---|---|---|---|---|---|---|
| Melt inclusions | 15jl22a05.xl | 0% | 15jl22a06.xl | 0% | 15jl22a07.xl | 0% | 15jl22a07.xl (copy) | 0% | 15jl22a10.xl | 0% | 15jl22a12.xl | 0% | 15jl22a12.xl (copy) | 0% | 15jl22a08.xl | 0% |
| SiO2 | 77.60 | 4% | 59.82 | 3% | <40.60 | | 130.83 | 7% | 61.66 | 4% | 54.72 | 3% | <41.12 | 2% | 78.89 | 3% |
| TiO2 | 0.44 | 13% | 0.54 | 8% | <0.79 | | 1.09 | 18% | 0.17 | 26% | 0.48 | 8% | 13.72 | 7% | 0.59 | 6% |
| Al2O3 | 15.69 | 1% | 15.72 | 0% | 15.69 | 3% | 15.63 | 1% | 15.75 | 0% | 15.83 | 0% | 15.69 | 0% | 15.61 | 0% |
| FeO | <1.51 | | 3.39 | 12% | <8.76 | | <3.84 | | 1.47 | 33% | 1.56 | 24% | 42.52 | 10% | <0.69 | |
| MnO | <0.04 | | 0.05 | 20% | 3.35 | 4% | <0.10 | | 0.22 | 6% | 0.14 | 6% | <0.18 | 9% | <0.02 | |
| MgO | <0.46 | | 0.47 | 26% | <2.86 | | <1.19 | | <0.34 | | 10.39 | 1% | 19.16 | | 3.55 | 4% |
| CaO | <3.65 | | 6.60 | 14% | 63.55 | 17% | <8.57 | | 9.00 | 12% | 2.12 | 36% | 57.96 | 12% | <1.55 | |
| Na2O | 3.35 | 1% | 3.29 | 1% | 9.47 | 2% | 4.18 | 2% | 3.90 | 1% | 2.91 | 1% | 0.66 | 0% | 3.43 | 1% |
| K2O | 8.22 | 0% | 6.38 | 0% | 8.38 | 1% | 13.33 | 0% | 5.67 | 0% | 7.85 | 0% | 6.42 | 0% | 7.68 | 0% |
| Total | 109.30 | 0% | 100.25 | 0% | 104.44 | 0% | 169.05 | 0% | 101.84 | 0% | 100.00 | 0% | 160.13 | 0% | 113.75 | 0% |
| mass factor | 0.14 | 0% | 0.21 | 0% | 0.01 | 0% | 0.03 | 0% | 0.16 | 0% | 0.28 | 0% | 0.03 | 0% | 0.11 | 0% |
| P3 | <709.20 | | -3.58<I<216.25 | | 4722.04 | 8% | <1064.39 | | 345.18 | 24% | 613.93 | 14% | <1926.16 | 1% | <275.22 | |
| Sc | <51.33 | | 45.52 | 26% | 342.91 | 43% | <117.63 | | 54.12 | 28% | <14.42 | | <218.96 | 27% | <21.22 | |
| V5 | <100.04 | | <54.97 | | <485.34 | | <228.05 | | 130.30 | 22% | <35.38 | | 3900.86 | 15% | 110.86 | 21% |
| Cr | <739.77 | | 528.40 | 24% | <2727.69 | | <1525.22 | | <292.80 | | <190.60 | | 3476.19 | | 803.77 | 12% |
| Co | <52.71 | | <33.91 | | <308.03 | | <136.05 | | <39.24 | | <18.84 | | <283.86 | | 43.35 | 32% |
| Ni | 206.92 | 38% | <130.74 | | <1110.98 | | <492.03 | | <152.94 | | <65.89 | | <995.37 | | 468.63 | 10% |
| Cu | 227.73 | 8% | 154.34 | 7% | <129.38 | | 917.32 | 5% | 249.22 | 5% | 54.33 | 15% | <161.35 | 4% | 131.23 | 10% |
| Rb | 434.67 | 3% | 328.47 | 3% | 527.62 | 5% | 721.02 | 3% | 379.51 | 3% | 221.55 | 2% | 280.33 | 2% | 402.18 | 1% |
| Sr | 293.22 | 6% | 234.82 | 5% | <184.04 | | 468.47 | 10% | 168.31 | 7% | 916.86 | 1% | 271.80 | 2% | 301.54 | 3% |
| Y8 | <28.90 | | 40.78 | 19% | <168.55 | | <74.00 | | 52.62 | 18% | <8.83 | | 142.77 | 6% | <13.04 | |
| Zr | 317.11 | 7% | 304.92 | 5% | <243.46 | | 310.56 | 20% | 258.80 | 7% | 129.12 | 11% | 284.90 | 3% | 362.03 | 4% |
| Nb | 20.96 | 14% | 17.24 | 12% | 39.06 | 22% | 38.23 | 13% | 34.69 | 8% | 12.86 | 9% | 55.65 | 6% | 20.98 | 7% |
| Ba | 936.58 | 4% | 712.33 | 4% | 757.04 | 8% | 1062.14 | 4% | 521.49 | 4% | 5658.68 | 1% | 1469.61 | 2% | 918.25 | 2% |
| Cs | 20.31 | 9% | 18.10 | 7% | 34.98 | 12% | 33.51 | 8% | 25.12 | 6% | 4.62 | 11% | 9.48 | 5% | 20.72 | 4% |
| La | 101.38 | 9% | 97.61 | 6% | 602.01 | 11% | 212.48 | 13% | 149.80 | 5% | 58.68 | 8% | 165.43 | 1% | 13.26 | 52% |
| Ce | 178.19 | 9% | 199.38 | 5% | 1050.85 | 11% | <92.33 | | 312.80 | 4% | 68.13 | 13% | <180.36 | 1% | <18.91 | |
| Nd | <71.81 | | 66.84 | 29% | <412.50 | | <180.90 | | 74.83 | 31% | <22.06 | | <331.63 | 4% | <33.29 | |
| Sm | <36.33 | | <23.16 | | <215.82 | | <94.64 | | 28.98 | 42% | <11.79 | | <177.60 | 12% | <16.39 | |
| Yb | <18.35 | | <11.00 | | <93.98 | | <41.16 | | <12.68 | | <5.71 | | <85.73 | 34% | <7.43 | |
| Pb | 89.44 | 7% | 73.62 | 6% | 75.51 | 31% | 166.25 | 8% | 96.92 | 5% | 65.16 | 5% | <48.30 | 3% | 89.26 | 3% |
| Th | 100.68 | 4% | 71.90 | 4% | 121.61 | 8% | 136.98 | 5% | 116.28 | 3% | 33.49 | 4% | 88.00 | 2% | 84.92 | 2% |
| U2 | 20.65 | 9% | 17.92 | 7% | 35.89 | 12% | 36.35 | 8% | 31.55 | 6% | 11.24 | 6% | 32.74 | 4% | 24.67 | 3% |
| Ho | <4.24 | | <2.50 | | <25.31 | | <11.08 | | 3.73 | 40% | <1.47 | | <22.08 | 20% | <1.86 | |
| B1 | <622.93 | | <160.40 | | <1198.89 | | <896.02 | | 55.28 | 44% | -137.90<I<91.37 | | <1583.70 | | <164.09 | |



Major oxide concentrations in wt%
Trace element concentrations in ppm